FUNDAMENTAL JOURNAL OF MATHEMATICS AND APPLICATIONS

VOLUME VI ISSUE II

FUJMA

www.dergipark.org.tr/en/pub/fujma

ISSN 2645-8845

VOLUME 6 ISSUE 2
ISSN 2645-8845

June 2023
www.dergipark.org.tr/en/pub/fujma

FUNDAMENTAL JOURNAL OF MATHEMATICS AND APPLICATIONS

Language Editor

Technical Editor

Editorial Secretariat

Contents

Research Articles

1 Constant Angle Ruled Surfaces in $\mathbb{E}_1^3$
Aykut Has, Beyhan Yılmaz, Yusuf Yaylı **78-88**

2 Flux Surfaces According to Killing Magnetic Vectors in Riemannian Space $\mathbb{S}ol3$
Nourelhouda Benmensour, Fouzi Hathout **89-100**

3 Parameter Estimation for a Class of Fractional Stochastic SIRD Models with Random Perturbations
Na Nie, Jun Jiang, Yuqiang Feng **101-106**

4 Berezin Radius Inequalities of Functional Hilbert Space Operators
Hamdullah Başaran, Mehmet Gürdal **107-116**

5 Ricci Soliton Lightlike Submanifolds with Co-Dimension 2
Erol KILIÇ Mehmet Gülbahar, Ecem Kavuk, Esra Erkan **117-127**

6 Qualitative Behavior of the Difference Equation $x_{n+1} = \frac{\alpha x_{n-m}+\eta x_{n-k}+\sigma x_{n-l}+\delta x_n}{\beta+\gamma x_{n-k}x_{n-l}(x_{n-k}+x_{n-l})}$
Mohamed Abd El-Moneam **128-136**

Fundamental Journal of Mathematics and Applications, 6 (2) (2023) 78-88
Research Article

FUJMA

Fundamental Journal of Mathematics and Applications

Journal Homepage: www.dergipark.org.tr/en/pub/fujma
ISSN: 2645-8845
doi: https://dx.doi.org/10.33401/fujma.1218966

Constant Angle Ruled Surfaces in $\mathbb{E}_1^3$

Aykut Has[1*], Beyhan Yılmaz[2] and Yusuf Yaylı[3]

[1*,2]*Department of Mathematics, Faculty of Science, Kahramanmaraş Sütçü İmam University, Kahramanmaraş, Türkiye*
[3]*Department of Mathematics, Faculty of Science, Ankara University, Ankara, Türkiye*
[*]*Corresponding author*

Article Info

Keywords: *Constant angle surface, Developable ruled surface, Isophote curve, Optic, Singularity, Spherical circle*
2010 AMS: *53A04, 53A05, 53A35, 78A05, 78A10*
Received: *14 December 2022*
Accepted: *18 April 2023*
Available online: *19 May 2023*

Abstract

In this study, for the first time, a method is given for a developable ruled surface to be a constant angle ruled surface. The general equations of constant angle surfaces have been shown in the studies done so far. In this study, a new method is given on how to obtain a constant angled surface when any constant direction is given in Minkowski 3−space.

1. Introduction

A constant angle surface is a surface whose tangent planes make a constant angle with a fixed vector field of space. In other words, constant angle surfaces whose unit normal forms a constant angle with an assigned direction field in the Euclidean 3−space. This surface is a generalization of a helical curve. An interesting motivation to study helix surfaces or constant angle surfaces arises from physics. The most basic known application areas of the constant angle surfaces are for light such as crystal, liquid and shape from shading problems. In recent years, many authors have studied these special surfaces to take advantage of their applications in mathematics and physics. Paolo and Scala discuss some properties of constant angel surfaces in terms of the Hamilton-Jacobi equation. They investigate the properties of a constant angle surface when the direction field is singular along a line or a point, [1]. Munteanu and Nistor obtain a classification for which the unit normal makes a constant angle with a fixed vector direction being the tangent direction to R in Euclidean 3−space [2]. Many studies have been done on constant angle surfaces and developable surfaces [3, 4]. In [5], the author investigates the constant angle ruled surfaces generated by Frenet frame vectors. Recently the theory of constant angle surfaces is extended to other ambient spaces. For example; in [6, 7], they study these surfaces in $\mathbb{E}_1^3$. Also, in [8]- [11], the authors extend the concept of constant angle surfaces to a Lorentzian ambient space. Also, in product spaces $\mathbb{S}^2 \times \mathbb{R}$ [12, 13], in $\mathbb{H}^2 \times \mathbb{R}$ [14] and in Heisenberg group [15, 16].
On the other hand, an isophote curve is defined as the locus of the surface points whose normal vectors make a constant angle with a given constant vector as seen in Figure 1.1. Therefore, we can say that the curves on the constant angle surface are isophote curves. The isophote curve is a nice corollary to Lambert's law of cosines in the optics branch of physics. This law states that the illuminance intensity on a diffused surface is proportional to the cosine of the angle formed between the normal vector of the surface and the light vector. So, we can say the geometric description of isophote curves on surfaces which are the surface normal vectors in points of the curve make a constant angle with a fixed light direction [17]. In recent years, there have been many applications of these curves in different branches. In [18], the authors developed a novel technique to detect caries lesions using isophote concepts. Also, in [19], they present the implementation of a real-time eye detection method that uses the properties of isophotes, to achieve robustness against changes in illumination, eye rotation and pupil size.

Email addresses and ORCID numbers: ahas@ksu.edu.tr, 0000-0003-0658-9365 (A. Has), beyhanyilmaz@ksu.edu.tr, 0000-0002-5091-3487 (B. Yılmaz), yayli@science.ankara.edu.tr, 0000-0003-4398-3855 (Y. Yaylı)
Cite as: A. Has, B. Yılmaz, Y. Yaylı, *Constant Angle Ruled Surfaces in* $\mathbb{E}_1^3$, Fundam. J. Math. Appl., 6(2) (2023), 78-88.

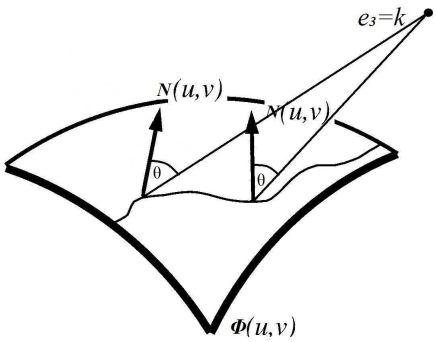

Figure 1.1: An isophote on a surface

In this present paper, we investigate the spherical circles and constant angle surfaces in $\mathbb{E}_1^3$. The difference of the present paper is a fixed angle surface is obtained with respect to any direction and some characterizations are given in three-dimensional Minkowski space. This constant angle surface is the developable ruled surface whose direction is the spherical circle in Minkowski space. Also, by the definition of isophote curves, the curves on this surface are isophote curves. These curves have applications in many fields. At the beginning of these is optics, which is its application in physics. There are many studies that bring together the optics branch of physics and the geometry branch of mathematics [20–24]. This study is one of them. Based on that, we can say that when we beam from a light source in a constant direction, the intensity of the light will be the same at every point on this constant angle surface. On the other hand, the singularity of the ruled surfaces has been studied by many authors. We also investigate the singularity types of this special surface. Finally, as an application, we give some illustrated examples which support the theory of the paper.

2. Preliminaries

Let $\mathbb{E}_1^3 = (\mathbb{R}^3, \langle,\rangle_L)$ be Minkowski 3−space which is given with the Lorentzian metric as follows

$$\begin{array}{rcl} \langle,\rangle_L & = & \mathbb{R}^3 \times \mathbb{R}^3 \to \mathbb{R} \\ (u,v) & \to & \langle u,v\rangle_L = u_1v_1 + u_2v_2 - u_3v_3, \end{array}$$

where $u = (u_1,u_2,u_3)$ and $v = (v_1,v_2,v_3)$ are general coordinates $\mathbb{E}_1^3$. In that case semi-Riemannian metric, an ordinary vector $u \in \mathbb{E}_1^3$ so-called spacelike if $\langle u,u\rangle_L > 0$ or $u = 0$, timelike if $\langle u,u\rangle_L < 0$ and null (lightlike) if $\langle u,u\rangle_L = 0$ but $u \neq 0$. The norm of a vector u is given by $\|u\|_L = \sqrt{|\langle u,u\rangle_L|}$ [25]. Considering the concept of the Lorentz cross product $\times : \mathbb{E}_1^3 \times \mathbb{E}_1^3 \to \mathbb{E}_1^3$. For $u,v \in \mathbb{E}_1^3$, the vector $u \times v$ is defined as

$$u \times v = (u_2v_3 - u_3v_2, u_3v_1 - u_1v_3, u_2v_1 - u_1v_2).$$

Definition 2.1 ([25]). *Let u and v be two vectors in Minkowski 3-space.*

a. *Let u and v be two time-like vectors. If these vectors span a vector subspace, there is a unique real number $\theta \geq 0$ such that*

$$\langle u,v\rangle_L = \|u\|_L \|v\|_L cosh\theta.$$

b. *Let u and v be vectors. If these two space-like vectors span a vector subspace, there is a unique real number $\theta \geq 0$ such that*

$$\langle u,v\rangle_L = \|u\|_L \|v\|_L cos\theta.$$

Definition 2.2 ([25]). *Let u and v be space-like and time-like vectors in $\mathbb{E}_1^3$, respectively. Then, there is a unique non-negative real number $\theta \geq 0$ satisfying*

$$\langle u,v\rangle_L = \|u\|_L \|v\|_L sinh\theta.$$

Definition 2.3 ([25]). *Let u and v be in the same timecone of $\mathbb{E}_1^3$. In this case, there is a unique non-negative real number $\theta \geq 0$ as follows:*

$$\langle u,v\rangle_L = -\|u\|_L \|v\|_L cosh\theta.$$

Let timelike and spacelike curves be vectors with spacelike or timelike normal vectors, respectively. Such curves are called Frenet curves. In this case, the Frenet equations are given by

$$\begin{pmatrix} T'(s) \\ N'(s) \\ B'(s) \end{pmatrix} = \begin{pmatrix} 0 & \kappa(s) & 0 \\ -\delta\kappa(s) & 0 & \tau(s) \\ 0 & \varepsilon\tau(s) & 0 \end{pmatrix} \begin{pmatrix} T(s) \\ N(s) \\ B(s) \end{pmatrix},$$

where $\langle T,T\rangle_L = \varepsilon$ and $\langle N,N\rangle_L = \delta$ [27]. Let the position vector of the surface M in the standard form of Lorentz Minkowski space $\mathbb{E}_1^3$ is

$$\Phi(u,v) = (\Phi_1(u,v),\Phi_2(u,v),\Phi_3(u,v)).$$

Definition 2.4 ([28]). *Surfaces formed by the movement of a line along a curve in space are called ruled surfaces. The parameterization of the ruled surface for any two differentiable curves α and γ is*

$$\Phi(u,v) = \alpha(v) + u\gamma(v)$$

where $\alpha(v)$ is called base curve of the ruled surface and $\gamma(v)$ is a unit direction vector of an oriented line in $\mathbb{E}_1^3$.

Theorem 2.5 ([29, 30]). *Let M be a regular ruled surface with the parameterization $\Phi(u,v) = \alpha(v) + u\gamma(v)$. If the Gaussian curvature of the surface M is zero, the surface M is called a developable surface. Also, another characterization for developable ruled surfaces is that* $\det(\alpha'(v),\gamma(v),\gamma'(v)) = 0$.

Definition 2.6 ([31]). *For the surface $\Phi(u,v) = \alpha(v) + u\gamma(v)$, line of striction is given by*

$$\bar{\alpha}(v) = \alpha(v) - \frac{\langle \gamma(v)\times\gamma'(v), \gamma(v)\times\alpha'(v)\rangle}{\|\gamma(v)\times\gamma'(v)\|^2}\gamma(v).$$

3. Main Results

This section is based on the definition of a constant angle ruled surface in 3-dimensional Minkowski space. In this section, constant angle ruled surfaces are studied with the help of any given direction and these surfaces are characterized. According to the casual characters of the orthonormal vectors, the direction vectors of the constant angle ruled surface can be obtained in different ways in the 3-dimensional Minkowski space.

Case 1. Let $\vec{e}_3$ be a timelike vector. So, $\{\vec{e}_1,\vec{e}_2\}$ are spacelike vectors. The Lorentz circle with the help of these orthonormal vectors in this space is as follows

$$\alpha(v) = \cosh\theta(\cos v\vec{e}_1 + \sin v\vec{e}_2) + \sinh\theta(\vec{e}_1\times\vec{e}_2). \tag{3.1}$$

Examining the casual character of the defined above curve α, provides

$$\langle\alpha,\alpha\rangle = 1.$$

So, we can easily say that α is spacelike and $\alpha\in S_1^2$. We take the derivative of the equation (3.1) with respect to v

$$\alpha'(v) = \cosh\theta\,(-\sin v\vec{e}_1 + \cos v\vec{e}_2). \tag{3.2}$$

The norm of the equation (3.2) is

$$\left\|\alpha'(v)\right\| = \cosh\theta.$$

Hence, the unit tangent vector of $\alpha(v)$ is obtained as follows

$$T(v) = \frac{\alpha'(v)}{\|\alpha'(v)\|} = -\sin v\vec{e}_1 + \cos v\vec{e}_2.$$

Examining the casual character of the tangent vector, we can see that it is a spacelike vector as

$$\langle T,T\rangle = 1.$$

If we cross product the spacelike curve $\alpha(v)$ and the spacelike tangent vector $T(v)$, we get

$$S(v) = \alpha(v)\times T(v) = -\sinh\theta(\cos v\vec{e}_1 + \sin v\vec{e}_2) - \cosh\theta\vec{e}_3$$

and we obtain the casual character of S is a timelike vector as

$$\langle S,S\rangle = -1.$$

Thus, the Sabban frame $\{\alpha(v), T(v), S(v)\}$ is obtained on S_1^2. If the necessary calculations are made, the derivative change of the frame is found

$$\frac{d}{dv}\begin{bmatrix} \alpha(v) \\ T(v) \\ S(v) \end{bmatrix} = \begin{bmatrix} 0 & \cosh\theta & 0 \\ -\cosh\theta & 0 & -\sinh\theta \\ 0 & -\sinh\theta & 0 \end{bmatrix} \begin{bmatrix} \alpha(v) \\ T(v) \\ S(v) \end{bmatrix}.$$

In addition, the Darboux vector of the Lorenz circle $\alpha(v)$ is a vector that determines the constant direction as

$$\omega = \sinh\theta\,\alpha(v) + \cosh\theta\, S(v).$$

In fact, if the necessary calculations are made here, it is easily seen that

$$\omega = (\vec{e}_1 \times \vec{e}_2) = -\vec{e}_3.$$

Theorem 3.1. *Let $\vec{e}_3$ be timelike and $\{\vec{e}_1, \vec{e}_2\}$ be spacelike vectors in 3−dimensional Minkowski space. The spacelike Lorentz circle on S_1^2 with the help of the orthonormal vectors in this space is*

$$\alpha(v) = \cosh\theta(\cos v\vec{e}_1 + \sin v\vec{e}_2) + \sinh\theta\vec{e}_3, \quad \theta \neq 0.$$

The surface defined below is a spacelike ruled surface

$$\Phi(u,v) \quad \rightarrow \quad \Phi(u,v) = \int_0^v [f(v)\alpha(v) + g(v)\alpha'(v)]\,dv + u\alpha(v) \tag{3.3}$$

and $S(v) = \alpha(v) \times T(v)$ is the timelike unit normal to ruled surface where f and g are the differentiable functions.

Proof. Considering the definition of ruled surfaces,

$$\int_0^v \left[f(v)\alpha(v) + g(v)\alpha'(v)\right] dv$$

is defined as the ruled surface directrix (also called the base curve) and the vector $\alpha(v)$ is defined as the direction vector of the surface. So, we can easily see that the surface $\Phi(u,v)$ is a ruled surface in 3−dimensional Minkowski space. To find the normal of the surface, we calculate the parameter curves of the surface

$$N = \frac{\Phi_u \times \Phi_v}{\|\Phi_u \times \Phi_v\|}.$$

If the derivatives of equation (3.3) are taken with respect to u and v, respectively, one immediately has

$$\Phi_u = (\cosh\theta\cos v, \cosh\theta\sin v, \sinh\theta)$$

and

$$\Phi_v = (f(v)\cosh\theta\cos v - (g(v)+u)\cosh\theta\sin v, f(v)\cosh\theta\sin v + (g(v)+u)\cosh\theta\cos v, f(v)\sinh\theta).$$

If the following calculations are made to find the normal of the surface, we obtain

$$\Phi_u \times \Phi_v = (-(g(v)+u)\cosh\theta\sinh\theta\cos v, -(g(v)+u)\cosh\theta\sinh\theta\sin v, -(g(v)+u)\cosh^2\theta)$$

and

$$\|\Phi_u \times \Phi_v\| = (g(v)+u)\cosh\theta.$$

Therefore, we can easily find the normal of the surface as follows:

$$N = (-\sinh\theta\cos v, -\sinh\theta\sin v, -\cosh\theta). \tag{3.4}$$

If necessary arrangements are made in equation (3.4), it can be seen that

$$\begin{aligned} N &= -\sinh\theta\,(\cos v\vec{e}_1 + \sin v\vec{e}_2) - \cosh\theta\vec{e}_3, \\ N &= S. \end{aligned}$$

Thus, we can say that $S(v)$ is the unit normal vector to the ruled surface $\Phi(u,v)$. If the casual character of the normal vector is computed here, one has

$$\langle N, N\rangle = -1.$$

Hence, the ruled surface $\Phi(u,v)$ is a spacelike surface.

□

Corollary 3.2. *Let $\vec{e}_3$ be timelike and $\{\vec{e}_1,\vec{e}_2\}$ be spacelike vectors in 3−dimensional Minkowski space. Suppose that the normal of the spacelike surface $\Phi(u,v)$ is N and $\omega=(\vec{e}_1\times\vec{e}_2)=-\vec{e}_3$ is the axis of the constant direction. Then, the surface $\Phi(u,v)$ is a spacelike constant angle ruled surface.*

Proof. Let the normal of the spacelike surface $\Phi(u,v)$ be N and $\omega=(\vec{e}_1\times\vec{e}_2)=-\vec{e}_3$ be the axis of the constant direction. Considering equation (3.4) and ω axis of the constant direction, we can write that

$$\langle N,\omega\rangle=-\cosh\theta=\text{constant}.$$

So, we can say that the surface $\Phi(u,v)$ is a spacelike constant angle ruled surface. □

Corollary 3.3. *The surface $\Phi(u,v)$ is a developable spacelike ruled surface.*

Proof. If we restate the base curve of the surface $\Phi(u,v)$ as

$$\varphi=\int_0^v\left[f(v)\alpha(v)+g(v)\alpha'(v)\right]dv,$$

and use the developable ruled surface condition, we obtain that

$$\det\left(\varphi'(v),\alpha(v),\alpha'(v)\right)=\det\left(f(v)\alpha(v)+g(v)\alpha'(v),\alpha(v),\alpha'(v)\right).$$

If necessary calculations are made, it can be easily seen that this determinant value is zero. So, we can say that $\Phi(u,v)$ is a spacelike developable ruled surface. □

Corollary 3.4. *The line of striction of the spacelike surface $\Phi(u,v)$ is*

$$\bar{\varphi}=\varphi+g(v)\alpha(v)$$

where $\varphi=\int_0^v\left[f(v)\alpha(v)+g(v)\alpha'(v)\right]dv$.

Proof. The line of striction of the surface is computed as follows

$$\bar{\varphi}=\varphi-\frac{\langle\alpha(v)\times\alpha'(v),\alpha(v)\times\varphi'(v)\rangle}{\|\alpha(v)\times\alpha'(v)\|^2}\alpha(v). \tag{3.5}$$

If the necessary calculations are made in equation (3.5), we find

$$\begin{aligned}\alpha(v)\times\alpha'(v) &= \left(-\sinh\theta\cosh\theta\cos v,-\sinh\theta\cosh\theta\sin v,\cosh^2\theta\right),\\ \alpha(v)\times\varphi'(v) &= \left(-g(v)\cosh\theta\sinh\theta\cos v,-g(v)\cosh\theta\sinh\theta\sin v,g(v)\cosh^2\theta\right).\end{aligned}$$

If the above equations are substituted in equation (3.5), the line of striction is obtained as

$$\begin{aligned}\bar{\varphi} &= \varphi+\frac{g(v)\cosh^2\theta}{\cosh^2\theta}\alpha(v),\\ \bar{\varphi} &= \varphi+g(v)\alpha(v).\end{aligned}$$

□

Corollary 3.5. *Considering the theory in the study, we can say that when we are given any axis, we can create a constant angle surface with the help of this axis. For example, we examine the problem of creating a constant angle ruled surface with axis $k=-\vec{e}_3$. To find the Lorentz circle $\alpha(v)$, the circle whose normal is $k=-\vec{e}_3$ must be written. This is found by writing the intersection curve of the light cone and the plane with $-\vec{e}_3$ normal. Let the $\{\vec{e}_1,\vec{e}_2\}$ be an orthonormal frame obtained in the plane whose normal is $-\vec{e}_3$. In this case, the intersection curve of the light cone and the plane is as follows*

$$\cos v\vec{e}_1+\sin v\vec{e}_2.$$

This curve is the Lorentz circle with radius $r=\cosh\theta$ given by

$$\alpha(v)=\cosh\theta\cos v\vec{e}_1+\cosh\theta\sin v\vec{e}_2+\sinh\theta\vec{e}_3.$$

The surface

$$\Phi(u,v)=\int_0^v\left[f(v)\alpha(v)+g(v)\alpha'(v)\right]dv+u\alpha(v)$$

obtained by this circle $\alpha(v)$ is a constant hyperbolic angle ruled surface with the axis $k=-\vec{e}_3$. The normal to this surface is

$$N=(-\sinh\theta\cos v,-\sinh\theta\sin v,-\cosh\theta)$$

and $\langle N,\vec{e}_3\rangle=-\cosh\theta$. According to the state of the θ hyperbolic angle, the angle that the surface makes with the axis is determined. Also, when the functions f and g are changed, they change on the constant angle surfaces.

Theorem 3.6. *Let $\Phi: I\times J\to\mathbb{E}^3$, $\Phi(u,v)=\int_0^v[f(v)\alpha(v)+g(v)\alpha'(v)]\,dv+u\alpha(v)$ be a spacelike constant angle ruled surface and $f,g: I\to\mathbb{R}$ be smooth functions with*

$$\frac{d}{dv}\left(\int_0^v\left[f(v)\alpha(v)+g(v)\alpha'(v)\right]dv\right)=f(v)\alpha(v)+g(v)\alpha'(v).$$

Also, let $(u_0,v_0)\in I\times J$ be a singular point of $\Phi(u,v)$ and put

$$x_0=\int_0^v\left[f(v_0)\alpha(v_0)+g(v_0)\alpha'(v_0)\right]dv+u_0\alpha(v_0)=\Phi(u_0,v_0).$$

The germ of $\Phi(u,v)$ at x_0 is locally diffeomorphic to $C\times\mathbb{R}$ and SW. Also, the germ of $\Phi(u,v)$ at x_0 isn't locally diffeomorphic to CCR.

Proof. Let $\Phi: I\times J\to\mathbb{E}^3$ be a spacelike constant angle ruled surface and $f,g: I\to\mathbb{R}$ be smooth functions. Considering the theory in [32,33], we calculated that

$$\det\left(\alpha(v),\alpha'(v),\alpha''(v)\right)=\sinh\theta\cosh^2\theta.$$

1. For $\theta\neq 0$ $(\theta\neq\frac{\pi}{2},\pi,\ldots)$, $\det(\alpha(v),\alpha'(v),\alpha''(v))\neq 0$. Then,
   a. Since $u_0=g(v_0)$ and $f(v_0)\neq g'(v_0)$, the germ of $\Phi(u,v)$ at x_0 is locally diffeomorphic to $C\times\mathbb{R}$.
   b. Since $u_0=g(v_0)$, $f(v_0)=g'(v_0)$ and $f'(v_0)\neq g''(v_0)$ the germ of $\Phi(u,v)$ at x_0 is locally diffeomorphic to SW.
2. For $\theta=0$ $\left(\theta=\frac{\pi}{2},\pi,\ldots\right)$, $\det(\alpha(v),\alpha'(v),\alpha''(v))=0$. Then, although $u_0=g(v_0)$, $f(v_0)\neq g'(v_0)$, $\det\left(\alpha(v),\alpha'(v),\alpha^{(3)}(v)\right)=0$. Hence, the germ of $\Phi(u,v)$ at x_0 isn't locally diffeomorphic to CCR.

□

Case 2. Let $\vec{e}_3$ be a timelike vector and $\{\vec{e}_1,\vec{e}_2\}$ be spacelike vectors. The Lorentz circle with the help of these orthonormal vectors in this space is

$$\alpha(v)=\sinh\theta(\cos v\vec{e}_1+\sin v\vec{e}_2)+\cosh\theta(\vec{e}_1\times\vec{e}_2). \tag{3.6}$$

If we examine the casual character of the defined above curve α, we get

$$\langle\alpha,\alpha\rangle=-1.$$

So, we can easily say that α is a timelike vector and $\alpha\in H_0^2$. If we take the derivative of the equation (3.6) with respect to v, we have

$$\alpha'(v)=\sinh\theta(-\sin v\vec{e}_1+\cos v\vec{e}_2). \tag{3.7}$$

The norm of the equation (3.7) is

$$\left\|\alpha'(v)\right\|=\sinh\theta.$$

Thus, the unit tangent vector of $\alpha(v)$ is obtained as follows

$$T(v)=\frac{\alpha'(v)}{\|\alpha'(v)\|}=-\sin v\vec{e}_1+\cos v\vec{e}_2.$$

Examining the casual character of the tangent vector, yields

$$\langle T,T\rangle=1.$$

Taking cross product the timelike curve $\alpha(v)$ and the spacelike tangent vector $T(v)$, provides

$$S(v) = \alpha(v) \times T(v) = \cosh\theta(\cos v\vec{e}_1 + \sin v\vec{e}_2) - \sinh\theta\vec{e}_3$$

and we obtain the casual character of S is spacelike as

$$\langle S, S\rangle = 1.$$

Hence, the Sabban frame $\{\alpha(v), T(v), S(v)\}$ is obtained on H_0^2. Moreover, the Darboux vector of the $\alpha(v)$ is the vector that determines the constant direction as

$$\omega = \cosh\theta\,\alpha(v) + \sinh\theta S(v).$$

If the necessary calculations are made here, we can easily see the timelike Darboux vector as

$$\langle \omega, \omega\rangle = -1.$$

With the same method as above, theorems and corollaries given in Case 1 can also be given for this case and other cases.

Case 3. Let $\vec{e}_3$ and $\vec{e}_1$ be a spacelike vectors and $\vec{e}_2$ be timelike vector. With the help of these orthonormal vectors, we get the Lorentz circle as

$$\alpha(v) = \cos\theta(\cosh v\vec{e}_1 + \sinh v\vec{e}_2) + \sin\theta(\vec{e}_1 \times \vec{e}_2). \tag{3.8}$$

Examining the casual character of the curve α, we get it as spacelike

$$\langle \alpha, \alpha\rangle = 1.$$

Taking the derivative of the equation (3.8) with respect to v, gives

$$\alpha'(v) = \cos\theta(\sinh v\vec{e}_1 + \cosh v\vec{e}_2).$$

The unit tangent vector of $\alpha(v)$ is obtained

$$T(v) = \sinh v\vec{e}_1 + \cosh v\vec{e}_2.$$

If we examine the casual character of the tangent vector, we have that it is a timelike vector. If we cross product the spacelike curve $\alpha(v)$ and the timelike tangent vector $T(v)$, one has

$$S(v) = \sin\theta(-\cosh v\vec{e}_1 + \sinh v\vec{e}_2) - \cos\theta\vec{e}_3$$

and we obtain the casual character of S vector is spacelike. Thus, the Sabban frame $\{\alpha(v), T(v), S(v)\}$ is obtained on S_1^2. So, from here we can say that if S and $\vec{e}_3$ span the spacelike sub-vector space, there is a single non-negative real number $\theta \geq 0$ such that $\langle S, \vec{e}_3\rangle = \cos\theta$.

Case 4. Let $\vec{e}_3$ and $\vec{e}_2$ be a spacelike vectors and $\vec{e}_1$ be timelike vector. Then the Lorentz circle is

$$\alpha(v) = \cos\theta(\sinh v\vec{e}_1 + \cosh v\vec{e}_2) + \sin\theta(\vec{e}_1 \times \vec{e}_2).$$

If we examine the casual character of the defined above α curve, we get it spacelike. The unit tangent vector of $\alpha(v)$ is obtained as follows

$$T(v) = \cosh v\vec{e}_1 + \sinh v\vec{e}_2.$$

If we cross product the spacelike curve $\alpha(v)$ and the timelike tangent vector $T(v)$, we get

$$S(v) = \sin\theta(-\sinh v\vec{e}_1 + \cosh v\vec{e}_2) - \cos\theta\vec{e}_3$$

and we obtain the casual character of S vector is spacelike. Thus, the Sabban frame $\{\alpha(v), T(v), S(v)\}$ is obtained on S_1^2. So, from here we can say that if S and $\vec{e}_3$ span the spacelike sub-vector space, there is a single non-negative real number $\theta \geq 0$ such that $\langle S, \vec{e}_3\rangle = \cos\theta$.
Given any direction, the equations and figures of the associated constant angle surfaces are discussed in the examples below.

Example 3.7. *We consider the equation of the constant angle surface with the axis*

$$k=\vec{e}_3=\left(\frac{1}{\sqrt{2}},\frac{1}{\sqrt{2}},\frac{2}{\sqrt{2}}\right)$$

and draw its graph.

$$\vec{e}_1=(1,1,1),\quad \vec{e}_2=\left(\frac{1}{\sqrt{2}},-\frac{1}{\sqrt{2}},0\right).$$

Note that $\vec{e}_3$ is a timelike vector, $\vec{e}_1$ is a spacelike vector, and $\vec{e}_2$ is a spacelike vector and $\vec{e}_1,\vec{e}_2,\vec{e}_3$ are the orthonormal vectors. Then, for $\theta=\ln 2$ the spherical circle $\alpha(v)$ is obtained as follows

$$\alpha(v)=\left(\frac{5}{4}\cos v+\frac{5}{4\sqrt{2}}\sin v-\frac{3}{4\sqrt{2}},\frac{5}{4}\cos v-\frac{5}{4\sqrt{2}}\sin v-\frac{3}{4\sqrt{2}},\frac{5}{4}\cos v-\frac{6}{4\sqrt{2}}\right).$$

For the functions $f(v)=\sin v$ and $g(v)=\cos v$, if the necessary calculations are made in equation (3.3), the equation of the spacelike constant angle ruled surface can be easily written as

$$\Phi(u,v)=(\Phi_1,\Phi_2,\Phi_3)$$

where

$$\begin{aligned}
\Phi_1(u,v) &= \frac{5v+3\cos v}{4\sqrt{2}}+\frac{5}{4}u\cos v+\frac{5}{4\sqrt{2}}u\sin v-\frac{3}{4\sqrt{2}}u,\\
\Phi_2(u,v) &= -\frac{5v-3\cos v}{4\sqrt{2}}+\frac{5}{4}u\cos v-\frac{5}{4\sqrt{2}}u\sin v-\frac{3}{4\sqrt{2}}u,\\
\Phi_3(u,v) &= \frac{3\cos v}{2\sqrt{2}}+\frac{5}{4}u\cos v-\frac{6}{4\sqrt{2}}u.
\end{aligned}$$

If we calculate the singular points for this surface according to Theorem 3.6, we can write that

$$\det\left(\alpha(v),\alpha'(v),\alpha''(v)\right)\neq 0 \quad for \quad \theta\neq 0\ \left(\theta\neq\frac{\pi}{2},\pi,\ldots\right).$$

a. For $f(v_0)=\sin v_0$, $g'(v_0)=-\sin v_0$,

$$\sin v_0\neq-\sin v_0$$

and

$$v_0\neq 0,\pi,2\pi,3\pi,\ldots,k\pi \quad for \quad k\in\mathbb{Z}.$$

Since $u_0=g(v_0)$, we can say that all points as (u_0,v_0) of $\Phi(u,v)$ satisfying the following condition are locally diffeomorphic to $C\times\mathbb{R}$

$$u_0=\cos v_0 \quad for \quad v_0\neq 0,\pi,2\pi,3\pi,\ldots,k\pi \quad for \quad k\in\mathbb{Z}.$$

b. For $f'(v)=\cos v$, $g'(v)=-\sin v$, $g''(v)=-\cos v$,

$$\begin{aligned}
f(v_0) &= \sin v,\\
g'(v_0) &= -\sin v.
\end{aligned}$$

From the equality of the above equations, we obtain that

$$v_0=0,\pi,2\pi,3\pi,\ldots,k\pi \quad for \quad k\in\mathbb{Z}.$$

Considering the following equations,

$$\begin{aligned}
f'(v_0) &= \cos v,\\
g''(v_0) &= -\cos v,
\end{aligned}$$

we have

$$f'(v_0)\neq g''(v_0) \quad for \quad v_0\neq\frac{\pi}{2},\frac{3\pi}{2},\frac{5\pi}{2},\ldots,\frac{k\pi}{2} \quad for \quad k=2n+1,\quad n\in\mathbb{Z}.$$

We obtain the other singular point as follows

$$u_0=g(v_0)=g\left(\frac{k\pi}{2}\right)=0 \quad for \quad k=2n+1,\quad n\in\mathbb{Z}.$$

So, the point $\Phi(u_0,v_0)=\Phi\left(0,\frac{k\pi}{2}\right)$ is locally diffeomorphic to SW. Also, according to Theorem 3.6, we know that the germ of $\Phi(u,v)$ isn't locally diffeomorphic to CCR. So, we give the figure of the spacelike constant angle ruled surface in Figure 3.1 as,

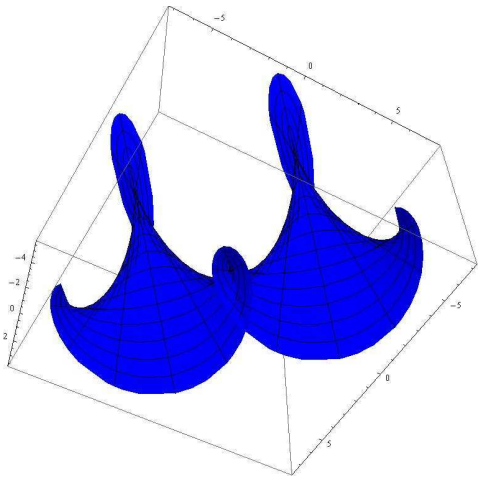

Figure 3.1: Spacelike constant angle ruled surface for $\ln 2$

Example 3.8. *We consider the equation of the constant angle surface with the axis*

$$k = \vec{e}_3 = \left(\frac{\sqrt{3}}{2}, \frac{\sqrt{3}}{3}, \frac{\sqrt{3}}{6} \right)$$

and

$$\vec{e}_1 = \left(\frac{2}{\sqrt{131}}, \frac{3}{\sqrt{131}}, \frac{12}{\sqrt{131}} \right), \quad \vec{e}_2 = \left(-\frac{7\sqrt{3}}{2\sqrt{131}}, \frac{17\sqrt{3}}{3\sqrt{131}}, \frac{5\sqrt{3}}{6\sqrt{131}} \right).$$

Note that $\vec{e}_3$ is a spacelike vector, $\vec{e}_1$ is a timelike vector, $\vec{e}_2$ is a spacelike vector and $\vec{e}_1, \vec{e}_2, \vec{e}_3$ are the orthonormal vectors. In this case, for $\theta = \frac{\Pi}{4}$ the spherical circle $\alpha(v)$ is obtained as follows

$$\alpha(v) = \left(\frac{2\sinh v}{\sqrt{262}} - \frac{7\sqrt{3}\cosh v}{2\sqrt{262}} + \frac{\sqrt{3}}{2\sqrt{2}}, \frac{3\sinh v}{\sqrt{262}} + \frac{17\sqrt{3}\cosh v}{3\sqrt{262}} + \frac{\sqrt{3}}{3\sqrt{2}}, \frac{12\sinh v}{\sqrt{262}} + \frac{5\sqrt{3}\cosh v}{6\sqrt{262}} + \frac{\sqrt{3}}{6\sqrt{2}} \right).$$

For the functions $f(v) = \cosh v$ and $g(v) = \sinh v$, if the necessary calculations are made, the equation of the timelike constant angle ruled surface can be written as

$$\Phi(u,v) = (\Phi_1, \Phi_2, \Phi_3)$$

where

$$\begin{aligned}
\Phi_1(u,v) &= \frac{1}{524}\left(2\sqrt{262}\cosh 2v + 131\sqrt{6}\sinh v - 7\sqrt{\frac{393}{2}}\sinh 2v \right) + \frac{2u\sinh v}{\sqrt{262}} - \frac{7\sqrt{3}u\cosh v}{2\sqrt{262}} + \frac{\sqrt{3}u}{2\sqrt{2}}, \\
\Phi_2(u,v) &= \frac{3\cosh 2v}{2\sqrt{262}} + \frac{\sinh v}{\sqrt{6}} + \frac{17\sinh 2v}{2\sqrt{786}} + \frac{3u\sinh v}{\sqrt{262}} + \frac{17\sqrt{3}u\cosh v}{3\sqrt{262}} + \frac{\sqrt{3}u}{3\sqrt{2}}, \\
\Phi_3(u,v) &= 3\sqrt{\frac{2}{131}}\cosh 2v + \frac{\sinh v}{2\sqrt{6}} + \frac{5\sinh 2v}{4\sqrt{786}} + \frac{12u\sinh v}{\sqrt{262}} + \frac{5\sqrt{3}u\cosh v}{6\sqrt{262}} + \frac{\sqrt{3}u}{6\sqrt{2}}.
\end{aligned}$$

So, we give the figure of the timelike constant angle ruled surface for $\theta = \frac{\Pi}{4}$ in Figure 3.2 as,

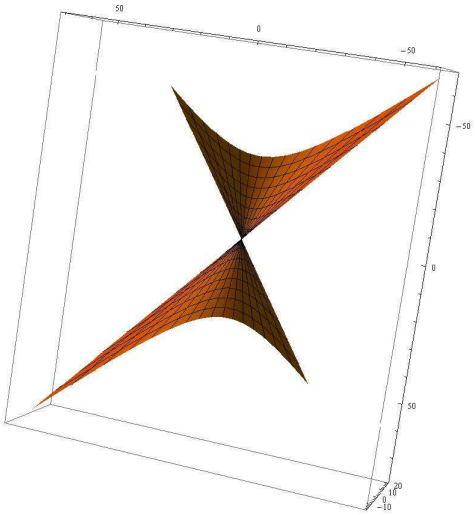

Figure 3.2: Timelike constant angle ruled surface for $\theta = \frac{\Pi}{4}$

4. Conclusion

In this paper, constant angle surfaces with respect to any direction are obtained and their characterizations are given in $\mathbb{E}_1^3$. The constant angle surface mentioned here is the developable ruled surface whose direction is the spherical circle in Minkowski space. It is also clear that the curves on this surface are isophote curves. This curve has many applications in physics, especially optics. Finally, the topics discussed in this article are expressed with some illustrated examples to support the theory of the article.

Article Information

Acknowledgements: The authors would like to express their sincere thanks to the editor and the anonymous reviewers for their helpful comments and suggestions.

Author's Contributions: All authors contributed equally to the writing of this paper. All authors read and approved the final manuscript.

Conflict of Interest Disclosure: No potential conflict of interest was declared by the author.

Supporting/Supporting Organizations: No grants were received from any public, private or non-profit organizations for this research.

Ethical Approval and Participant Consent: It is declared that during the preparation process of this study, scientific and ethical principles were followed and all the studies benefited from are stated in the bibliography.

Plagiarism Statement: This article was scanned by the plagiarism program. No plagiarism was detected.

Availability of Data and Materials: Not applicable.

References

[1] P. Cermelli, A. J. Di Scala, *Constant angle surfaces in liquid crystals*, Philos. Mag., **87** (2007), 1871-1888.
[2] M. I. Munteanu, A. I. Nistor, *A new approach on constant angle surfaces in* $\mathbb{E}^3$, Turkish J. Math., **33**(2) (2009), 1-10.
[3] A. I. Nistor, *Certain constant angle surfaces constructed on curves*, Int. Electron. J. Geom., **4** (2011), 79-87.
[4] S. Özkaldı, Y. Yaylı, *Constant angle surfaces and curves in* $\mathbb{E}^3$, Int. Electron. J. Geom., **4**(1) (2011), 70-78.
[5] A. T. Ali, *A constant angle ruled surfaces*, Int. Electron. J. Geom., **7**(1) (2018), 69-80.
[6] C. Y. Li, C. G. Zhu, *Construction of the spacelike constant angle surface family in Minkowski* $3-$*space*, AIMS Math., **5**(6) (2020), 6341-6354.
[7] S. Özkaldı Karakuş, *Certain constant angle surfaces constructed on curves in Minkowski* $3-$*space*, Int. Electron. J. Geom., **11**(1) (2018), 37-47.
[8] R. López, M. I. Munteanu, *Constant angle surfaces in Minkowski space*, Bull. Belg. Math. Soc. Simon Stevin, **18**(2) (2011), 271-286.
[9] A. T. Ali, *Non-lightlike constant angle ruled surfaces in Minkowski 3-space*, J. Geom. Phys., **157** (2020), 103833.
[10] F. Güler, G. Şaffak, E. Kasap, *Timelike constant angle surfaces in Minkowski space* R_1^3, Int. J. Contemp. Math. Sciences, **6**(44) (2011), 2189-2200.

[11] G. U. Kaymanlı, C. Ekici, Y. Ünlütürk, *Constant angle ruled surfaces due to the Bishop frame in Minkowski* $3-$*space*, J. Sci. Arts, **22**(1) (2022), 105-114.

[12] F. Dillen, J. Fastenakels, J. Van de Veken, L. Vrancken, *Constant angle surfaces in* $\mathbb{S}^2 \times \mathbb{R}$, Monatsh. Math., **152** (2007), 89-96.

[13] S. Özkaldı Karakuş, *Quaternionic approach on constant angle surfaces in* $\mathbb{S}^2 \times \mathbb{R}$, Appl. Math. E-Notes, **19** (2019), 497-506.

[14] F. Dillen, M. I. Munteanu, *Constant angle surfaces in* $\mathbb{H}^2 \times \mathbb{R}$, Bull. Braz. Math. Soc., **40** (2009), 85-97.

[15] J. Fastenakels, M. I. Munteanu, J. Van Der Veken, *Constant angle surfaces in the Heisenberg group*, Acta Math. Sin. (Engl. Ser.), **27**(4) (2011), 747-756.

[16] I. I. Onnis, P. Piu, *Constant angle surfaces in the Lorentzian Heisenberg group*, Arch. Math., **109** (2017), 575-589.

[17] F. Doğan, Y. Yayli, *On isophote curves and their characterizations*, Turkish J. Math., **39**(5) (2015), 650-664.

[18] C. E. Ordoñez, E. Blotta, J. I. Pastore, *Isophote based low computing power eye detection embedded system*, IEEE Latin America Transactions, **18**(02) (2020), 336-343.

[19] S. Datta, N. Chaki, B. Modak, *A novel technique to detect caries lesion using isophote concepts*, IRBM, **40**(3) (2019), 174-182.

[20] T. Körpınar, R. C. Demirkol, Z. Körpınar, *Polarization of propagated light with optical solitons along the fiber in de-sitter space* S_1^2, Optik-International Journal for Light and Electron Optics, **226** (2021), 165872.

[21] T. Körpinar, R. C. Demirkol, *Electromagnetic curves of the linearly polarized light wave along an optical fiber in a 3D Riemannian manifold with Bishop equations*, Optik, **200** (2020), 163334.

[22] Z. Özdemir, *A new calculus for the treatment of Rytov's law in the optical fiber*, Optik, **216** (2020), 164892.

[23] B. Yılmaz, *A new type electromagnetic curves in optical fiber and rotation of the polarization plane using fractional calculus*, Optik, **247** (2021), 168026.

[24] Z. Özdemir, F. N. Ekmekçi, *Electromagnetic curves and Rytov curves based on the hyperbolic split quaternion algebra*, Optik, **251** (2022), 168359.

[25] B. O'neill, *Semi-Riemannian Geometry with Applications to Relativity*, Academic press, Los Angeles, 1983.

[26] D. J. Struik, *Lectures on Classical Differential Geometry*, Addison-Wesley Publishing, New York, 1961.

[27] R. López, *Differential geometry of curves and surfaces in Lorentz-Minkowski space*, Int. Electron. J. Geom., **7**(1) (2014), 44-107.

[28] H. H. Hacısalihoğlu, *Diferensiyel Geometri*, İnonu University, Faculty of Arts and Sciences Publications, Malatya, 1983.

[29] A. Sabuncuoğlu, *Diferensiyel Geometri*, Nobel Publications, Ankara, 2004.

[30] M. P. Do Carmo, *Differential Geometry of Curves and Surfaces, Prentice-Hall*, Englewood Cliffs., New Jersey, 1976.

[31] M. Özdemir, *Diferansiyel Geometri*, Altı Nokta Publications, İzmir, 2020.

[32] S. Izumiya, *Generating families of developable surfaces in* $\mathbb{R}^3$, Hokkaido Univ. Pre. Series in Mathematics, **512** (2001), 1-18.

[33] S. Izumiya, N. Takeuchi, *Singularities of ruled surfaces in* $\mathbb{R}^3$, In Mathematical Proceedings of the Cambridge Philosophical Society, Cambridge University Press, **130**(1) (2001), 1-11.

Fundamental Journal of Mathematics and Applications, 6 (2) (2023) 89-100
Research Article

Fundamental Journal of Mathematics and Applications

Journal Homepage: www.dergipark.org.tr/en/pub/fujma
ISSN: 2645-8845
doi: https://dx.doi.org/10.33401/fujma.1163741

Flux Surfaces According to Killing Magnetic Vectors in Riemannian Space $\mathbb{S}ol3$

Norelhouda Benmansour[1] **and Fouzi Hathout**[2*]

[1]*Master's student in Department of Mathematics, Faculty of Sciences, Saida University, 20000 Saida, Algeria*
[2]*Department of Mathematics, Faculty of Sciences, Saida University, 20000 Saida, Algeria*
[*]*Corresponding author*

Article Info

Keywords: *Flux, Flux surface, Killing magnetic, Scalar flux function, $\mathbb{S}ol3$ manifold*
2010 AMS: *53A35, 53C21, 37C10*
Received: *16 September 2023*
Accepted: *30 April 2023*
Available online: *19 May 2023*

Abstract

In this paper, we define flux surface as surfaces in which its normal vector is orthogonal to the vector corresponding to a flux with its associate scalar flux functions in ambient manifold M. Next, we determine, in 3-dimensional homogenous Riemannian manifold $\mathbb{S}ol3$, the parametric flux surfaces according to the flux corresponding to the Killing magnetic vectors and we calculate its associate scalar flux functions. Finally, examples of such surfaces are presented with their graphical representation in Euclidean space.

1. Introduction

An effect, which passes or moves through a surface or substance, is called a flux or flow. It has many applications that we can cited a fluid mechanics, thermodynamics, electromagnetism, radiation, energy and in particular particle flux. Surfaces that do not disturb the flux are called flux surface, it plays an important role in physics, particulary the magnetism, and geometry (see [1–5] and [6–10]).
Geometrically, let $\mathbb{M}$ be a smooth surface in Riemannian manifold $(\mathbb{N}, g)$, $\overrightarrow{\mathbf{n}}$ is the normal vector and $\overrightarrow{V}$ is a smooth vector field on $\mathbb{N}$. The flux $\mathscr{F}$ corresponding to the smooth vector $\overrightarrow{V}$, (to simplify, we denote the vectors $\overrightarrow{V}$, $\overrightarrow{\mathbf{n}}$ by $V, \mathbf{n}$) passing through the surface $\mathbb{M}$ is given by

$$\mathscr{F} = \int_{\mathbb{M}} g(V, \mathbf{n}) ds.$$

The smooth surface $\mathbb{M}$ is called a *flux surface* of a smooth vector field V if

$$g(V, \mathbf{n}) = 0$$

everywhere on $\mathbb{M}$. We denoted $\mathbb{M}$ by *V-flux surface* (see Figure 1.1).

Email addresses and ORCID numbers: benmansournorelhouda97@gmail.com, 0000-0002-6774-5256 (N. Benmansour), f.hathout@gmail.com & fouzi.hathout@univ-saida.dz, 0000-0001-5278-5944 (F. Hathout)
Cite as: N. Benmansour, F. Hathout, *Flux surfaces according to Killing magnetic vectors in Riemannian space* $\mathbb{S}ol3$, Fundam. J. Math. Appl., 6(2) (2023), 89-100.

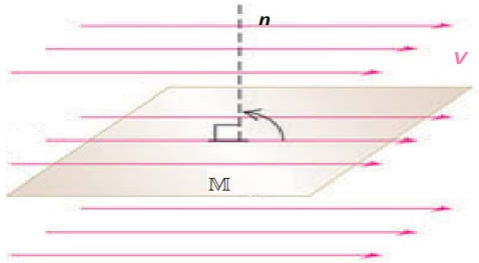

Figure 1.1: Flux surface $\mathbb{M}$ for linear flux in $(\mathbb{R}^3, g_{euc})$

When V is magnetic vector fields which is zero divergence according to Biot and Savart's law ([11]), V does not cross the surface $\mathbb{M}$ anywhere, i.e. the magnetic flux traversing $\mathbb{M}$ is zero, then $\mathbb{M}$ is called flux surface corresponding to the magnetic vector V. In this case $\mathbb{M}$ is denoted by *Magnetic V-flux surface.*
Hence, we can define a scalar flux function f according to the *magnetic vector* V, such that its value is constant on the surface $\mathbb{M}$, and

$$g(V, \nabla f) = 0$$

where ∇f is Riemannian gradient on $\mathbb{M}$.
Moreover, If V is a Killing i.e. magnetic vector fields satisfying the Killing equation

$$g(\nabla_X V, Y) + g(\nabla_Y V, X) = 0 \tag{1.1}$$

then $\mathbb{M}$ is called *Killing magnetic V-flux surface, where* ∇ is a connection and X, Y are a vector fields on $\mathbb{M}$.
The plasma is an example of flux surfaces. Considered as fourth state of matter, it is a hot ionized gas made up of approximately equal numbers of positively charged ions and negatively charged electrons which makes it a good electrical conductor. The electrical conductivity creates currents flowing in a plasma that interact with magnetic fields to produce the forces necessary for containment. Ordinary matter ionizes and forms a plasma at temperatures above about 5000 K, and most of the visible matter in the universe is in the plasma state (see for more detail [1, 5, 10–12]).
In magnetic confinement fusion, a flux surface is a surface on which magnetic field lines lie. Poincare-Hopf prove that such surfaces must be either a torus, or a knot (see [13]). Another applications of a flux surfaces, in Minkowski context, on the dynamics of solitons and dispersive effects can be found in ([6–8]).
In [2] and [9], the Killing V-magnetic flux surfaces was determined in Heisenberg three group and in Euclidean space, respectively. In our study, we determine all Killing V-magnetic flux surfaces and its associate Killing scalar flux functions in three-dimensional Riemannian manifold $\mathbb{S}ol3$ which is among the eight models of the geometry of Thurston ([14]).
The paper is organized as follow. In Section 2, we present the geometry of $\mathbb{S}ol3$ and its three Killing vectors representations. We determine, in the Section 3, all parameterizations of Killing V-flux surfaces and its associate Killing V-magnetic scalar flux functions with examples.
We use the computer software "Wolfram Mathematica" to present the computer graphics in Euclidean 3-space.

2. Geometry of Riemannian Space $\mathbb{S}ol3$

The $\mathbb{S}ol3$ space is seen as $\mathbb{R}^3$ with the standard representation in $SL(3,\mathbb{R})$ as

$$\mathbb{S}ol3 = \left\{ \begin{pmatrix} e^{-z} & 0 & x \\ 0 & e^{z} & y \\ 0 & 0 & 1 \end{pmatrix} \mid (x,y,z) \in \mathbb{R}^3 \right\}$$

endowed with the multiplication

$$(x_1,y_1,z_1)(x_2,y_2,z_2) = (x_1 + e^{-z}x_2, y_1 + e^{z}y_2, z_1 + z_2).$$

The Riemannian metrics on the $\mathbb{S}ol3$ is given by

$$g_{\mathbb{S}ol_3} = e^{2z}dx^2 + e^{-2z}dy^2 + dz^2. \tag{2.1}$$

We define an orthonormal basis $(e_i)_{i=\overline{1,3}}$ as

$$e_1 = e^{-z}\partial x, \;\; e_2 = e^{z}\partial y, \;\; e_3 = \partial z, \tag{2.2}$$

and its dual basis $\left(\omega^i\right)_{i=\overline{1,3}}$ by

$$\omega^1 = e^{z}dx; \;\; \omega^2 = e^{-z}dy; \;\; \omega^3 = dz.$$

The Lie bracket of the basis $(e_i)_{i=\overline{1,3}}$ are given by the following identities

$$[e_1,e_2]=0;\quad [e_2,e_3]=-e_2,\quad [e_1,e_3]=e_1. \tag{2.3}$$

The Levi-Civita connection ∇ of the metric $g_{\mathbb{S}ol_3}$ with respect to the orthonormal basis $(e_i)_{i=\overline{1,3}}$ is

$$\left\{\begin{array}{lll} \nabla_{e_1}e_1=-e_3 & \nabla_{e_2}e_1=0 & \nabla_{e_3}e_1=0 \\ \nabla_{e_1}e_2=0 \quad ; & \nabla_{e_2}e_2=e_3 \quad ; & \nabla_{e_3}e_2=0 \quad . \\ \nabla_{e_1}e_3=e_1 & \nabla_{e_2}e_3=-e_2 & \nabla_{e_3}e_3=0 \end{array}\right. \tag{2.4}$$

The algebra of Killing vector field of $\mathbb{S}ol3$ it is generated by the basis $\mathbb{K}=(\mathbf{K}_i)_{i=\overline{1,3}}$, which are solutions of Eq. (1.1), where the Killing vectors $(\mathbf{K}_i)_{i=\overline{1,3}}$ are presented in the following

$$\mathbf{K}_1=\partial x,\ \ \mathbf{K}_2=\partial y \text{ and } \ \mathbf{K}_3=x\partial x-y\partial y-\partial z.$$

The Killing vectors, in the base $(e_i)_{i=\overline{1,3}}$ from the Eq. (2.2), are

$$\mathbf{K}_1=e^z e_1,\ \ \mathbf{K}_2=e^{-z}e_2 \text{ and } \quad \mathbf{K}_3=xe^z e_1-ye^{-z}e_2-e_3, \tag{2.5}$$

(for more detail see [3,4,15]).

3. Killing V-flux Surfaces in $\mathbb{S}ol3$

Definition 3.1. *Let M be a smooth surface in a Riemannian manifold (N,g) and $\mathbf{n}$ be its normal vector field. We call M a flux surface of a smooth vector field V (denoted by V-flux surface) on (N,g) if*

$$g(V,\mathbf{n})=0$$

everywhere on M.
Moreover, if V is a Killing field then we call M flux surface according to the Killing vector V denoted by Killing V-flux surface.

Lemma 3.2. *Let f be a scalar function in (N,g), then the Riemannian gradient of f is*

$$\nabla f=f_x\partial x+f_y\partial y+f_z\partial z=e^z f_x e_1+e^{-z}f_y e_2+f_z e_3.$$

The determination of flux surfaces needs the resolution of partial differential equations denoted by PDE, therefore we use the resolution method in the following proposition.

Proposition 3.3. *Let P and Q two functions in real parameters s and t. The general solutions of the PDE*

$$P(s,t)h_s+Q(s,t)\partial_t h_t=R(s,t) \tag{3.1}$$

are in the following form:
1. *When the PDE (3.1) is homogeneous (i.e. $R\equiv 0$)*

i. If $P\equiv 0$ (resp. $Q\equiv 0$) then $h(s,t)=h(s)$ (resp. $h(s,t)=h(t)$)

ii. If P and Q are non null functions, then

$$h(s,t)=\varphi\left(\psi(s,t)\right)$$

where $\psi(s,t)=c$ (c is a constant) is the solution of ODE

$$\frac{ds}{P}=\frac{dt}{Q} \tag{3.2}$$

and φ is arbitrary real function.

2. *When the PDE (3.1) is nonhomogeneous (i.e. $R\neq 0$)*

i. If $P\equiv 0$ (resp. $Q\equiv 0$) then $h(s,t)=\int\frac{R}{Q}dt$ (resp. $h(s,t)=\int\frac{R}{P}ds$)

ii. If P and Q are non null functions, then the solution h is given implicitly from

$$\overline{\psi}_1(s,t,h)=\varphi\left(\overline{\psi}_2(s,t,h)\right)$$

where $\overline{\psi}_{1,2}(s,t)=c_{1,2}$ ($c_{1,2}$ are a constants) are the choice of two functions among three functions solutions of three ODEs

$$\frac{ds}{P}=\frac{dt}{Q}=\frac{dh}{R}$$

and φ is arbitrary function in $\mathbb{R}$. (See the method to solve linear PDE in [16]).

3.1. Killing K_1-flux surfaces in $\mathbb{S}ol3$

Let $\mathbb{M}$ be a surface in $\mathbb{S}ol3$ and $X(s,t)=(x(s,t),y(s,t),z(s,t))$ its parametrization. The tangent vectors X_s and X_t are described by

$$\begin{cases} X_s = x_s\partial x + y_s\partial y + z_s\partial z = e^z x_s e_1 + e^{-z} y_s e_2 + z_s e_3 \\ X_t = x_t\partial x + y_t\partial y + z_t\partial z = e^z x_t e_1 + e^{-z} y_t e_2 + z_t e_3. \end{cases}$$

Its normal vector $\mathbf{n}$, in the base $(e_i)_{i=\overline{1,3}}$, is

$$\mathbf{n} = \frac{X_s \times X_t}{\|X_s \times X_t\|} = \frac{1}{\|X_s \times X_t\|} \begin{pmatrix} (y_s z_t - y_t z_s)\, e^{-z} \\ (x_t z_s - x_s z_t)\, e^{z} \\ x_s y_t - x_t y_s \end{pmatrix}. \tag{3.3}$$

Now, we have the theorem.

Theorem 3.4. *Let $\mathbb{M}$ be a surface in $\mathbb{S}ol3$ and $X(s,t)=(x(s,t),y(s,t),z(s,t))$ its parametrization. Then $\mathbb{M}$ is a Killing K_1-flux surface if and only if*

$$y_s z_t - y_t z_s = 0 \tag{3.4}$$

Proof. It's a direct consequence by using the inner product given in Eq. (2.1), in the orthonormal base $(e_i)_{i=\overline{1,3}}$ defined in the Definition 3.1, of the normal vector $\mathbf{n}$ given from the Eq. (3.3) and the Killing vector K_1. □

Proposition 3.5. *All Killing K_1-flux surfaces in $\mathbb{S}ol3$ are parameterized by*

$$\begin{aligned} \mathbf{1}.\ X(s,t) &= (x(s,t),y(s,t),\varphi(\psi_2(s,t))), \\ \mathbf{2}.\ X(s,t) &= (x(s,t),\varphi(\psi_3(s,t)),z(s,t)), \\ \mathbf{3}.\ X(s,t) &= (x(s,t),\varphi_1(s),\varphi_2(s)), \\ \mathbf{4}.\ X(s,t) &= (x(s,t),\varphi_1(t),\varphi_2(t)), \end{aligned}$$

where x,y,z and φ ,$\varphi_{1,2}$ are arbitrary smooth functions in $\mathbb{R}^2$ and $\mathbb{R}$, respectively.

Proof. Using the Proposition 3.3(1-ii), the parameterizations $X(s,t)$ are a general solution of the first order linear PDE given in the Theorem 3.4 for arbitrary functions x,y and x,z for the assertions 1 and 2, respectively. For the assertions 3 and 4, it's a direct consequence from the Proposition 3.3(1-i). □

Example 3.6. ***1.*** *Let $y(s,t)=\cos st$, from the Proposition 3.5-1(ii) and substituting the value of y in the Eq. (3.4), we have $P=y_s$ and $Q=y_t$ and*

$$\frac{ds}{s\sin st} = \frac{-dt}{t\sin st}$$

its solution is

$$\psi_2(s,t) = st = c,\ c \text{ is a constant}$$

then the surface $\mathbb{M}_{1.1}$ parameterized by

$$X(s,t) = (x(s,t),\cos st,\varphi(st))$$

is Killing K_1-flux surface in $\mathbb{S}ol3$, where φ and x are arbitrary smooth functions in $\mathbb{R}$ and $\mathbb{R}^2$ respectively. We present the surface $\mathbb{M}_{1.1}$ in the Figure 3.1 for $(s,t)\in[-\pi,\pi]^2$ in Euclidean space $\left(\mathbb{R}^3, g_{euc}\right)$.

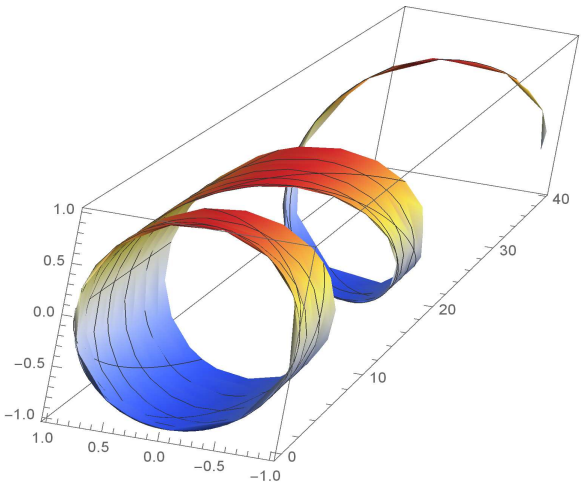

Figure 3.1: Killing K_1-flux surface $\mathbb{M}_{1.1} = \left((s+t)^2, \cos st, \sin st\right)$

2. *Let $z(s,t) = e^{st}$, similarly the Eq. (3.4) turns to*

$$sy_s - ty_t = 0$$

we have $P = s, Q = t$ and

$$\frac{ds}{s} = \frac{-dt}{t}$$

its solution is

$$\psi_3(s,t) = st = c,\ c \text{ is a constant}$$

Using the assertion 2 of Proposition 3.5, then the surface $\mathbb{M}_{1.2}$ parameterized by

$$X(s,t) = \left(x(s,t), \varphi(st), e^{st}\right)$$

is Killing K_1-flux surface in $\mathbb{S}ol3$, where φ and x are arbitrary smooth functions in $\mathbb{R}$ and $\mathbb{R}^2$ respectively.
3. *Let $z(s,t) = e^{s+t}$, we have*

$$\frac{ds}{e^{s+t}} = \frac{-dt}{e^{s+t}}$$

its solution is

$$\psi_3(s,t) = s+t = c,\ c \text{ is a constant}$$

By the assertion 2 of Proposition 3.5, the surface $\mathbb{M}_{1.3}$ parameterized by

$$X(s,t) = \left(x(s,t), \varphi(s+t), e^{s+t}\right)$$

is Killing K_1-flux surface in $\mathbb{S}ol3$, where φ and x are arbitrary smooth functions in $\mathbb{R}$ and $\mathbb{R}^2$, respectively.

3.1.1. Scalar flux functions

Definition 3.7. *Let f be a function on (N,g). Then f is called a scalar flux function corresponding to the magnetic vector field V if its value is constant on the surface M, and*

$$g(V, \nabla f) = 0$$

we denoted here f, to simplify, a V-magnetic scalar flux function. Moreover, if V is Killing, f is denoted Killing V-magnetic scalar flux function.

Now, we can present the following theorem.

Theorem 3.8. *Let $\mathbb{M}$ be a Killing magnetic K_1-flux surface in $\mathbb{S}ol3$. Then the function f given by*

$$f(x,y,z) = f(y,z)\ (f \text{ depend only on parameters } y,z)$$

and constant on $\mathbb{M}$ is Killing K_1-magnetic scalar flux function to $\mathbb{M}$, where ψ is arbitrary smooth function in $\mathbb{R}$.

Proof. Using the Definition 3.7 and the Lemma 3.2, we have

$$g_{\mathbb{S}ol_3}(K_1, \nabla f) = e^{2z} f_x = 0$$

by solving the above first order PDE we get

$$f(x,y,z) = f(y,z)$$

and f must be also constant on $\mathbb{M}$ to be Killing K_1-magnetic scalar flux function on $\mathbb{M}$ □

Example 3.9. *Using the Example 3.6(3), the surface $\mathbb{M}_{1.3}$ parameterized by*

$$X(s,t) = \left(\cos st, \sqrt{e^{s+t}}, e^{s+t}\right)$$

is Killing magnetic K_1-flux surface. The Killing K_1-magnetic scalar flux function f to $\mathbb{M}_{1.3}$, from the Theorem 3.7, is in the form $f(x,y,z) = f(y,z)$ and it must be constant on $\mathbb{M}$, (i.e. $f(X(s,t)) \equiv C$, C is a constant). Let

$$f(x,y,z) = y^2 - z + a,\ a \in \mathbb{R}$$

We have

$$f(X(s,t)) = a$$

then $f(x,y,z) = y^2 - z + a$ is Killing K_1-magnetic scalar flux function to the Killing magnetic K_1-flux surface $\mathbb{M}_{1.3}$ parameterized by $X(s,t) = \left(\cos st, \sqrt{e^{s+t}}, e^{s+t}\right)$.

3.2. Killing K_2-flux surfaces in $\mathbb{S}ol3$

Similar as Section 3.1, we characterise and present all Killing K_2-flux surfaces given in the Eq. (2.5_2).

Theorem 3.10. *Let $\mathbb{M}$ be a surface in $\mathbb{S}ol3$ and $X(s,t) = (x(s,t), y(s,t), z(s,t))$ its parametrization. Then $\mathbb{M}$ is a Killing K_2-flux surface if and only if*

$$x_u z_v - x_v z_u = 0.$$

Proof. The proof is similar as the proof of the Theorem 3.4 using the Killing vector K_2 given in Eq. (2.5_2). □

Proposition 3.11. *All Killing K_1-flux surfaces in $\mathbb{S}ol3$ are parameterized by*

$$\begin{aligned}
&\mathbf{1}.\ X(s,t) &&= (x(s,t), y(s,t), \varphi(\psi_1(u,v))),\\
&\mathbf{2}.\ X(s,t) &&= (\varphi(\psi_3(s,t)), y(s,t), z(s,t)),\\
&\mathbf{3}.\ X(s,t) &&= (\varphi_1(s), y(s,t), \varphi_2(s)),\\
&\mathbf{4}.\ X(s,t) &&= (\varphi_1(t), y(s,t), \varphi_2(t)),
\end{aligned}$$

where x, y, z and φ, $\varphi_{1,2}$ are arbitrary smooth functions in $\mathbb{R}^2$ and $\mathbb{R}$, respectively.

Proof. The proof is similar as the proof of the Proposition 3.5. □

Example 3.12. ***1.*** *Let $x(s,t) = \sin(s+t)$, from the assertion 1 of Proposition 3.5-1(ii) and same computations as the Example 3.6, we have*

$$\psi_1(s,t) = s + t = c,\ c \text{ is a constant,}$$

then the surface $\mathbb{M}_{2.1}$ parameterized by

$$X(s,t) = (\sin(s+t), y(s,t), \varphi(s+t))$$

is Killing K_2-flux surface in $\mathbb{S}ol3$.

2. *Similarly, from the assertion 2 of Proposition 3.5, let $z(s,t) = (1+\cos t)\sin s$, we have*

$$\psi_3(s,t) = (1+\cos t)\sin s = c,\ c \text{ is a constant,}$$

then the Killing K_2-flux surface $\mathbb{M}_{2.2}$ in $\mathbb{S}ol3$ have the parametrization

$$X(s,t) = (\varphi((1+\cos t)\sin s), y(s,t), (1+\cos t)\sin s),$$

where φ and y are arbitrary smooth functions in $\mathbb{R}$ and $\mathbb{R}^2$ respectively. The following Figure 3.2 presents the surface $\mathbb{M}_{2.2}$ in $\left(\mathbb{R}^3, g_{euc}\right)$ for parameters $(s,t) \in [-\pi, 2\pi] \times [-\pi, \pi]$.

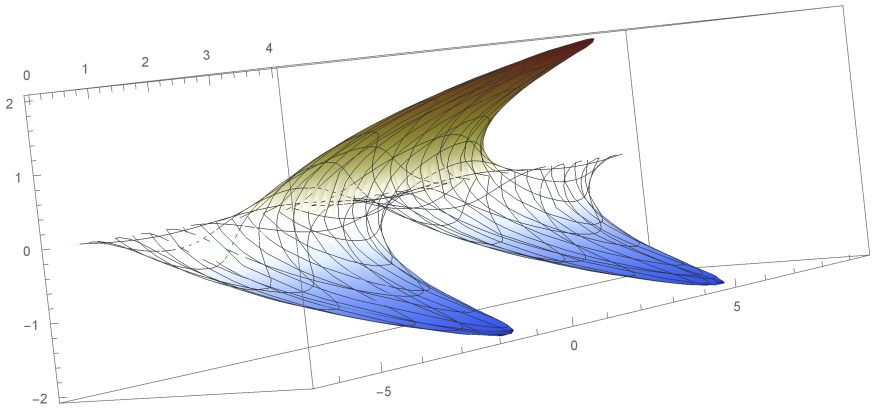

Figure 3.2: Killing K_2-flux surface $\mathbb{M}_2 = (((1+\cos t)\sin s)^2, s+t, (1+\cos t)\sin s)$

3. *Similarly, from the assertion* 4 *of Proposition* 3.5*, the surface* $\mathbb{M}_{2.3}$ *parameterized by* $X(s,t) = (t\cos t, s^3+t, t\sin t)$ *is Killing* K_2*-flux surface in* $\mathbb{S}ol3$*. The Figure* 3.3 *presents* $\mathbb{M}_{2.3}$ *for* $(s,t) \in [-3,3]\times[-2\pi,2\pi]$ *..*

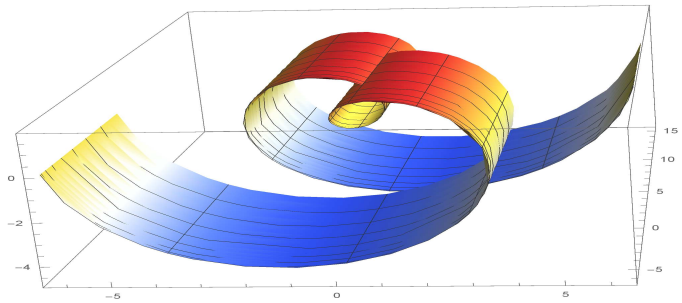

Figure 3.3: Killing K_2-flux Surface $\mathbb{M}_{2.3}$

3.2.1. Killing K_2-magnetic scalar flux functions

We present the Killing K_2-magnetic scalar flux functions in the following theorem.

Theorem 3.13. *Let* $\mathbb{M}$ *be a Killing magnetic* K_2*-flux surface in* $\mathbb{S}ol3$*. Then the function* f *given by*

$$f(x,y,z) = f(x,z)$$

and constant on $\mathbb{M}$ *is Killing* K_2*-magnetic scalar flux function to* $\mathbb{M}$*.*

Proof. Using the Definition 3.7 and the Lemma 3.2, we have

$$g(K_2, \nabla f) = e^{-2z} f_y = 0$$

we get Killing K_2-magnetic scalar flux function f by solving the above linear first order PDE and f must be constant on $\mathbb{M}$. □

Example 3.14. *From the Theorem* 3.13*, the Killing* K_2*-magnetic scalar flux function corresponding to the* $\mathbb{M}$ *parameterized by*

$$X(s,t) = \left(\sin(s+t), \cos(s^2+t^2), \arcsin(s+t)\right)$$

given in Example 3.12 *is in the form* $f(x,y,z) = f(x,z) = \arcsin x - \sin z + a$*;* $a \in \mathbb{R}$ *and* $f(X(s,t)) = a$*, i.e.* f *is constant on* $\mathbb{M}$*. See Figure* 3.4 *(here* $(s,t) \in [-\pi,\pi]^2$*).*

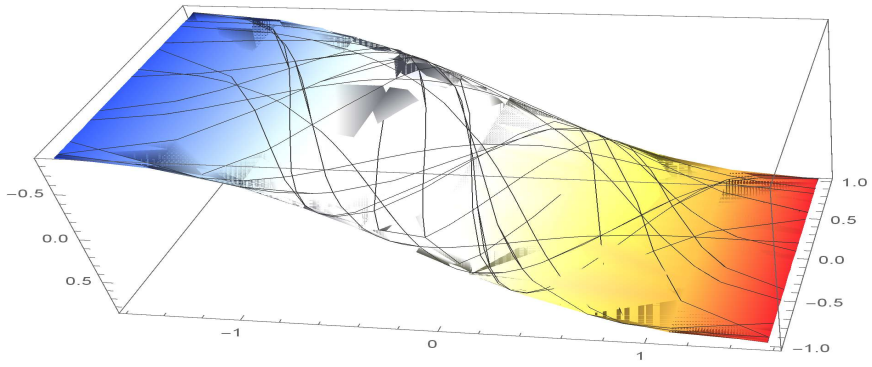

Figure 3.4: Flux surface $\mathbb{M}$ of Killing K_2-magnetic scalar flux function f

3.3. Killing K_3-flux surfaces in $\mathbb{S}ol3$

Following the above subsections, we have the following theorem.

Theorem 3.15. *Let $\mathbb{M}$ be a surface in $\mathbb{S}ol3$ and $X(s,t)=(x(s,t),y(s,t),z(s,t))$ its parametrization. Then $\mathbb{M}$ is a Killing K_3-flux surface if and only if*

$$x_t y_s - x_s y_t + x y_s z_t - x y_t z_s + y x_s z_t - y x_t z_s = 0. \tag{3.5}$$

Proof. The proof is similar as the Theorem 3.4 using the Killing vector K_3 given in Eq. (2.5_3). □

The surface $\mathbb{M}$ in $\mathbb{S}ol3$ parameterized by $X(s,t)=(x(s,t),y(s,t),z(s,t))$ is Killing K_3-flux surface if the Eq. (3.5) holds. However, the Eq. (3.5) have three cases to solve. The first case is where we assume that $x(s,t)$ and $y(s,t)$ are arbitrary functions and find the solution $z(s,t)$ of the Eq. (3.5) in the form

$$[y x_t + x y_t] z_s - [x y_s + y x_s] z_t + [x_s y_t - x_t y_s] = 0.$$

The second and the third cases are when we assume $x(s,t)$, $z(s,t)$ and $y(s,t)$, $z(s,t)$ to be arbitrary functions and find the solutions $y(s,t)$ and $x(s,t)$, respectively. We present in the following proposition only the first case. A similar result, with a similar method, can be obtained for the second and third cases which will not be presented in this paper.

Proposition 3.16. *The parametric surfaces in $\mathbb{S}ol3$ with the parametrization $X(s,t)$ given by*

$$\begin{cases} \textbf{1}.\ X(s,t)=(x(s,t),\varphi_1(x(s,t)),\varphi_4(\psi(s,t))), \\ \textbf{2}.\ X(s,t)=\left(x(s,t),\frac{\varphi_2(s)}{x(s,t)},z(s)\right), \\ \textbf{3}.\ X(s,t)=\left(x(s,t),\frac{\varphi_3(t)}{x(s,t)},z(t)\right), \\ \textbf{4}.\ X(s,t)=(x(s,t),y(s,t),\overline{\psi}(s,t)), \end{cases}$$

are Killing K_3-flux surfaces, where x,y,z and $\varphi_{\overline{1,4}}$ are arbitrary smooth functions in $\mathbb{R}^2$ and $\mathbb{R}$, the functions $\psi,\overline{\psi}$ are given in the Eqs. (3.7) and (3.8), respectively, and we assume that $\frac{\partial(x,y)}{\partial(s,t)}\neq 0$.

Proof. (case 1). Let $x(s,t)$ and $y(s,t)$ be an arbitrary smooth functions then the Eq. (3.5) turns to the PDE

$$\left(\underbrace{x y_t + y x_t}_{P}\right) z_s + \left(\underbrace{-x y_s - y x_s}_{Q}\right) z_t + \left(\underbrace{x_s y_t - x_t y_s}_{R}\right) = 0 \tag{3.6}$$

in the form of the PDE in Eq. (3.1), with respect to z.

i. If $R(s,t)=x_t y_s - x_s y_t = 0$ (i.e. the Eq. (3.6) is homogeneous PDE), using the assertion 1 of the Proposition 3.3, then y must be

$$y(s,t)=\varphi_1(x(s,t))$$

With cases when $y(s,t)=\frac{\varphi_2(s)}{x(s,t)}$ (i.e. $P\equiv 0$) (resp. $y(s,t)=\frac{\varphi_3(t)}{x(s,t)}$ (i.e. $Q\equiv 0$), by using again the assertion 1(i) of the Proposition 3.3, we obtain $z=z(t)$ (resp. $z=z(s)$), which prove the assertions 2 and 3. If $P,Q\neq 0$ then

$$z(s,t)=\varphi_4(\psi(s,t)) \tag{3.7}$$

where ψ is solution of the OED

$$\frac{dt}{xy_s + yx_s} = -\frac{ds}{xy_t + yx_t}$$

and $\varphi_{\overline{1,4}}$ are arbitrary real smooth functions, then the assertion 1 is proved.

ii. If $P = 0$ $\left(\text{i.e. } y(s,t) = \frac{\varphi_2(s)}{x(s,t)}\right)$ we obtain $R = 0$ as (i), and similarly when $Q = 0$.

iii. If $P, R, Q \neq 0$ then the solution $z(s,t) = \overline{\psi}(s,t)$ of the nonhomogeneous PDE (3.6), using the assertion 2(ii) of the Proposition 3.3, is given implicitly from the equation

$$\overline{\psi}_1(s,t,z) = \varphi\left(\overline{\psi}_2(s,t,z)\right), \tag{3.8}$$

which prove the assertion 4.

□

Example 3.17. *We construct an example using the assertion* 1 *of the Proposition 3.16. Let* $x(s,t) = st$ *and* $y(s,t) = (st)^2$, *using the Proposition 3.3, we have*

$$P = 3s^3t^2,\ Q = -3s^2t^3 \text{ and } R = 0$$

and the ODE

$$\frac{ds}{P} = \frac{dt}{Q}$$

with solution

$$\psi_1(s,t) = s^3t^3 = c,\ c \text{ is a constant}$$

then the surface $\mathbb{M}_{3.1}$ *parameterized by* $X(s,t) = \left(st, (st)^2, \varphi(s^3t^3)\right)$ *is Killing* K_3*-flux surface in* $\mathbb{S}ol3$, *where* φ *is arbitrary real smooth function. We present, in* $(\mathbb{R}^3, g_{euc})$, *the Killing* K_3*-flux surface* $X(s,t) = \left(st, (st)^2, \sin(s^3t^3 + 1)\right)$ *in* $\mathbb{S}ol3$ *in Figure 3.5, where* $(s,t) \in \left[-\frac{\pi}{2}, \frac{\pi}{2}\right] \times [-\pi, \pi]$

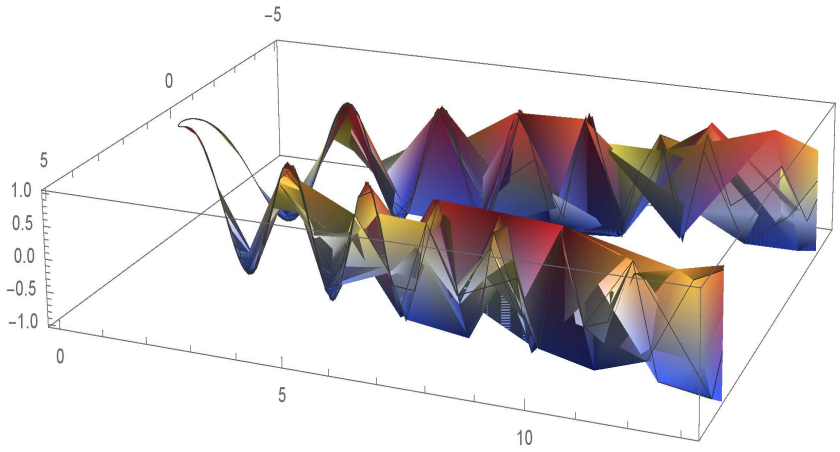

Figure 3.5: Killing K_3-flux surface $\mathbb{M}_{3.1}$

Example 3.18. *We present an example, using the assertion* 2 *of the Proposition 3.16, of Killing* K_3*-flux surface* $\mathbb{M}_{3.2}$ *in* $\mathbb{S}ol3$ *parameterized by* $X(s,t) = \left(st, \frac{s}{t}, \cos s\right)$ *see Figure 3.6* $(s,t) \in [-2\pi, 2\pi]^2$.

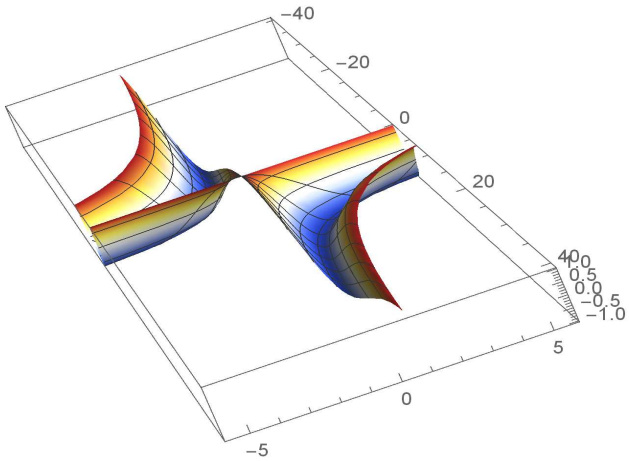

Figure 3.6: Killing K_3-Flux surface $\mathbb{M}_{3.2}$

Example 3.19. *Now, we consider the assertion* 4 *of the Proposition 3.16. Let* $x(s,t)=\cos(s+t)$ *and* $y(s,t)=st^2$, *then the Eq. (3.6) turns to an nonhomogeneous PDE given by*

$$s\left[\cos(s+t)-t\sin(s+t)\right]z_s+t\left[s\sin(s+t)-\cos(s+t)\right]z_t-\left[s\sin(s+t)+t\sin(s+t)\right]=0 \tag{3.9}$$

using the Proposition 3.3-2(ii), we must make a choice of two functions among three functions which are solutions of three following ODEs

$$\underbrace{\frac{ds}{s\left[\cos(s+t)-t\sin(s+t)\right]}}_{(1)}=\underbrace{\frac{dt}{t\left[s\sin(s+t)-\cos(s+t)\right]}}_{(2)}=\underbrace{\frac{-dz}{\left[s\sin(s+t)+t\sin(s+t)\right]}}_{(3)}$$

The ODE $(1=2)$ *has a solution* $\psi_1(s,t,z)=-2st\cos(s+t)=c_1$ *and the solution of the ODE* $(1=3)$ *has a solution* $\psi_2(s,t,z)=(s+t+tz)\cos(s+t)-(1+stz)\sin(s+t)=c_2$, *where* $c_{1,2}$ *are a real constants.*
Hence, the solution z *of the Eq. (3.9) is given implicitly from the equation*

$$\psi_1(s,t,h)=\varphi\left(\psi_2(s,t,h)\right)$$

which turns, after substitution the values of $\psi_{1,2}$, *to*

$$-2st\cos(s+t)=\varphi\left((s+t+tz)\cos(s+t)-(1+stz)\sin(s+t)\right)$$

where φ *is arbitrary function in* $\mathbb{R}$. *By taking* $\varphi=Id_{\mathbb{R}}$, *we get*

$$z(s,t)=\frac{\sin(s+t)-(s+t+2st)\cos(s+t)}{t\cos(s+t)+st\sin(s+t)}$$

and the surface $\mathbb{M}_{3.3}$ *parameterized by*

$$X(s,t)=\left(\cos(s+t),st^2,\frac{\sin(s+t)-(s+t+2st)\cos(s+t)}{t\cos(s+t)+st\sin(s+t)}\right)$$

is Killing K_3*-flux surface in* $\mathbb{S}ol3$. *We present, in* $(\mathbb{R}^3,g_{euc})$, *the Killing* K_3*-flux surface* $\mathbb{M}_{3.3}$, *in* $\mathbb{S}ol3$, *in Figure 3.7 where* $(s,t)\in\left[-\frac{\pi}{2},-\frac{\pi}{2}\right]^2$.

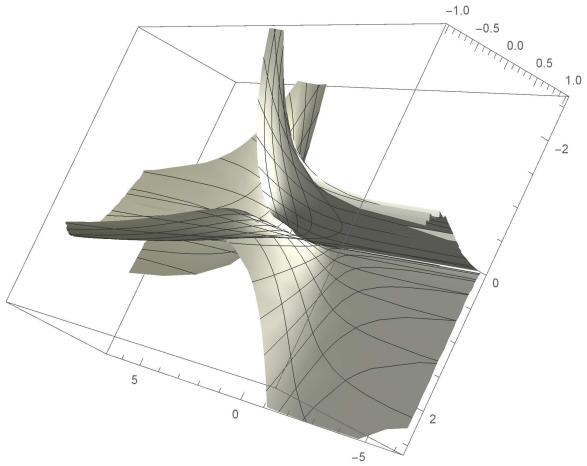

Figure 3.7: Killing K_3-flux surface $\mathbb{M}_{3.3}$

3.3.1. Killing K_3-magnetic scalar flux functions

For the Killing K_2-magnetic Scalar flux functions, we have the following theorem.

Theorem 3.20. *Let $\mathbb{M}$ be a Killing magnetic K_3-flux surface in $\mathbb{S}ol3$. Then the function f given by*

$$f(x,y,z) = \Psi\left(2\ln x + e^{2z}, 2\ln y - e^{-2z}\right)$$

and constant on $\mathbb{M}$ is Killing K_3-magnetic scalar flux function to $\mathbb{M}$.

Proof. Using the Definition 3.7 and the Lemma 3.2, we have

$$g_{\mathbb{S}ol3}(K_3, \nabla f) = xe^{2z} f_x - ye^{-2z} f_y - f_z = 0$$

solving the above linear first order PDE, we get

$$f(x,y,z) = \Psi\left(2\ln x + e^{2z}, 2\ln y - e^{-2z}\right)$$

Killing magnetic K_3-scalar flux function f and constant on $\mathbb{M}$, where Ψ is arbitrary function. □

Example 3.21. *Using the the assertion 2 of the Proposition 3.16, let $\mathbb{M}$ be a Killing magnetic K_3-flux surface in $\mathbb{S}ol3$ parameterized by*

$$X(s,t) = \left(st, \frac{\varphi(s)}{st}, z(s)\right)$$

Next, the Killing K_3-magnetic scalar flux function f is in the form

$$\begin{aligned} f(x,y,z) &= \Psi\left(2\ln x + e^{2z}, 2\ln y - e^{-2z}\right) \\ &= \Psi\left(2\ln(st) + e^{2z(s)}, 2\ln\frac{\varphi(s)}{st} - e^{-2z(s)}\right) \end{aligned}$$

and constant on $\mathbb{M}$. By choosing

$$\Psi(u,v) = u + v;\ \varphi(s) = -\sinh 2z(s)$$

we get

$$f(x,y,z) = 2(\ln xy + \sinh 2z) \text{ and } f(X(s,t)) = \Psi(0)$$

then f is constant on $\mathbb{M}$ parameterized by $X(s,t) = \left(st, \frac{-\sinh 2z(s)}{st}, z(s)\right)$.

Conclusion

The flux surface are surfaces that appear in many phenomena that we can cited, in Euclidean context, magnetic confinement fusion, dynamics of solitons and dispersive effects and plasma state. These surfaces are characterized that its normal vector is orthogonal to the vector corresponding to a flux in ambient spaces. Moreover, if the flux is magnetic (i.e. the associate vector to the flux is magnetic vector), we can define flux functions is which its gradient is orthogonal to the magnetic vector and constant on the associate flux surface. Inspired by the determination of the flux surfaces and associate flux function in Euclidean and Heisenberg group as three-dimensional manifolds. We have extended this determination, in this paper, to three-dimensional Riemannian space Sol3.

Article Information

Acknowledgements: The authors thank the referees for valuable comments and suggestions which improved the presentation of this paper.

Author's Contributions: All authors contributed equally to the writing of this paper. All authors read and approved the final manuscript.

Conflict of Interest Disclosure: No potential conflict of interest was declared by the author.

Supporting/Supporting Organizations: No grants were received from any public, private or non-profit organizations for this research.

Ethical Approval and Participant Consent: It is declared that during the preparation process of this study, scientific and ethical principles were followed and all the studies benefited from are stated in the bibliography.

Plagiarism Statement: This article was scanned by the plagiarism program. No plagiarism detected.

Availability of Data and Materials: Not applicable.

References

[1] A. H. Boozer, *Physics of magnetically confined plasmas*, Rev. Mod. Phys., **76** (2004), 1071–1141.
[2] H. M. Dida, F. Hathout, *Killing magnetic flux surfaces in the Heisenberg three group*, Facta Universitatis (NIS) Ser. Math. Inform., **37**(5) (2022), 975–991.
[3] Z. Erjavec, J. Inoguchi, *Killing magnetic curves in Sol space*, Math. Phys. Anal. Geom., **21**(2018), 15.
[4] Z. Erjavec, J. Inoguchi, *Magnetic curves in Sol*3, J. Nonlinear Math. Phys., **25**(2)(2018), 198-210.
[5] R. D. Hazeltine, J. D. Meiss, *Plasma Confinement*, Dover Publications, inc. Mineola, New York, 2003.
[6] T. Körpinar, R. C. Demirkol, Z. Körpinar, *Approximate solutions for the inextensible Heisenberg antiferromagnetic flow and solitonic magnetic flux surfaces in the normal direction in Minkowski space*, Optik, **238** (2021), 166403.
[7] T. Körpinar, R. C. Demirkol, Z. Körpinar, *New analytical solutions for the inextensible Heisenberg ferromagnetic flow and solitonic magnetic flux surfaces in the binormal direction*, Phys. Scr., **96** (2021), 085219.
[8] Talat Körpinaret, R. C. Demirkol, V. Asil, Z. Körpinar, *Magnetic flux surfaces by the fractional Heisenberg antiferromagnetic flow of magnetic b-lines in binormal direction in Minkowski space*, J. Magn. Magn. Mater., **549** (2022), 168952.
[9] Z. Özdemir, İ. Gök, Y. Yaylı, F. N. Ekmekçi, *Killing magnetic flux surfaces in Euclidean 3-space*, Honam Math. J. **41**(2) (2019), 329–342.
[10] T.S. Pedersen, A. H. Boozer, *Confinement of nonneutral plasmas on magnetic surfaces*, Phys. Rev. Lett. **88** (2002), 205002.
[11] M. Barros, A. Romero, *Magnetic vortices*, EPL **77** (2007), 34002.
[12] R. B. Bird, W. E. Stewart, E. N. Lightfoot, *Transport Phenomena*, Wiley, ISBN 0-471-07392-X, 1960.
[13] S. R. Hudson, E. Startsev, E. Feibush, *A new class of magnetic confinement device in the shape of a knot*, Phys. Plasmas, **21**(1) (2014), 010705.
[14] W. Thurston, *Three-dimensional geometry and topology*, Princenton Math. Ser. 35, Princenton Univ. Press, Princenton, NJ, (1997).
[15] M. Troyanov, *L'horizon de SOL*. Expo. Math., **16** (1998), 441–479.
[16] Walter. A. Strauss, *Partial differential equations: An introduction*, Math. Gaz., **77**(479) (1993), 286–287 ISBN 0-471-57364-7, Wiley.

Fundamental Journal of Mathematics and Applications, 6 (2) (2023) 101-106
Research Article

FUJMA

Fundamental Journal of Mathematics and Applications

Journal Homepage: www.dergipark.org.tr/en/pub/fujma
ISSN: 2645-8845
doi: https://dx.doi.org/10.33401/fujma.1212268

Parameter Estimation for a Class of Fractional Stochastic SIRD Models with Random Perturbations

Na Nie[1], Jun Jiang[1,2] and Yu Qiang Feng[1,2*]

[1]*College of Science, Wuhan University of Science and Technology, Hubei, China*
[2]*Hubei Province Key Laboratory of Systems Science in Metallurgical Process, Hubei, China*
[*]*Corresponding author*

Article Info

Keywords: *COVID-19, Fractional stochastic SIRD model, Maximum likelihood estimation*
2010 AMS: *92F05*
Received: *30 November 2022*
Accepted: *15 May 2023*
Available online: *24 May 2023*

Abstract

The classical SIRD model is extended to the conformable fractional stochastic SIRD model. The differences between the fractional stochastic SIRD model and the integer stochastic SIRD model are analyzed and compared using COVID-19 data from India. The results show that when the order of the fractional stochastic SIRD model is between $[0.93, 0.99]$, the root mean square error between the simulated value and the real value of the number of infections is smaller than that of the integer stochastic SIRD model. Then, the maximum likelihood estimation of the parameters of the conformable fractional stochastic SIRD model is carried out, and compared with the maximum likelihood estimation results of the parameters of the integer stochastic SIRD model, It can be seen that the root mean square error of the fractional stochastic SIRD model is smaller when the fractional order is between $[0.93, 0.99]$.

1. Introduction

In recent years, with the wide spread of COVID-19, the loss of individuals and society has gradually increased. And the study of mathematical models of infectious diseases has become an increasingly important topic, which can be divided into deterministic models and stochastic models [1]. Stochastic models have been studied mainly for models corresponding to transitions of individuals into different epidemic regimes over time.

The SIR model was first proposed by Kermack and Mckendrick in 1927 [2], which laid the foundation for the study of the dynamics of infectious diseases. Becker used the least square method and maximum likelihood method to estimate the parameters of the model and defined the initial infection rate [3]. Timmer discussed the parameter estimation problem of nonlinear stochastic differential equations based on the sampled time series [4]. Buckingham-Jeffery et al. considered the Gaussian process approximation based on the approximation of random moment closure and the approximation based on the approximation of linear time non-uniform SDE to infer the parameter characteristics of the random SEIR model [5]. Senel proposed a single-parameter estimation method to avoid potential problems such as limited and noisy data when using SIR Model to estimate COVID-19 [6]. Morato et al. formulated a nonlinear model predictive control scheme based on the SIRD model with time-varying parameters, and they proposed an identification method consisting of analytical regression, least squares optimization, and autoregressive model fitting, which can fully predict the infection curve in a large range [7].

In recent years, fractional infectious disease models have begun to attract a surge of research. Farman et al. applied the Laplace Adomian decomposition method to give the approximate solution of the nonlinear system of the Caputo SEIR model [8]. Rajagopal et al. compared the predictive ability of the fractional SEIRD model and the classical SEIRD model by using Italian COVID-19 data [9]. Basti et al. proposed an improved mathematical model for fractional SIRD in the sense

Email addresses and ORCID numbers: 1583712215@qq.com, 0000-0002-3742-5585 (N. Nie), jiangjun@wust.edu.cn, 0000-0002-2241-3450 (J. Jiang), yqfeng6@126.com, 0000-0002-1208-0509 (Y. Q. Feng)
Cite as: N. Nie, J. Jiang, Y. Q. Feng, *Parameter estimation for a class of fractional stochastic SIRD models with random perturbations*, Fundam. J. Math. Appl., 6(2) (2023), 101-106.

of Caputo-Katugampola fractional derivatives. The existence and uniqueness of the solution of the improved SIRD model are studied by applying the properties of Schauder and Banach's fixed point theorems [10]. Mohammadi et al. proposed a SIRD model in the sense of Caputo fractional order, discussed the stability of the model and the existence and uniqueness of nonnegative solutions, and obtained approximate responses by implementing the fractional Euler method [11]. Fouladi et al. analyzed the identifiability and sensitivity of the integer and Caputo fractional SEIRD models and proved that the fractional infectious disease model was more suitable for predicting the real situation by comparing the quality of fitting [12].
In 2014, Khalil et al. proposed Conformable fractional derivatives, which is a natural expansion of integer derivatives [13]. Several scholars have applied conformable fractional derivatives to models in mathematics, physics, transportation, and other fields. In 2021, Akinyemi et al. established a time-varying nonlinear differential equation in the sense of conformable fractional order and obtained the exact solution of the equation by using the sub-equation method [14]. In 2022, Ashraf et al. studied the $(2+1)$ dimensional Conformable fractional transmission line equation in a nonlinear system. By combining exponential, polynomial, trigon, and hyperbolic functions, Multi-wave, M-shaped rational, and interaction solutions are obtained [15]. In 2022, Yuxiao Kang et al. established a conformable fractional time-varying gray Riccati traffic flow model based on viscoelastic fluid and applied it to modeling traffic flow and traffic congestion degree in multiple scenarios [16]. The relevant definitions and properties are introduced below.

Definition 1.1 ([13]). *Given the function $f(t):[0,\infty)\to R$, for all $t>0$, $\alpha\in(0,1]$, the α-order conformable fractional derivative of $f(t)$ is defined as*

$$T_\alpha f(t)=\lim_{\varepsilon\to 0}\frac{f\left(t+\varepsilon t^{1-\alpha}\right)-f(t)}{\varepsilon},$$

when $t=0$, $T_\alpha f(0)=\lim\limits_{t\to 0^+}T_\alpha f(t)$.

Lemma 1.2 ([13]). *The relationship between the α-order conformable fractional derivative of $f(t)$ and the first derivative of $f(t)$ can be represented as*

$$T_\alpha f(t)=t^{1-\alpha}\frac{\mathrm{d}f(t)}{\mathrm{d}t},$$

specifically, $T_1 f(t)=\frac{\mathrm{d}f(t)}{\mathrm{d}t}$.

In this paper, we propose a stochastic SIRD model in the sense of conformable fractional order and obtain maximum likelihood estimates for the model parameters, taking into account the impact of various uncertainties on infectious diseases in real-world situations. Finally, the COVID-19 data from April 1, 2020, to July 31, 2020, in India is used for example analysis to compare the effect of fitting the raw data with a fractional stochastic SIRD model at different fractional orders. The parameter estimates for the fractional stochastic SIRD model are computed using maximum likelihood estimation. The results show that when the order of the fractional stochastic SIRD model is between $[0.93,0.99]$, the root mean square error between the simulated value and the real value of the number of infections is smaller than that of the integer stochastic SIRD model. Moreover, compared with the maximum likelihood estimation of the parameters of the integer stochastic SIRD model, it can be seen that when the fractional order is between $[0.93,0.99]$, the root mean square error of the fractional stochastic SIRD model is smaller.

2. Model Introduction

The SIRD model divides the tested population into Susceptible(S), Infected(I), Recovered(R), and Dead(D) populations. A susceptible person is a person who has not been infected, lacks immunity and is susceptible to infection after contact with an infected person; An infected population is already infected; Recovered populations are those that have been cured of their disease; Dead populations refers to a person who has died as a result of illness and is no longer involved in the process of infection and contagion. The classical SIRD model can be expressed as the following system of differential equations [17]

$$\begin{cases}\dfrac{\mathrm{d}S(t)}{\mathrm{d}t}=-\dfrac{\beta S(t)I(t)}{N},\\ \dfrac{\mathrm{d}I(t)}{\mathrm{d}t}=\dfrac{\beta S(t)I(t)}{N}-\gamma I(t)-\mu I(t),\\ \dfrac{\mathrm{d}R(t)}{\mathrm{d}t}=\gamma I(t),\\ \dfrac{\mathrm{d}D(t)}{\mathrm{d}t}=\mu I(t),\end{cases}\tag{2.1}$$

where $t\geq 0$, $S(0)\geq 0$, $I(0)\geq 0$, $R(0)\geq 0$, $D(0)\geq 0$. Let the total population of the area be N, satisfying $S(t)+I(t)+R(t)+D(t)=N$. β is the infection rate, and it represents the probability of a susceptible person being infected; γ is the recovery rate, and it indicates the likelihood of recovery of the infected person; μ is the mortality rate, all of which are positive numbers.
The classical SIRD model has a stable and interference-resistant performance, and considering the advantage that the fractional SIRD model can better fit the data by adjusting the order of the fractional derivatives in the model, in this paper we extend

the classical SIRD model to the conformable fractional SIRD model by using the definition and properties of conformable fractional derivatives.

$$\begin{cases} T_\alpha S(t) = t^{1-\alpha}\dfrac{\mathrm{d}S(t)}{\mathrm{d}t} = -\dfrac{\beta S(t)I(t)}{N}, \\ T_\alpha I(t) = t^{1-\alpha}\dfrac{\mathrm{d}I(t)}{\mathrm{d}t} = \dfrac{\beta S(t)I(t)}{N} - \gamma I(t) - \mu I(t), \\ T_\alpha R(t) = t^{1-\alpha}\dfrac{\mathrm{d}R(t)}{\mathrm{d}t} = \gamma I(t), \\ T_\alpha D(t) = t^{1-\alpha}\dfrac{\mathrm{d}D(t)}{\mathrm{d}t} = \mu I(t). \end{cases} \tag{2.2}$$

α is the order of the fractional order derivative of conformable, and $\alpha \in (0,1]$. Since the parameters β, γ, and μ of the real-life SIRD model are easily affected by the variable environment, and there is some randomness in the number of susceptibilities, infections, recoveries, and deaths at the next moment, we give a conformable fractional stochastic SIRD model.
Let $B_1(t)$, $B_2(t)$, $B_3(t)$, $B_4(t)$ be a set of mutually independent standard Brownian motions, $\sigma_i\,(i=1,2,3,4)$ be a non-negative white noise intensity, and build the following Conformable fractional stochastic SIRD model

$$\begin{cases} \mathrm{d}S(t) = -t^{\alpha-1}\dfrac{\beta S(t)I(t)}{N}\mathrm{d}t + \sigma_1 S(t)\mathrm{d}B_1(t), \\ \mathrm{d}I(t) = t^{\alpha-1}\left(\dfrac{\beta S(t)I(t)}{N} - \gamma I(t) - \mu I(t)\right)\mathrm{d}t + \sigma_2 I(t)\mathrm{d}B_2(t), \\ \mathrm{d}R(t) = t^{\alpha-1}\gamma I(t)\mathrm{d}t + \sigma_3 R(t)\mathrm{d}B_3(t), \\ \mathrm{d}D(t) = t^{\alpha-1}\mu I(t)\mathrm{d}t + \sigma_4 D(t)\mathrm{d}B_4(t). \end{cases} \tag{2.3}$$

Parameter estimation is an extremely important ingredient in the study of infectious disease models. Considering that the maximum likelihood estimator is widely used and converges well, the following discussion deals with the maximum likelihood estimator for the parameters β, γ, and μ of the conformable fractional stochastic SIRD model.

3. Parameter Estimation

The discretization of equation (2.3) using Euler's method gives

$$\begin{cases} S(t+1) = S(t) - t^{\alpha-1}\dfrac{\beta S(t)I(t)}{N}\Delta t + \sigma_1 S(t)\Delta B_1(t), \\ I(t+1) = I(t) + t^{\alpha-1}\left(\dfrac{\beta S(t)I(t)}{N} - \gamma I(t) - \mu I(t)\right)\Delta t + \sigma_2 I(t)\Delta B_2(t), \\ R(t+1) = R(t) + t^{\alpha-1}\gamma I(t)\Delta t + \sigma_3 R(t)\Delta B_3(t), \\ D(t+1) = D(t) + t^{\alpha-1}\mu I(t)\Delta t + \sigma_4 D(t)\Delta B_4(t), \end{cases} \tag{3.1}$$

where $\Delta B_i(t) = B_i(t+\Delta t) - B_i(t)$, $i = 1,2,3,4$. Taking into account the reasonableness of the division of time, let $\Delta t = 1$. Since $B_1(t), B_2(t), B_3(t), B_4(t)$ are independent of each other. Based on the properties of the multidimensional normal distribution [18], we can get the probability density function of the fractional stochastic SIRD model as

$$f(t) = \frac{1}{A}\exp\left\{-\frac{1}{2}\left[\begin{array}{c}\left(\dfrac{S(t+1)-S(t)+t^{\alpha-1}\frac{\beta S(t)I(t)}{N}}{\sigma_1 S(t)}\right)^2 + \left(\dfrac{I(t+1)-I(t)-t^{\alpha-1}(\frac{\beta S(t)I(t)}{N}-\gamma I(t)-\mu I(t))}{\sigma_2 I(t)}\right)^2 \\ + \left(\dfrac{R(t+1)-R(t)-t^{\alpha-1}\gamma I(t)}{\sigma_3 R(t)}\right)^2 + \left(\dfrac{D(t+1)-D(t)-t^{\alpha-1}\mu I(t)}{\sigma_4 D(t)}\right)^2\end{array}\right]\right\} \tag{3.2}$$

where $A = 4\pi^2\sigma_1 S(t)\sigma_2 I(t)\sigma_3 R(t)\sigma_4 D(t)$. The joint probability density function, the maximum likelihood function $L(\theta)$, is computed from the above equations as follows.

$$L(\theta) = \prod_{t=1}^{n-1}\left\{\frac{1}{A}\exp\left[-\frac{1}{2}\left(\begin{array}{c}\left(\dfrac{S(t+1)-S(t)+t^{\alpha-1}\frac{\beta S(t)I(t)}{N}}{\sigma_1 S(t)}\right)^2 + \left(\dfrac{D(t+1)-D(t)-t^{\alpha-1}\mu I(t)}{\sigma_4 D(t)}\right)^2 \\ + \left(\dfrac{I(t+1)-I(t)-t^{\alpha-1}\left(\frac{\beta S(t)I(t)}{N}-\gamma I(t)-\mu I(t)\right)}{\sigma_2 I(t)}\right)^2 + \left(\dfrac{R(t+1)-R(t)-t^{\alpha-1}\gamma I(t)}{\sigma_3 R(t)}\right)^2\end{array}\right)\right]\right\}, \tag{3.3}$$

Taking the logarithm of $L(\theta)$, this gives the log-likelihood function of the fractional stochastic SIRD model as

$$\ln L(\theta) = -\sum_{t=1}^{n-1}\left\{\ln A - \frac{1}{2}\left[\begin{array}{l}\left(\frac{S(t+1)-S(t)+t^{\alpha-1}\frac{\beta S(t)I(t)}{N}}{\sigma_1 S(t)}\right)^2+\left(\frac{I(t+1)-I(t)-t^{\alpha-1}\left(\frac{\beta S(t)I(t)}{N}-\gamma I(t)-\mu I(t)\right)}{\sigma_2 I(t)}\right)^2\\ +\left(\frac{R(t+1)-R(t)-t^{\alpha-1}\gamma I(t)}{\sigma_3 R(t)}\right)^2+\left(\frac{D(t+1)-D(t)-t^{\alpha-1}\mu I(t)}{\sigma_4 D(t)}\right)^2\end{array}\right]\right\}. \tag{3.4}$$

The maximum likelihood estimates of the parameters β, γ and μ in the fractional stochastic SIRD model are thus obtained as

$$\begin{pmatrix}\hat{\beta}\\ \hat{\gamma}\\ \hat{\mu}\end{pmatrix} = \begin{pmatrix}\sigma_2^2C_2+\sigma_1^2C_1 & -\sigma_1^2NC_3 & -\sigma_1^2NC_3\\ -\sigma_3^2C_3 & \sigma_3^2NC_4+\sigma_2^2NC_5 & \sigma_3^2NC_4\\ -\sigma_4^2C_3 & \sigma_4^2NC_4 & \sigma_4^2NC_4+\sigma_2^2NC_6\end{pmatrix}^{-1}\begin{pmatrix}\sigma_1^2NA_2-\sigma_2^2NA_1\\ \sigma_2^2NA_4-\sigma_3^2NA_3\\ \sigma_2^2NA_5-\sigma_4^2NA_3\end{pmatrix}, \tag{3.5}$$

where

$$A_1=\sum_{t=1}^{n-1}\frac{t^{\alpha-1}(S(t+1)-S(t))I(t)}{S(t)},\quad A_2=\sum_{t=1}^{n-1}\frac{t^{\alpha-1}(I(t+1)-I(t))S(t)}{I(t)},\quad A_3=\sum_{t=1}^{n-1}\frac{t^{\alpha-1}(I(t+1)-I(t))}{I(t)},$$
$$A_4=\sum_{t=1}^{n-1}\frac{t^{\alpha-1}(R(t+1)-R(t))I(t)}{R^2(t)},\quad A_5=\sum_{t=1}^{n-1}\frac{t^{\alpha-1}(D(t+1)-D(t))I(t)}{D^2(t)},$$
$$C_1=\sum_{t=1}^{n-1}t^{2\alpha-2}S^2(t),\quad C_2=\sum_{t=1}^{n-1}t^{2\alpha-2}I^2(t),\quad C_3=\sum_{t=1}^{n-1}t^{2\alpha-2}S(t),\quad C_4=\sum_{t=1}^{n-1}t^{2\alpha-2},\quad C_5=\sum_{t=1}^{n-1}\frac{t^{2\alpha-2}I^2(t)}{R^2(t)},\quad C_6=\sum_{t=1}^{n-1}\frac{t^{2\alpha-2}I^2(t)}{D^2(t)}.$$

Maximum likelihood estimates of infection rate β, recovery rate γ, and mortality rate μ can are obtained by calculating equation (3.5) using MATLAB software. The fractional stochastic SIRD model can have the lowest possible estimation error by finding a suitable value between $(0,1]$.

4. Example Analysis

Data for the COVID-19 epidemic in India from April 1, 2020, to July 31, 2020, are summarized from Worldometers and the WHO website, and the raw data for the number of infections are plotted in MATLAB as shown in Figure 4.1.

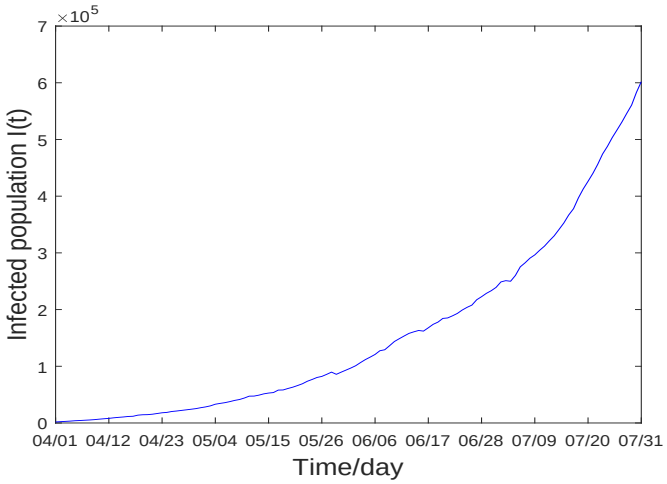

Figure 4.1: Graph of raw data on the number of infections

According to the parameter values of the SIRD model in reference [19], the initial parameters $\beta = 0.0559$, $\gamma = 7.3594\times10^{-4}$ and $\mu = 1.3030\times10^{-5}$ of the fractional SIRD model are obtained by using the lsqcurvefit function in MATLAB software. Using the second-order Adams-Bashforth method [20], numerical solutions of the number of infected people when α is $1, 0.99$, and 0.98 are obtained, as shown in Figure 4.2. The three curves in Figure 4.2 are in good agreement with the true data curves in Figure 4.1, but there is a gap between the simulated and true values for the number of infected people at the intermediate epoch. The fractional SIRD model can make the simulated values of the number of infections as close as possible to the true values by a reasonable choice of the fractional order. The fractional order was continuously adjusted to observe the effect of fitting the fractional SIRD model to the raw data, and the fit was found to be better when α was equal to 0.99. Consider next the stochastic SIRD model. Here $\alpha = 1$, the fractional SIRD model, is the integer SIRD model.

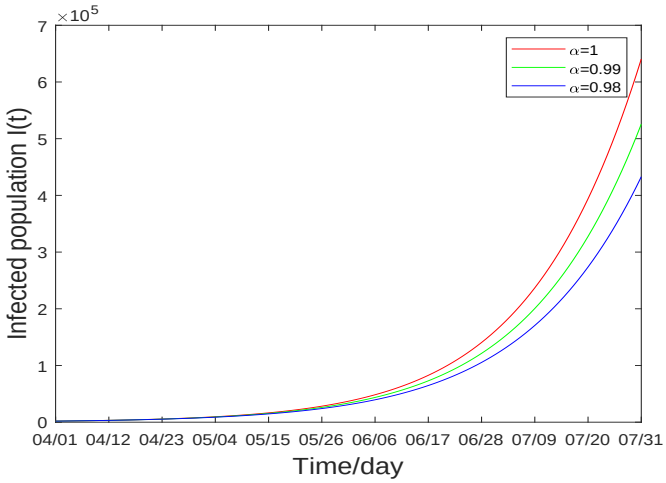

Figure 4.2: Simulation of the number of infected people in the fractional SIRD model

A series of simulation values for the number of infected individuals can be obtained by adjusting the values of the fractional order α, and the noise strength σ_2, of the stochastic SIRD model of the infected population. It can be seen from Table 4.1 that under different noise intensities, when $\alpha = 0.98$, the root mean square error reaches the minimum. And α is between $[0.93, 0.99]$, the root mean square error of the fractional stochastic SIRD model is smaller than that of the integer stochastic SIRD model. The smaller the value of the root mean square error, the better the fit, so the fractional stochastic SIRD model has a better fit than the integer stochastic SIRD model when $\alpha \in [0.93, 0.99]$, and the best result is when $\alpha = 0.98$, respectively.

	$\sigma_2 = 0.0001$	$\sigma_2 = 0.0002$	$\sigma_2 = 0.0003$	$\sigma_2 = 0.0004$
$\alpha = 1$	1.36×10^5	1.38×10^5	1.39×10^5	1.40×10^5
$\alpha = 0.99$	8.04×10^4	8.10×10^4	8.16×10^4	8.19×10^4
$\alpha = 0.98$	5.25×10^4	5.28×10^4	5.28×10^4	5.30×10^4
$\alpha = 0.97$	5.91×10^4	5.88×10^4	5.85×10^4	5.81×10^4
$\alpha = 0.93$	1.34×10^5	1.33×10^5	1.33×10^5	1.33×10^5
$\alpha = 0.92$	1.46×10^5	1.46×10^5	1.46×10^5	1.45×10^5

Table 4.1: RMSE of the number of infected people in the stochastic SIRD model

The maximum likelihood estimates of the parameters β, γ, and μ of the integer and fractional stochastic SIRD models are carried out respectively, the root mean square error between the simulation value and the true value of the number of infected people is calculated at the same time. The parameter results and root mean square errors are shown in Table 4.2. It can be seen from Table 4.2 that when $\alpha = 0.98$, the root mean square error reaches the minimum 5.2452×10^4, and when $\alpha \in [0.93, 0.99]$, the root mean square error of the fractional stochastic SIRD model is smaller than that of the integer stochastic SIRD model. Thus, when $\alpha \in [0.93, 0.99]$, the maximum likelihood estimator for the fractional stochastic SIRD model yields better results than that for the integer stochastic SIRD model.

	$\hat{\beta}$	$\hat{\gamma}$	$\hat{\mu}$	RMSE
$\alpha = 1$	0.0559	7.3646×10^{-4}	1.3046×10^{-5}	1.3589×10^5
$\alpha = 0.99$	0.0559	7.3647×10^{-4}	1.3047×10^{-5}	7.9728×10^4
$\alpha = 0.98$	0.0559	7.3652×10^{-4}	1.3048×10^{-5}	5.2452×10^4
$\alpha = 0.97$	0.0559	7.3660×10^{-4}	1.3057×10^{-5}	5.9574×10^4
$\alpha = 0.93$	0.0559	7.3669×10^{-4}	1.3069×10^{-5}	1.3407×10^5
$\alpha = 0.92$	0.0559	7.3678×10^{-4}	1.3077×10^{-5}	1.4668×10^5

Table 4.2: Maximum likelihood estimation results and RMSE of stochastic SIRD model parameters

This section analyzes the goodness-of-fit of the fractional stochastic SIRD model and the integer stochastic SIRD model to the raw data and compares and analyzes the maximum likelihood estimation results for the parameters of the integer stochastic SIRD model and the fractional stochastic SIRD model. The results show that when the value of α is between $[0.97, 0.99]$, the root mean square error estimated by the fraction stochastic SIRD model is smaller than that of the integer stochastic SIRD model, indicating that the fraction stochastic SIRD model has better estimation effect than the integer stochastic SIRD model, which also indicates that the fraction stochastic SIRD model is more suitable for the actual situation.

5. Conclusion

In this paper, we propose a conformable fractional stochastic SIRD model and perform maximum likelihood estimation of the parameters in the model. Moreover, data from the COVID-19 outbreak in India is used for example analysis. By comparing the simulation graphs of the number of infected persons between the integer stochastic SIRD model and the fractional stochastic SIRD model, the results show that the fitting ability of the original data can be greatly improved by adjusting the order of the fractional stochastic SIRD model reasonably. Also, maximum likelihood estimation results for the parameters of the integer and fractional stochastic SIRD models are compared. It is found that the root mean square error of the fractional stochastic SIRD model is smaller than that of the integer stochastic SIRD model when the fractional order number is between $[0.97, 0.99]$, and when the fractional order is 0.98, the fractional stochastic SIRD model has the best parameter estimation effect. It has been shown that a reasonable choice of the fractional order has a certain effect on the correct understanding and estimation of the model parameters of infectious diseases, and a positive effect on the prediction and prevention of infectious diseases. In recent years, infectious diseases have been ravaging the globe. The study of infectious diseases has become a hot topic. With the deepening of infectious disease models, the estimation of model parameters is becoming more and more important. In future studies, parameter estimation of more complex fractional infectious disease models, such as the SEIRDV model, or models that take into account parameters such as vaccine coverage and level of government intervention, should be considered. It can better adapt to the more complex situation in the present era and optimize parameter estimation methods to reduce estimation errors, leading to more accurate predictions of infectious disease trends and reasonable measures to control the epidemic situation promptly.

Article Information

Acknowledgements: The authors thank the referees for valuable comments and suggestions which improved the presentation of this paper.

Author's Contributions: All authors contributed equally to the writing of this paper. The author has seen the final version of the article and approved its publication.

Conflict of Interest Disclosure: No potential conflict of interest was declared by the author.

Supporting/Supporting Organizations: This research is partially supported by the State Key Program of National Natural Science Foundation of China (72031009), and the College Students' innovation and entrepreneurship training program of China (202210488007).

Ethical Approval and Participant Consent: It is declared that during the preparation process of this study, scientific and ethical principles were followed and all the studies benefited from are stated in the bibliography.

Plagiarism Statement: This article was scanned by the plagiarism program. No plagiarism detected.

Availability of Data and Materials: Not applicable.

References

[1] P. Giles, *The mathematical theory of infectious diseases and its applications*, J. Oper. Res. Soc., **28**(2) (1977), 479-480.
[2] W. O. Kermack, A. G. Mckendrick. *Contributions to the mathematical theory of epidemics–I 1927*, Bull. Math. Biol., **53**(1-2) (1991), 33-55.
[3] N. Becker, *Estimation for an epidemic model*, Biom., **32**(4) (1976), 769-777.
[4] J. Timmer, *Parameter estimation in nonlinear stochastic differential equations*, Chaos. Soliton. Fract., **11**(15) (2000), 2571-2578.
[5] E. Buckingham-Jeffery, V. Isham, T. House, *Gaussian process approximations for fast inference from infectious disease data*, Math. Biosci., **301** (2018), 111-120.
[6] K. Senel, M. Ozdinc, S. Ozturkcan, *Single parameter estimation approach for robust estimation of SIR model with limited and noisy data: The case for COVID-19*, Disaster. Med. Public., **3**(15) (2021), E8-E22.
[7] M. M. Morato, I. M. L. Pataro, M. V. Americano da Costa, J. E. Normey-Rico, *A parametrized nonlinear predictive control strategy for relaxing COVID-19 social distancing measures in Brazil*, Isa. T., **124** (2022), 198-214.
[8] M. Farman, M. U. Saleem, A. Ahmad, M. O. Ahmad, *Analysis and numerical solution of SEIR epidemic model of measles with non-integer time fractional derivatives by using Laplace Adomian Decomposition Method*, Ain. Shams. Eng. J., **9**(4) (2018), 3391-3397.
[9] K. Rajagopal, N. Hasanzaden, F. Parastesh, et al, *A fractional-order model for the novel coronavirus (COVID-19) outbreak*, Nonlinear. Dynam., **101**(1) (2020), 711-718.
[10] B. Basti, N. Hammami, I. Berrabah, F. Nouioua, R. Djemiat, N. Benhamidouche, *Stability analysis and existence of solutions for a modified SIRD model of COVID-19 with fractional derivatives*, Symmetry, **13**(8) (2021), 1431.
[11] H. Mohammadi, S. Rezapour, A. Jajarmi. *On the fractional SIRD mathematical model and control for the transmission of COVID-19: The first and the second waves of the disease in Iran and Japan*, Isa. T., **124** (2022), 103-114.
[12] S. Fouladi, M. Kohandel, B. Eastman. *A comparison and calibration of integer and fractional-order models of COVID-19 with stratified public response*, Math. Biosci. Eng., **19**(12) (2022), 12792-12813.
[13] L. Akinyemi, M Senol, O. S. Iyiola. *Exact solutions of the generalized multidimensional mathematical physics models via sub-equation method*, Math. Comput. Simulat., **182**, (2021), 211-233.
[14] F. Ashraf, A. R. Seadawy, S. Rizvi, et al. *Multi-wave, M-shaped rational and interaction solutions for fractional nonlinear electrical transmission line equation*, JGP., **177**, (2022), 104503.
[15] Y. X. Kang, S. H. Mao, Y. H. Zhang, *Fractional time-varying grey traffic flow model based on viscoelastic fluid and its application*, Transport. Res. B-Meth., **157**, (2022), 149-174.
[16] R. Khalil, M. A. Horani, A. Yousef, et al. *A new definition of fractional derivative*, J. Comput. Appl. Math., **264**(5) (2014), 65-70.
[17] D. Fanelli, F. Piazza, *Analysis and forecast of COVID-19 spreading in China, Italy and France*, Chaos. Sol. Frac., **134** (2020), 109761.
[18] X. M. Wang, *Applied multivariate analysis*. ShangHai: Shanghai University of Finance and Economics Press, (2014).
[19] R. Behl, M. Mishra, *COVID-19 and India: what next?*, Inf. Discov. Deliv., **49**(3) (2020), 250-258.
[20] Y. Wang, Y. Q. Feng, *COVID-19 model and numerical solution based on fractional derivative of Conformable*, Complex. Syst. Complex. Sci., **19**(03) (2022), 27-32.

Fundamental Journal of Mathematics and Applications, 6 (2) (2023) 107-116
Research Article

Fundamental Journal of Mathematics and Applications

Journal Homepage: www.dergipark.org.tr/en/pub/fujma
ISSN: 2645-8845
doi: https://dx.doi.org/10.33401/fujma.1254301

Berezin Radius Inequalities of Functional Hilbert Space Operators

Hamdullah Başaran[1*] **and Mehmet Gürdal**[1]

[1]*Department of Mathematics, Faculty of Science and Arts, Süleyman Demirel University, Isparta, Türkiye*
[*]*Corresponding author*

Article Info

Keywords: *Berezin norm, Berezin radius, Functional Hilbert space*
2010 AMS: *47A30, 47A63, 15A60, 47A12*
Received: *21 February 2023*
Accepted: *27 May 2023*
Available online: *7 June 2023*

Abstract

We investigate new upper bounds for the Berezin radius and Berezin norm of 2×2 operator matrices using the Cauchy-Buzano inequality, and we propose a required condition for the equality case in the triangle inequalities for the Berezin norms. We also show various Berezin radius inequalities for matrices with 2×2 operators.

1. Introduction

Let $\mathbb{L}(\mathscr{H})$ denote the C^*-algebra of all bounded linear operators defined on a complex Hilbert space $(\mathscr{H},\langle .,.\rangle)$. Throughout the paper, we work on functional Hilbert space (FHS), which are complete inner product spaces made up of complex-valued functions defined on a non-empty set Υ with bounded point evaluation. If $\langle Px,x\rangle > 0$ for all $x\in\mathscr{H}$, then an operator $P\in\mathbb{L}(\mathscr{H})$ is called positive. Recall that a functional Hilbert space $\mathscr{H}=\mathscr{H}(\Upsilon)$ is a complex Hilbert space on a (nonempty) Υ, which has the property that point evaluations are continuous for each $\omega\in\Upsilon$ there is a unique element $k_\omega\in\mathscr{H}$ such that $f(\omega)=\langle f,k_\omega\rangle$, for all $f\in\mathscr{H}$. The family $\{k_\omega:\omega\in\Upsilon\}$ is called the reproducing kernel $\mathscr{H}$. If $\{e_n\}_{n\geq 0}$ is an orthonormal basis for FHS, the reproducing kernel is shown by $k_\omega=\sum_{n=0}^{\infty}\overline{e_n(\omega)}e_n(z)$; (see, [1]). For $\omega\in\Upsilon$, $\widehat{k}_\omega=\frac{k_\omega}{\|k_\omega\|}$ is called the normalized reproducing kernel. For $P\in\mathbb{L}(\mathscr{H})$, the function $\widetilde{P}$ defined on Υ by $\widetilde{P}(\omega)=\left\langle P\widehat{k}_\omega,\widehat{k}_\omega\right\rangle$ is the Berezin symbol (or Berezin transform) of P. The Berezin symbol firstly has been introduced by Berezin in [2]. The Berezin set and Berezin radius (or number) of the operator P are defined by

$$\mathrm{Ber}(P)=\left\{\widetilde{P}(\omega):\omega\in\Upsilon\right\}\quad\text{and}\quad\mathrm{ber}(P)=\sup\left\{\left|\widetilde{P}(\omega)\right|:\omega\in\Upsilon\right\},$$

respectively. In some recent works, several Berezin radius inequalities have been examined by authors in [3–10].
We also define the so-called Berezin norm of operators $P\in\mathscr{B}(\mathscr{H})$ as follows:

$$\|P\|_{\mathrm{Ber}}:=\sup_{\varepsilon\in\Upsilon}\left\|P\widehat{k}_\omega\right\|.$$

It is obvious that $\|P\|_{\mathrm{Ber}}$ determines a new operator norm in $\mathbb{L}(\mathscr{H}(\Upsilon))$. It is also obvious that $\mathrm{ber}(P)\leq\|P\|_{\mathrm{Ber}}\leq\|P\|$.
A significant inequality for $\mathrm{ber}(P)$ is the power inequality stating that

$$\mathrm{ber}(P^n)\leq\mathrm{ber}^n(P)$$

Email addresses and ORCID numbers: 07hamdullahbasaran@gmail.com, 0000-0002-9864-9515 (H. Başaran), gurdalmehmet@sdu.edu.tr, 0000-0003-0866-1869 (M. Gürdal)
Cite as: H. Başaran, M. Gürdal, *Berezin radius inequalities of functional Hilbert space operators*, Fundam. J. Math. Appl., 6(2) (2023), 107-116.

for $n = 1,2,\ldots$; more generally, if P is not nilpotent, then

$$C_1 \text{ber}^n(P) \leq \text{ber}(P^n) \leq C_2 \text{ber}^n(P),$$

for some constant $C_1, C_2 > 0$. In a FHS, the Berezin range of an operator P is a subset of numerical range of P, i.e.,

$$\text{Ber}(P) \subseteq W(P).$$

Hence $\text{ber}(P) \leq w(P)$.
The numerical range and numerical radius of $P \in \mathbb{L}(\mathscr{H})$ are denoted by

$$W(P) = \{\langle Px,x\rangle : x \in \mathscr{H} \text{ and } \|x\| = 1\} \text{ and } w(P) = \sup\{|\langle Px,x\rangle| : x \in \mathscr{H} \text{ and } \|x\| = 1\},$$

respectively. The absolute value of positive operator is denoted by $|P| = (P^*P)^{\frac{1}{2}}$. The numerical range has several intriguing features. For example, it is usually assumed that an operator's spectrum is confined in the closure of its numerical range. For an illustration of how this and other numerical radius inequalities were addressed in those sources, we urge the reader read [11–14].
It is well known that

$$\frac{\|P\|}{2} \leq w(P) \leq \|P\|$$

and

$$\text{ber}(P) \leq w(P) \leq \|P\|$$

for any $P \in \mathbb{L}(\mathscr{H})$. Also shown by Karaev in [15] are the Berezin range and Berezin radius of operators, which are numerical features of operators on the FHS. In 2022, Huban et al. [16, 17] have proved the following results:

$$\text{ber}(P) \leq \frac{1}{2}\||P| + |P^*|\|_{\text{ber}} \leq \frac{1}{2}\left(\|P\|_{\text{ber}} + \|P\|_{\text{ber}}^{\frac{1}{2}}\right) \tag{1.1}$$

and

$$\text{ber}^{2r}(P) \leq \frac{1}{2}\left\||P|^{2r} + |P^*|^{2r}\right\|_{\text{ber}} \quad \text{where} \quad r \geq 1.$$

Başaran et al. [18] have showed the following inequality:

$$\text{ber}^2(P) \leq \frac{1}{2}\left\||P|^2 + |P^*|^2\right\|_{\text{ber}}. \tag{1.2}$$

The direct sum of two copies of $\mathscr{H}$ is denoted by $\mathscr{H}^2 = \mathscr{H} \oplus \mathscr{H}$. If $P,R,S,T \in \mathbb{L}(\mathscr{H})$, then the operator matrix $A = \begin{bmatrix} P & R \\ S & T \end{bmatrix}$ can be considered as an operator in $\mathbb{L}(\mathscr{H} \oplus \mathscr{H})$, which is defined by $Ax = \begin{pmatrix} Px_1 + Rx_2 \\ Sx_1 + Tx_2 \end{pmatrix}$ for every vector $x = \begin{pmatrix} x_1 \\ x_2 \end{pmatrix} \in \mathscr{H} \oplus \mathscr{H}$. In 2018, Bakherad, has proved Berezin radius inequalities of block matrix of the form $\begin{bmatrix} 0 & X \\ Y & 0 \end{bmatrix}$ (see, [19–21]). As one can see in [22, 23], where operator norm and numerical radius inequalities were researched and implemented, operator matrices and their properties and inequalities have attracted a lot of attention in the literature.
In order to complete the inequalities for the Berezin number, the numerical radius, and the operator norm, we offer Berezin number inequalities for operator matrices in this study. Our work consists of three sections. In the first section, It has been given introduction. In the second section, it has been given known lemmas. In the third section, it has obtained new upper bounds for the Berezin radius and Berezin norm of 2×2 operator matrices by Cauchy-Buzano inequality. Also, it has been given a necessary condition for the equality case in the triangle inequalities for the Berezin norms. Finally, it has been proven some Berezin radius inequalities for 2×2 operator matrices.

2. Main Results

2.1. Auxiliary theorems

To start our work, we need the following lemmas. The first lemma is found by Bakherad in [19].

Lemma 2.1. *Let $P \in \mathbb{L}(\mathscr{H}_1(\Upsilon))$, $R \in \mathbb{L}(\mathscr{H}_2(\Upsilon), \mathscr{H}_1(\Upsilon))$, $S \in \mathbb{L}(\mathscr{H}_1(\Upsilon), \mathscr{H}_2(\Upsilon))$, $T \in \mathbb{L}(\mathscr{H}_2(\Upsilon))$. Then the following statements holds:*

$$\text{ber}\left(\begin{bmatrix} P & 0 \\ 0 & T \end{bmatrix}\right) = \max\{\text{ber}(P), \text{ber}(T)\} \tag{2.1}$$

and

$$\text{ber}\left(\begin{bmatrix} 0 & R \\ S & 0 \end{bmatrix}\right) = \frac{1}{2}(\|R\| + \|S\|). \tag{2.2}$$

The second lemma arises from the spectral theorem for positive operators and Jensen inequality.

Lemma 2.2 ([24]). *Let $P \in \mathbb{L}(\mathscr{H})$ be a positive operator, and $u \in \mathscr{H}$ is an unit vector. Then*

$$\langle Pu,u\rangle^r \leq \langle P^r u,u\rangle \quad \text{for all} \quad r \geq 1. \tag{2.3}$$

Aujla and Silva provide the third lemma, a norm inequality involving convex functions of positive operators (see [25]).

Lemma 2.3. *let f be a non-negative convex function on $[0,\infty)$, and let $P,R \in \mathbb{L}(\mathscr{H})$ be a positive operators. Then*

$$\left\| f\left(\frac{P+R}{2}\right)\right\| \leq \left\|\frac{f(P)+f(R)}{2}\right\|. \tag{2.4}$$

In particular, if $r \geq 1$, then

$$\left\|\left(\frac{P+R}{2}\right)^r\right\| \leq \left\|\frac{P^r+R^r}{2}\right\|. \tag{2.5}$$

The fourth lemma is shown by Kittaneh (see [24]).

Lemma 2.4. *Let $P \in \mathbb{L}(\mathscr{H})$ and let $u,v \in \mathscr{H}$ be any vectors. Then*

$$|\langle Pu,v\rangle|^2 \leq \langle |P|u,v\rangle \langle |P^*|v,v\rangle. \tag{2.6}$$

The fifth lemma may be found in [26, Lemma 2.2], and it is based on the corollary of Cauchy-Buzano inequality.

Lemma 2.5. *Let $u,v,e \in \mathscr{H}$ and $\|e\| = 1$. Then*

$$|\langle u,e\rangle \langle e,v\rangle|^2 \leq \frac{1}{4}\left(3\|u\|^2\|v\|^2 + \|u\|\|v\| + |\langle u,v\rangle|\right). \tag{2.7}$$

For any positive operators A,B, the classic Arithmetic Mean-Geometric Mean inequality, often known as AM-GM inequality, states that $\sqrt{AB} \leq \frac{A+B}{2}$.

2.2. Some Berezin radius inequalities

Our findings are presented in this section. Now, we can the prove the first theorem.

Theorem 2.6. *Let $P,R \in \mathbb{L}(\mathscr{H})$. Then*

$$\operatorname{ber}\left(\begin{bmatrix} P & R \\ R & P \end{bmatrix}\right) = \max\{\operatorname{ber}(P+R), \operatorname{ber}(P-R)\} \tag{2.8}$$

In particular,

$$\operatorname{ber}\left(\begin{bmatrix} 0 & R \\ R & 0 \end{bmatrix}\right) = \operatorname{ber}(R).$$

Proof. Assume $U = \frac{1}{\sqrt{2}}\begin{bmatrix} I & I \\ -I & I \end{bmatrix}$ and $T = \begin{bmatrix} P & R \\ R & P \end{bmatrix}$. It can easy that

$$U^*TU = \begin{bmatrix} P-R & 0 \\ 0 & P+R \end{bmatrix}.$$

Using the inequality (2.1) and $\operatorname{ber}(U^*TU) = \operatorname{ber}(T)$, we have

$$\operatorname{ber}(T) = \max\{\operatorname{ber}(P+R), \operatorname{ber}(P-R)\}.$$

For $P = 0$, we get

$$\operatorname{ber}\left(\begin{bmatrix} 0 & R \\ R & 0 \end{bmatrix}\right) = \operatorname{ber}(R).$$

□

Theorem 2.7. *Let $\mathscr{H} = \mathscr{H}(\Upsilon)$ be a FHS and $P,R,S,T \in \mathbb{L}(\mathscr{H})$. Then*

$$\begin{aligned} \operatorname{ber}^2\left(\begin{bmatrix} P & R \\ S & T \end{bmatrix}\right) &= \max\left\{\operatorname{ber}^2(P), \operatorname{ber}^2(T)\right\} + \operatorname{ber}^2\left(\begin{bmatrix} 0 & R \\ S & 0 \end{bmatrix}\right) \\ &\quad + \max\{\|P\|_{\mathrm{Ber}}, \|T\|_{\mathrm{Ber}}\} \max\{\|R\|_{\mathrm{Ber}}, \|S\|_{\mathrm{Ber}}\} + \operatorname{ber}\left(\begin{bmatrix} 0 & S^*T \\ R^*P & 0 \end{bmatrix}\right). \end{aligned} \tag{2.9}$$

Proof. For every $(\omega_1,\omega_2),(\varkappa_1,\varkappa_2)\in\Upsilon_1\times\Upsilon_2$, let $\widehat{k}_w=\widehat{k}_{(\omega_1,\omega_2)}=\begin{bmatrix}k_{\omega_1}\\k_{\omega_2}\end{bmatrix}$, $\widehat{k}_\varkappa=\widehat{k}_{(\varkappa_1,\varkappa_2)}=\begin{bmatrix}k_{\varkappa_1}\\k_{\varkappa_2}\end{bmatrix}$ be a normalized reproducing kernel in $\mathscr{H}(\Upsilon_1)\oplus\mathscr{H}(\Upsilon_2)$. Then we have

$$\begin{aligned}
\left|\left\langle\begin{bmatrix}P&R\\S&T\end{bmatrix}\widehat{k}_w,\widehat{k}_\varkappa\right\rangle\right|^2 &= \left|\left\langle\left(\begin{bmatrix}P&0\\0&T\end{bmatrix}+\begin{bmatrix}0&R\\S&0\end{bmatrix}\right)\widehat{k}_w,\widehat{k}_\varkappa\right\rangle\right|^2\\
&\le \left|\left\langle\begin{bmatrix}P&0\\0&T\end{bmatrix}\widehat{k}_w,\widehat{k}_\varkappa\right\rangle+\left\langle\begin{bmatrix}0&R\\S&0\end{bmatrix}\widehat{k}_w,\widehat{k}_\varkappa\right\rangle\right|^2\\
&\le \left(\left|\left\langle\begin{bmatrix}P&0\\0&T\end{bmatrix}\widehat{k}_w,\widehat{k}_\varkappa\right\rangle\right|+\left|\left\langle\begin{bmatrix}0&R\\S&0\end{bmatrix}\widehat{k}_w,\widehat{k}_\varkappa\right\rangle\right|\right)^2\\
&= \left|\left\langle\begin{bmatrix}P&0\\0&T\end{bmatrix}\widehat{k}_w,\widehat{k}_\varkappa\right\rangle\right|^2+\left|\left\langle\begin{bmatrix}0&R\\S&0\end{bmatrix}\widehat{k}_w,\widehat{k}_\varkappa\right\rangle\right|^2+2\left|\left\langle\begin{bmatrix}P&0\\0&T\end{bmatrix}\widehat{k}_w,\widehat{k}_\varkappa\right\rangle\right|\left|\left\langle\begin{bmatrix}0&R\\S&0\end{bmatrix}\widehat{k}_w,\widehat{k}_\varkappa\right\rangle\right|\\
&= \left|\left\langle\begin{bmatrix}P&0\\0&T\end{bmatrix}\widehat{k}_w,\widehat{k}_w\right\rangle\right|^2+\left|\left\langle\begin{bmatrix}0&R\\S&0\end{bmatrix}\widehat{k}_w,\widehat{k}_w\right\rangle\right|^2+2\left|\left\langle\begin{bmatrix}P&0\\0&T\end{bmatrix}\widehat{k}_w,\widehat{k}_\varkappa\right\rangle\right|\left|\left\langle\widehat{k}_\varkappa,\begin{bmatrix}0&R\\S&0\end{bmatrix}\widehat{k}_w\right\rangle\right|\\
&\le \left|\left\langle\begin{bmatrix}P&0\\0&T\end{bmatrix}\widehat{k}_w,\widehat{k}_\varkappa\right\rangle\right|^2+\left|\left\langle\begin{bmatrix}0&R\\S&0\end{bmatrix}\widehat{k}_w,\widehat{k}_\varkappa\right\rangle\right|^2+\left\|\begin{bmatrix}P&0\\0&T\end{bmatrix}\widehat{k}_w\right\|\left\|\begin{bmatrix}0&R\\S&0\end{bmatrix}\widehat{k}_w\right\|\\
&\quad+\left|\left\langle\begin{bmatrix}0&S^*T\\R^*P&0\end{bmatrix}\widehat{k}_w,\widehat{k}_w\right\rangle\right|.
\end{aligned}$$

where the sixth inequality follows from Buzano's inequality (see [27]), i.e., if $u,v,e\in\mathscr{H}$ and $\|e\|=1$, then

$$|\langle u,e\rangle\langle e,v\rangle|\le\frac{1}{2}\left(\|u\|\|v\|+|\langle u,v\rangle|\right). \tag{2.10}$$

So, we get

$$\begin{aligned}
\left|\left\langle\begin{bmatrix}P&R\\S&T\end{bmatrix}\widehat{k}_w,\widehat{k}_\varkappa\right\rangle\right|^2 &\le \left|\left\langle\begin{bmatrix}P&0\\0&T\end{bmatrix}\widehat{k}_w,\widehat{k}_\varkappa\right\rangle\right|^2+\left|\left\langle\begin{bmatrix}0&R\\S&0\end{bmatrix}\widehat{k}_w,\widehat{k}_\varkappa\right\rangle\right|^2+\left\|\begin{bmatrix}P&0\\0&T\end{bmatrix}\widehat{k}_w\right\|\left\|\begin{bmatrix}0&R\\S&0\end{bmatrix}\widehat{k}_w\right\|\\
&\quad+\left|\left\langle\begin{bmatrix}0&S^*T\\R^*P&0\end{bmatrix}\widehat{k}_w,\widehat{k}_w\right\rangle\right|.
\end{aligned}$$

Now, taking the supremum over $(\omega_1,\omega_2),(\varkappa_1,\varkappa_2)\in\Upsilon_1\times\Upsilon_2$ with $(\omega_1,\omega_2)=(\varkappa_1,\varkappa_2)$ and then applying inequality (2.1) in the above inequality, we have

$$\begin{aligned}
\mathrm{ber}^2\left(\begin{bmatrix}P&R\\S&T\end{bmatrix}\right) &= \max\left\{\mathrm{ber}^2(P),\mathrm{ber}^2(T)\right\}+\mathrm{ber}^2\left(\begin{bmatrix}0&R\\S&0\end{bmatrix}\right)\\
&\quad+\max\left\{\|P\|_{\mathrm{Ber}},\|T\|_{\mathrm{Ber}}\right\}\max\left\{\|R\|_{\mathrm{Ber}},\|S\|_{\mathrm{Ber}}\right\}+\mathrm{ber}\left(\begin{bmatrix}0&S^*T\\R^*P&0\end{bmatrix}\right).
\end{aligned}$$

The proof is now complete. □

Several inequalities for Berezin radius inequalities of operator matrices are included in the preceding theorem. The following corollaries show these inequities.

Corollary 2.8. *If $(\omega_1,\omega_2)\neq(\varkappa_1,\varkappa_2)$, then we have*

$$\begin{aligned}
\left\|\begin{bmatrix}P&R\\S&T\end{bmatrix}\right\|^2 &= \max\left\{\|P\|^2,\|T\|^2\right\}+\max\left\{\|R\|^2,\|S\|^2\right\}\\
&\quad+\max\left\{\|P\|_{\mathrm{Ber}},\|T\|_{\mathrm{Ber}}\right\}\max\left\{\|R\|_{\mathrm{Ber}},\|S\|_{\mathrm{Ber}}\right\}+\mathrm{ber}\left(\begin{bmatrix}0&S^*T\\R^*P&0\end{bmatrix}\right).
\end{aligned}$$

Corollary 2.9. *If we apply the inequality (2.2) to inequality (2.9), we have*

$$\begin{aligned}
\mathrm{ber}^2\left(\begin{bmatrix}P&R\\S&T\end{bmatrix}\right) &= \max\left\{\mathrm{ber}^2(P),\mathrm{ber}^2(T)\right\}+\frac{1}{4}\left(\|R\|+\|S\|\right)^2\\
&\quad+\max\left\{\|P\|_{\mathrm{Ber}},\|T\|_{\mathrm{Ber}}\right\}\max\left\{\|R\|_{\mathrm{Ber}},\|S_{\mathrm{Ber}}\|\right\}+\frac{1}{4}\left(\|R^*P\|+\|S^*T\|\right).
\end{aligned}$$

The following corollary follows easily from the inequality (2.8) in Theorem 2.6.

Corollary 2.10. *If we take $P=T$ and $R=S$ in the Theorem 2.7 and Corollary 2.8, we get*

(i) $\operatorname{ber}^2\left(\begin{bmatrix} P & R \\ R & P \end{bmatrix}\right) = \max\left\{\operatorname{ber}^2(P+R), \operatorname{ber}^2(P-R)\right\} \leq \operatorname{ber}^2(P) + \operatorname{ber}^2(R) + \|P\|\|R\| + \operatorname{ber}(R^*P)$,

(ii) $\left\|\begin{bmatrix} P & R \\ R & P \end{bmatrix}\right\|^2 = \max\left\{\|P+R\|^2, \|P-R\|^2\right\} \leq \|P\|^2 + \|R\|^2 + \|P\|\|R\| + \operatorname{ber}(R^*P)$.

After that, it is simple that to prove Corollary 2.10 may be used to provide a required condition for the equality case in the triangle inequality for Berezin radius.

Proposition 2.11. *Let $\mathscr{H} = \mathscr{H}(\Upsilon)$ be a FHS and $P, R \in \mathbb{L}(\mathscr{H})$.*

(i) If $\operatorname{ber}(P+R) = \operatorname{ber}(P) + \operatorname{ber}(R)$, then we have $2\operatorname{ber}(P)\operatorname{ber}(R) - \operatorname{ber}(R^*P) = \|P\|_{\text{Ber}}\|R\|_{\text{Ber}}$.
(ii) If $\|P+R\| = \|P\| + \|R\|$, then we have $\operatorname{ber}(R^*P) = \|P\|_{\text{Ber}}\|R\|_{\text{Ber}}$.

Proof. By using $\operatorname{ber}(P+R) = \operatorname{ber}(P) + \operatorname{ber}(R)$ and $\|P+R\| = \|P\| + \|R\|$ in Corollary 2.10, respectively, we get the required inequalities. □

Theorem 2.12. *Let $P, R, S, T \in \mathbb{L}(\mathscr{H})$. Then*

$$\begin{aligned} \operatorname{ber}^2\left(\begin{bmatrix} P & R \\ S & T \end{bmatrix}\right) &= \max\left\{\operatorname{ber}^2(P), \operatorname{ber}^2(T)\right\} + \operatorname{ber}^2\left(\begin{bmatrix} 0 & R \\ S & 0 \end{bmatrix}\right) \\ &\quad + \frac{1}{2}\max\left\{\left\||P|^2 + |R^*|^2\right\|_{\text{ber}}, \left\||T|^2 + |S^*|^2\right\|_{\text{ber}}\right\} + \operatorname{ber}\left(\begin{bmatrix} 0 & RT \\ SP & 0 \end{bmatrix}\right). \end{aligned} \tag{2.11}$$

Proof. For every $(\omega_1, \omega_2) \in \Upsilon_1 \times \Upsilon_2$, let $\widehat{k}_w = \widehat{k}_{(\omega_1,\omega_2)} = \begin{bmatrix} k_{\omega_1} \\ k_{\omega_2} \end{bmatrix}$ be a normalized reproducing kernel in $\mathscr{H}(\Upsilon_1) \oplus \mathscr{H}(\Upsilon_2)$. Using the AM-GM inequality and (2.10), we establish the following inequality using the same approach as in Theorem 2.7:

$$\begin{aligned} \left|\left\langle \begin{bmatrix} P & R \\ S & T \end{bmatrix}\widehat{k}_w, \widehat{k}_w \right\rangle\right|^2 &= \left|\left\langle \left(\begin{bmatrix} P & 0 \\ 0 & T \end{bmatrix} + \begin{bmatrix} 0 & R \\ S & 0 \end{bmatrix}\right)\widehat{k}_w, \widehat{k}_w \right\rangle\right|^2 \\ &\leq \left|\left\langle \begin{bmatrix} P & 0 \\ 0 & T \end{bmatrix}\widehat{k}_w, \widehat{k}_w \right\rangle + \left\langle \begin{bmatrix} 0 & R \\ S & 0 \end{bmatrix}\widehat{k}_w, \widehat{k}_w \right\rangle\right|^2 \\ &\leq \left(\left|\left\langle \begin{bmatrix} P & 0 \\ 0 & T \end{bmatrix}\widehat{k}_w, \widehat{k}_w \right\rangle\right| + \left|\left\langle \begin{bmatrix} 0 & R \\ S & 0 \end{bmatrix}\widehat{k}_w, \widehat{k}_w \right\rangle\right|\right)^2 \\ &= \left|\left\langle \begin{bmatrix} P & 0 \\ 0 & T \end{bmatrix}\widehat{k}_w, \widehat{k}_w \right\rangle\right|^2 + \left|\left\langle \begin{bmatrix} 0 & R \\ S & 0 \end{bmatrix}\widehat{k}_w, \widehat{k}_w \right\rangle\right|^2 + 2\left|\left\langle \begin{bmatrix} P & 0 \\ 0 & T \end{bmatrix}\widehat{k}_w, \widehat{k}_w \right\rangle\right|\left|\left\langle \begin{bmatrix} 0 & R \\ S & 0 \end{bmatrix}\widehat{k}_w, \widehat{k}_w \right\rangle\right| \\ &= \left|\left\langle \begin{bmatrix} P & 0 \\ 0 & T \end{bmatrix}\widehat{k}_w, \widehat{k}_w \right\rangle\right|^2 + \left|\left\langle \begin{bmatrix} 0 & R \\ S & 0 \end{bmatrix}\widehat{k}_w, \widehat{k}_w \right\rangle\right|^2 + 2\left|\left\langle \begin{bmatrix} P & 0 \\ 0 & T \end{bmatrix}\widehat{k}_w, \widehat{k}_w \right\rangle\right|\left|\left\langle \widehat{k}_w, \begin{bmatrix} 0 & R \\ S & 0 \end{bmatrix}\widehat{k}_w \right\rangle\right| \\ &\leq \left|\left\langle \begin{bmatrix} P & 0 \\ 0 & T \end{bmatrix}\widehat{k}_w, \widehat{k}_w \right\rangle\right|^2 + \left|\left\langle \begin{bmatrix} 0 & R \\ S & 0 \end{bmatrix}\widehat{k}_w, \widehat{k}_w \right\rangle\right|^2 + \left\|\begin{bmatrix} P & 0 \\ 0 & T \end{bmatrix}\widehat{k}_w\right\|\left\|\begin{bmatrix} 0 & R \\ S & 0 \end{bmatrix}\widehat{k}_w\right\| \\ &\quad + \left|\left\langle \begin{bmatrix} P & 0 \\ 0 & T \end{bmatrix}\widehat{k}_w, \begin{bmatrix} 0 & S^* \\ R^* & 0 \end{bmatrix}\widehat{k}_w \right\rangle\right| \\ &\leq \left|\left\langle \begin{bmatrix} P & 0 \\ 0 & T \end{bmatrix}\widehat{k}_w, \widehat{k}_w \right\rangle\right|^2 + \left|\left\langle \begin{bmatrix} 0 & R \\ S & 0 \end{bmatrix}\widehat{k}_w, \widehat{k}_w \right\rangle\right|^2 + \sqrt{\left\langle \left|\begin{bmatrix} P & 0 \\ 0 & T \end{bmatrix}\right|^2 \widehat{k}_w, \widehat{k}_w \right\rangle\left\langle \left|\begin{bmatrix} 0 & S^* \\ R^* & 0 \end{bmatrix}\right|^2 \widehat{k}_w, \widehat{k}_w \right\rangle} \\ &\quad + \left|\left\langle \begin{bmatrix} 0 & RT \\ SP & 0 \end{bmatrix}\widehat{k}_w, \widehat{k}_w \right\rangle\right| \\ &\leq \left|\left\langle \begin{bmatrix} P & 0 \\ 0 & T \end{bmatrix}\widehat{k}_w, \widehat{k}_w \right\rangle\right|^2 + \left|\left\langle \begin{bmatrix} 0 & R \\ S & 0 \end{bmatrix}\widehat{k}_w, \widehat{k}_w \right\rangle\right|^2 + \frac{1}{2}\left\langle \begin{bmatrix} |P|^2 + |R^*|^2 & 0 \\ 0 & |T|^2 + |S^*|^2 \end{bmatrix}\widehat{k}_w, \widehat{k}_w \right\rangle \\ &\quad + \left|\left\langle \begin{bmatrix} 0 & RT \\ SP & 0 \end{bmatrix}\widehat{k}_w, \widehat{k}_w \right\rangle\right|. \end{aligned}$$

By taking the supremum over $(\omega_1, \omega_2) \in \Upsilon_1 \times \Upsilon_2$ and applying the inequality (2.1) in the above inequality, we have

$$\begin{aligned} \operatorname{ber}^2\left(\begin{bmatrix} P & R \\ S & T \end{bmatrix}\right) &= \max\left\{\operatorname{ber}^2(P), \operatorname{ber}^2(T)\right\} + \operatorname{ber}^2\left(\begin{bmatrix} 0 & R \\ S & 0 \end{bmatrix}\right) \\ &\quad + \frac{1}{2}\max\left\{\left\||P|^2 + |R^*|^2\right\|_{\text{ber}}, \left\||T|^2 + |S^*|^2\right\|_{\text{ber}}\right\} + \operatorname{ber}\left(\begin{bmatrix} 0 & RT \\ SP & 0 \end{bmatrix}\right). \end{aligned}$$

We have desired result. □

Several Berezin radius inequalities for operator matrices are contained in Theorem 2.12. The following corollaries demonstrate some of these inequalities.

Corollary 2.13. *If we apply the inequality (2.2) to inequality (2.11), then we have*

$$\begin{aligned}\operatorname{ber}^2\left(\begin{bmatrix}P & R\\ S & T\end{bmatrix}\right) &= \max\left\{\operatorname{ber}^2(P),\operatorname{ber}^2(T)\right\}+\frac{1}{4}\left(\|R\|+\|S\|\right)^2\\ &\quad+\frac{1}{2}\max\left\{\left\||P|^2+|R^*|^2\right\|_{\text{ber}},\left\||T|^2+|S^*|^2\right\|_{\text{ber}}\right\}+\frac{1}{2}\left(\|RT\|+\|SP\|\right).\end{aligned}$$

The inequality (2.8) in Theorem 2.6 simply leads to the following consequence.

Corollary 2.14. *If we take $P=T$ and $R=S$ in Theorem 2.12, then we get*

$$\operatorname{ber}^2\left(\begin{bmatrix}P & R\\ R & P\end{bmatrix}\right)=\max\left\{\operatorname{ber}^2(P+R),\operatorname{ber}^2(P-R)\right\}\leq\operatorname{ber}^2(P)+\operatorname{ber}^2(R)+\frac{1}{2}\left\||P|^2+|R^*|^2\right\|_{\text{ber}}+\operatorname{ber}(RP).$$

Corollary 2.15. *If we take $P=R$ in Corollary 2.14, then we have*

$$\operatorname{ber}^2(P)\leq\frac{1}{4}\left\||P|^2+|P^*|^2\right\|_{\text{ber}}+\frac{1}{2}\operatorname{ber}\left(P^2\right),$$

(see, [28, Corollary 2.14]).

Theorem 2.16. *Let $P,R,S,T\in\mathbb{L}(\mathscr{H})$. Then*

$$\begin{aligned}\operatorname{ber}^2\left(\begin{bmatrix}P & R\\ S & T\end{bmatrix}\right) &= \max\left\{\operatorname{ber}^2(P),\operatorname{ber}^2(T)\right\}+\frac{1}{4}\max\left\{\left\||S|^2+|R^*|^2\right\|_{\text{ber}},\left\||R|^2+|S^*|^2\right\|_{\text{ber}}\right\}\\ &\quad+\max\left\{\operatorname{ber}(P),\operatorname{ber}(T)\right\}\max\left\{\||S|+|R^*|\|_{\text{ber}},\||R|+|S^*|\|_{\text{ber}}\right\}+\frac{1}{2}\max\left\{\operatorname{ber}(SR),\operatorname{ber}(RS)\right\}.\end{aligned}$$

Proof. For every $(\omega_1,\omega_2)\in\Upsilon_1\times\Upsilon_2$, let $\widehat{k}_w=\widehat{k}_{(\omega_1,\omega_2)}=\begin{bmatrix}k_{\omega_1}\\ k_{\omega_2}\end{bmatrix}$ be a normalized reproducing kernel in $\mathscr{H}(\Upsilon_1)\oplus\mathscr{H}(\Upsilon_2)$. Following the same procedure as in Theorem 2.7 and by using the AM-GM inequality, (2.6) and (2.10), the following inequality is obtained:

$$\begin{aligned}\left|\left\langle\begin{bmatrix}P & R\\ S & T\end{bmatrix}\widehat{k}_w,\widehat{k}_w\right\rangle\right|^2 &= \left|\left\langle\left(\begin{bmatrix}P & 0\\ 0 & T\end{bmatrix}+\begin{bmatrix}0 & R\\ S & 0\end{bmatrix}\right)\widehat{k}_w,\widehat{k}_w\right\rangle\right|^2\\ &\leq\left(\left|\left\langle\begin{bmatrix}P & 0\\ 0 & T\end{bmatrix}\widehat{k}_w,\widehat{k}_w\right\rangle\right|+\left|\left\langle\begin{bmatrix}0 & R\\ S & 0\end{bmatrix}\widehat{k}_w,\widehat{k}_w\right\rangle\right|\right)^2\\ &\leq\left(\left|\left\langle\begin{bmatrix}P & 0\\ 0 & T\end{bmatrix}\widehat{k}_w,\widehat{k}_w\right\rangle\right|+\left|\left\langle\begin{bmatrix}0 & R\\ S & 0\end{bmatrix}\widehat{k}_w,\widehat{k}_w\right\rangle\right|\right)^2\\ &=\left|\left\langle\begin{bmatrix}P & 0\\ 0 & T\end{bmatrix}\widehat{k}_w,\widehat{k}_w\right\rangle\right|^2+2\left|\left\langle\begin{bmatrix}P & 0\\ 0 & T\end{bmatrix}\widehat{k}_w,\widehat{k}_w\right\rangle\right|\left|\left\langle\begin{bmatrix}0 & R\\ S & 0\end{bmatrix}\widehat{k}_w,\widehat{k}_w\right\rangle\right|+\left|\left\langle\begin{bmatrix}0 & R\\ S & 0\end{bmatrix}\widehat{k}_w,\widehat{k}_w\right\rangle\right|^2\\ &\leq\left|\left\langle\begin{bmatrix}P & 0\\ 0 & T\end{bmatrix}\widehat{k}_w,\widehat{k}_w\right\rangle\right|^2+2\left|\left\langle\begin{bmatrix}P & 0\\ 0 & T\end{bmatrix}\widehat{k}_w,\widehat{k}_w\right\rangle\right|\sqrt{\left\langle\left|\begin{bmatrix}0 & R\\ S & 0\end{bmatrix}\right|\widehat{k}_w,\widehat{k}_w\right\rangle\left\langle\left|\begin{bmatrix}0 & S^*\\ R^* & 0\end{bmatrix}\right|\widehat{k}_w,\widehat{k}_w\right\rangle}\\ &\quad+\frac{1}{2}\left(\sqrt{\left\langle\left|\begin{bmatrix}0 & R\\ S & 0\end{bmatrix}\right|^2\widehat{k}_w,\widehat{k}_w\right\rangle\left\langle\left|\begin{bmatrix}0 & S^*\\ R^* & 0\end{bmatrix}\right|^2\widehat{k}_w,\widehat{k}_w\right\rangle}+\left|\left\langle\begin{bmatrix}0 & R\\ S & 0\end{bmatrix}\widehat{k}_w,\begin{bmatrix}0 & S^*\\ R^* & 0\end{bmatrix}\widehat{k}_w\right\rangle\right|\right)\\ &\leq\left|\left\langle\begin{bmatrix}P & 0\\ 0 & T\end{bmatrix}\widehat{k}_w,\widehat{k}_w\right\rangle\right|^2+\left|\left\langle\begin{bmatrix}P & 0\\ 0 & T\end{bmatrix}\widehat{k}_w,\widehat{k}_w\right\rangle\right|\left(\left\langle\left|\begin{bmatrix}0 & R\\ S & 0\end{bmatrix}\right|\widehat{k}_w,\widehat{k}_w\right\rangle+\left\langle\left|\begin{bmatrix}0 & S^*\\ R^* & 0\end{bmatrix}\right|\widehat{k}_w,\widehat{k}_w\right\rangle\right)\\ &\quad+\frac{1}{4}\left(\left\langle\left|\begin{bmatrix}0 & R\\ S & 0\end{bmatrix}\right|^2\widehat{k}_w,\widehat{k}_w\right\rangle+\left\langle\left|\begin{bmatrix}0 & S^*\\ R^* & 0\end{bmatrix}\right|^2\widehat{k}_w,\widehat{k}_w\right\rangle\right)+\frac{1}{2}\left|\left\langle\begin{bmatrix}RS & 0\\ 0 & SR\end{bmatrix}\widehat{k}_w,\widehat{k}_w\right\rangle\right|\\ &\leq\left|\left\langle\begin{bmatrix}P & 0\\ 0 & T\end{bmatrix}\widehat{k}_w,\widehat{k}_w\right\rangle\right|^2+\left|\left\langle\begin{bmatrix}P & 0\\ 0 & T\end{bmatrix}\widehat{k}_w,\widehat{k}_w\right\rangle\right|\left(\left\langle\begin{bmatrix}|S|+|R^*| & 0\\ 0 & |R|+|S^*|\end{bmatrix}\widehat{k}_w,\widehat{k}_w\right\rangle\right)\\ &\quad+\frac{1}{4}\left(\left\langle\left|\begin{bmatrix}|S|^2+|R^*|^2 & 0\\ 0 & |R|^2+|S^*|^2\end{bmatrix}\right|^2\widehat{k}_w,\widehat{k}_w\right\rangle\right)+\frac{1}{2}\left|\left\langle\begin{bmatrix}RS & 0\\ 0 & SR\end{bmatrix}\widehat{k}_w,\widehat{k}_w\right\rangle\right|,\end{aligned}$$

and, so

$$\begin{aligned}\left|\left\langle\begin{bmatrix}P & R\\ S & T\end{bmatrix}\widehat{k}_w,\widehat{k}_w\right\rangle\right|^2 &\leq \left|\left\langle\begin{bmatrix}P & 0\\ 0 & T\end{bmatrix}\widehat{k}_w,\widehat{k}_w\right\rangle\right|^2+\left|\left\langle\begin{bmatrix}P & 0\\ 0 & T\end{bmatrix}\widehat{k}_w,\widehat{k}_w\right\rangle\right|\left(\left\langle\begin{bmatrix}|S|+|R^*| & 0\\ 0 & |R|+|S^*|\end{bmatrix}\widehat{k}_w,\widehat{k}_w\right\rangle\right)\\ &\quad+\frac{1}{4}\left(\left\langle\left|\begin{bmatrix}|S|^2+|R^*|^2 & 0\\ 0 & |R|^2+|S^*|^2\end{bmatrix}\right|^2\widehat{k}_w,\widehat{k}_w\right\rangle\right)+\frac{1}{2}\left|\left\langle\begin{bmatrix}RS & 0\\ 0 & SR\end{bmatrix}\widehat{k}_w,\widehat{k}_w\right\rangle\right|.\end{aligned}$$

By taking the supremum over $(\omega_1,\omega_2)\in\Upsilon_1\times\Upsilon_2$ and using inequality (2.1) in the above inequality, we have

$$\begin{aligned}\mathrm{ber}^2\left(\begin{bmatrix}P & R\\ S & T\end{bmatrix}\right) &= \max\left\{\mathrm{ber}^2(P),\mathrm{ber}^2(T)\right\}+\frac{1}{4}\max\left\{\left\||S|^2+|R^*|^2\right\|_{\mathrm{ber}},\left\||R|^2+|S^*|^2\right\|_{\mathrm{ber}}\right\}\\ &\quad+\max\left\{\mathrm{ber}(P),\mathrm{ber}(T)\right\}\max\left\{\||S|+|R^*|\|_{\mathrm{ber}},\||R|+|S^*|\|_{\mathrm{ber}}\right\}\\ &\quad+\frac{1}{2}\max\left\{\mathrm{ber}(RS),\mathrm{ber}(SR)\right\}.\end{aligned}$$

□

The inequality (2.8) in Theorem 2.6 and a particular application of Theorem 2.16 lead to the following conclusion, which is straightforward to deduce.

Corollary 2.17. *If $P=T$ and $R=S$, then it follows from Theorem 2.16 that*

$$\mathrm{ber}^2\left(\begin{bmatrix}P & R\\ R & P\end{bmatrix}\right)=\max\left\{\mathrm{ber}^2(P+R),\mathrm{ber}^2(P-R)\right\}\leq\mathrm{ber}^2(P)+\frac{1}{4}\left\||R|^2+|R^*|^2\right\|_{\mathrm{ber}}+\mathrm{ber}(P)\||R|+|R^*|\|_{\mathrm{ber}}+\frac{1}{2}\mathrm{ber}\left(R^2\right).$$

Corollary 2.18. *If we take $P=R$ in Corollary 2.17, then we get the inequality (1.2)*

$$\mathrm{ber}^2(P)\leq\frac{1}{2}\left\||P|^2+|P^*|^2\right\|_{\mathrm{ber}}$$

(see, [18, Theorem 3.2]).

Proof. From Corollary 2.17, we reach

$$4\mathrm{ber}^2(P)\leq\mathrm{ber}^2(P)+\frac{1}{4}\left\||P|^2+|P^*|^2\right\|_{\mathrm{ber}}+\mathrm{ber}(P)\||P|+|P^*|\|_{\mathrm{ber}}+\frac{1}{2}\mathrm{ber}\left(P^2\right).$$

Also, by using the inequality (1.1), we have

$$3\mathrm{ber}^2(P)\leq\frac{1}{4}\left\||P|^2+|P^*|^2\right\|_{\mathrm{ber}}+\mathrm{ber}(P)\||P|+|P^*|\|_{\mathrm{ber}}+\frac{1}{2}\mathrm{ber}^2(P).$$

Then using the inequalities (1.1) and (2.5), we get

$$\begin{aligned}\frac{5}{2}\mathrm{ber}^2(P) &\leq \frac{1}{4}\left\||P|^2+|P^*|^2\right\|_{\mathrm{ber}}+\frac{1}{2}\||P|+|P^*|\|_{\mathrm{ber}}^2\\ &= \frac{1}{4}\left\||P|^2+|P^*|^2\right\|_{\mathrm{ber}}+\left\|\frac{|P|+|P^*|}{2}\right\|_{\mathrm{ber}}^2\\ &\leq \frac{1}{4}\left\||P|^2+|P^*|^2\right\|_{\mathrm{ber}}+\left\|\frac{|P|^2+|P^*|^2}{2}\right\|_{\mathrm{ber}}\\ &\leq \frac{1}{4}\left\||P|^2+|P^*|^2\right\|_{\mathrm{ber}}+\left\||P|^2+|P^*|^2\right\|_{\mathrm{ber}}\\ &\leq \frac{5}{4}\left\||P|^2+|P^*|^2\right\|_{\mathrm{ber}}\end{aligned}$$

and

$$\mathrm{ber}^2(P)\leq\frac{1}{2}\left\||P|^2+|P^*|^2\right\|_{\mathrm{ber}}$$

as desired. □

Taking $P=0$ and $P=T=0$ in Corollary 2.17 and Theorem 2.16, respectively, we obtain the following corollary.

Remark 2.19. *$\mathscr{H}=\mathscr{H}(\Upsilon)$ be a FHS and $R,S\in\mathbb{L}(\mathscr{H})$. Then*

$$\operatorname{ber}^2(R)\leq\frac{1}{4}\left\||R|^2+|R^*|^2\right\|_{\operatorname{ber}}+\frac{1}{2}\operatorname{ber}\left(R^2\right)$$

(see, [28, Corollary 2.14]) and

$$\operatorname{ber}^2\left(\begin{bmatrix}0&R\\S&0\end{bmatrix}\right)=\frac{1}{4}\max\left\{\left\||S|^2+|R^*|^2\right\|_{\operatorname{ber}},\left\||R|^2+|S^*|^2\right\|_{\operatorname{ber}}\right\}+\frac{1}{2}\max\left\{\operatorname{ber}(RS),\operatorname{ber}(SR)\right\}.$$

Theorem 2.20. *Let $P,R,S,T\in\mathbb{L}(\mathscr{H})$. Then*

$$\begin{aligned}\operatorname{ber}^4\left(\begin{bmatrix}P&R\\S&T\end{bmatrix}\right)&\leq 8\max\left\{\operatorname{ber}^4(P),\operatorname{ber}^4(T)\right\}+3\max\left\{\left\||S|^4+|R^*|^4\right\|_{\operatorname{ber}},\left\||R|^4+|S^*|^4\right\|_{\operatorname{ber}}\right\}\\&\quad+\max\left\{\operatorname{ber}(SR),\operatorname{ber}(RS)\right\}\max\left\{\left\||S|^2+|R^*|^2\right\|_{\operatorname{ber}},\left\||R|^2+|S^*|^2\right\|_{\operatorname{ber}}\right\}.\end{aligned}$$

Proof. For every $(\omega_1,\omega_2)\in\Upsilon_1\times\Upsilon_2$, let $\widehat{k}_w=\widehat{k}_{(\omega_1,\omega_2)}=\begin{bmatrix}k_{\omega_1}\\k_{\omega_2}\end{bmatrix}$ be a normalized reproducing kernel in $\mathscr{H}(\Upsilon_1)\oplus\mathscr{H}(\Upsilon_2)$. Then

$$\begin{aligned}\left|\left\langle\begin{bmatrix}P&R\\S&T\end{bmatrix}\widehat{k}_w,\widehat{k}_w\right\rangle\right|^4&=\left|\left\langle\left(\begin{bmatrix}P&0\\0&T\end{bmatrix}+\begin{bmatrix}0&R\\S&0\end{bmatrix}\right)\widehat{k}_w,\widehat{k}_w\right\rangle\right|^4\\&\leq\left(\left|\left\langle\begin{bmatrix}P&0\\0&T\end{bmatrix}\widehat{k}_w,\widehat{k}_w\right\rangle\right|+\left\langle\begin{bmatrix}0&R\\S&0\end{bmatrix}\widehat{k}_w,\widehat{k}_w\right\rangle\right|\right)^4\\&\leq\left(\left|\left\langle\begin{bmatrix}P&0\\0&T\end{bmatrix}\widehat{k}_w,\widehat{k}_w\right\rangle\right|+\left|\left\langle\begin{bmatrix}0&R\\S&0\end{bmatrix}\widehat{k}_w,\widehat{k}_w\right\rangle\right|\right)^4\\&=\left(\frac{2\left|\left\langle\begin{bmatrix}P&0\\0&T\end{bmatrix}\widehat{k}_w,\widehat{k}_w\right\rangle\right|+2\left|\left\langle\begin{bmatrix}0&R\\S&0\end{bmatrix}\widehat{k}_w,\widehat{k}_w\right\rangle\right|}{2}\right)^4.\end{aligned}$$

By convexity of $f(t)=t^4$, the inequality (2.7) with $M=\begin{bmatrix}0&R\\S&0\end{bmatrix}$, the AM-GM inequality and inequality (2.3), we get

$$\begin{aligned}\left|\left\langle\begin{bmatrix}P&R\\S&T\end{bmatrix}\widehat{k}_w,\widehat{k}_w\right\rangle\right|^4&\leq 8\left(\left|\left\langle\begin{bmatrix}P&0\\0&T\end{bmatrix}\widehat{k}_w,\widehat{k}_w\right\rangle\right|^4+\left|\left\langle\begin{bmatrix}0&R\\S&0\end{bmatrix}\widehat{k}_w,\widehat{k}_w\right\rangle\right|^4\right)\\&\leq 8\left|\left\langle\begin{bmatrix}P&0\\0&T\end{bmatrix}\widehat{k}_w,\widehat{k}_w\right\rangle\right|^4\\&\quad+2\left(3\left\|M\widehat{k}_w\right\|^2\left\|M^*\widehat{k}_w\right\|^2+\left\|M\widehat{k}_w\right\|\left\|M^*\widehat{k}_w\right\|\left|\left\langle M\widehat{k}_w,M^*\widehat{k}_w\right\rangle\right|\right)\\&=8\left|\left\langle\begin{bmatrix}P&0\\0&T\end{bmatrix}\widehat{k}_w,\widehat{k}_w\right\rangle\right|^4+2\left(3\left\langle|M|^2\widehat{k}_w,\widehat{k}_w\right\rangle\left\langle|M^*|^2\widehat{k}_w,\widehat{k}_w\right\rangle\right.\\&\quad\left.+\sqrt{\left\langle|M|^2\widehat{k}_w,\widehat{k}_w\right\rangle\left\langle|M^*|^2\widehat{k}_w,\widehat{k}_w\right\rangle}\left|\left\langle M\widehat{k}_w,M^*\widehat{k}_w\right\rangle\right|\right)\\&\leq 8\left|\left\langle\begin{bmatrix}P&0\\0&T\end{bmatrix}\widehat{k}_w,\widehat{k}_w\right\rangle\right|^4+3\left\langle\left(|M|^2+|M^*|^2\right)\widehat{k}_w,\widehat{k}_w\right\rangle\\&\quad+\left\langle\left(|M|^2+|M^*|^2\right)\widehat{k}_w,\widehat{k}_w\right\rangle\left|\left\langle M^2\widehat{k}_w,\widehat{k}_w\right\rangle\right|\\&=8\left|\left\langle\begin{bmatrix}P&0\\0&T\end{bmatrix}\widehat{k}_w,\widehat{k}_w\right\rangle\right|^4+3\left\langle\begin{bmatrix}|S|^4+|R^*|^4&0\\0&|R|^4+|S^*|^4\end{bmatrix}\widehat{k}_w,\widehat{k}_w\right\rangle\\&\quad+\left\langle\begin{bmatrix}|S|^2+|R^*|^2&0\\0&|R|^2+|S^*|^2\end{bmatrix}\widehat{k}_w,\widehat{k}_w\right\rangle\left|\left\langle\begin{bmatrix}RS&0\\0&SR\end{bmatrix}\widehat{k}_w,\widehat{k}_w\right\rangle\right|.\end{aligned}$$

and, so

$$\begin{aligned}\left|\left\langle\begin{bmatrix}P&R\\S&T\end{bmatrix}\widehat{k}_w,\widehat{k}_w\right\rangle\right|^4&\leq 8\left|\left\langle\begin{bmatrix}P&0\\0&T\end{bmatrix}\widehat{k}_w,\widehat{k}_w\right\rangle\right|^4+3\left\langle\begin{bmatrix}|S|^4+|R^*|^4&0\\0&|R|^4+|S^*|^4\end{bmatrix}\widehat{k}_w,\widehat{k}_w\right\rangle\\&\quad+\left\langle\begin{bmatrix}|S|^2+|R^*|^2&0\\0&|R|^2+|S^*|^2\end{bmatrix}\widehat{k}_w,\widehat{k}_w\right\rangle\left|\left\langle\begin{bmatrix}RS&0\\0&SR\end{bmatrix}\widehat{k}_w,\widehat{k}_w\right\rangle\right|.\end{aligned}$$

Taking the supremum over $(\omega_1,\omega_2)\in\Upsilon_1\times\Upsilon_2$ and then applying the inequality (2.1) in the above inequality, we have

$$\begin{aligned}\mathrm{ber}^4\left(\begin{bmatrix}P & R\\ S & T\end{bmatrix}\right) \leq\ & 8\max\left\{\mathrm{ber}^4(P),\mathrm{ber}^4(T)\right\}+3\max\left\{\left\||S|^4+|R^*|^4\right\|_{\mathrm{ber}},\left\||R|^4+|S^*|^4\right\|_{\mathrm{ber}}\right\}\\ &+\max\left\{\mathrm{ber}(SR),\mathrm{ber}(RS)\right\}\max\left\{\left\||S|^2+|R^*|^2\right\|_{\mathrm{ber}},\left\||R|^2+|S^*|^2\right\|_{\mathrm{ber}}\right\}.\end{aligned}$$

This completes the proof. □

Now, considering $P=T$ and $R=S$ in Theorem 2.20, we obtain the following case.

Corollary 2.21. *Let $\mathscr{H}=\mathscr{H}(\Upsilon)$ be a FHS and $P,R\in\mathbb{L}(\mathscr{H})$. Then we have*

$$\mathrm{ber}^4\left(\begin{bmatrix}P & R\\ R & P\end{bmatrix}\right)\leq\max\left\{\mathrm{ber}^4(P+R),\mathrm{ber}^4(P-R)\right\}\leq 8\mathrm{ber}^4(P)+3\left\||R|^4+|R^*|^4\right\|_{\mathrm{ber}}+\left\||R|^2+|R^*|^2\right\|_{\mathrm{ber}}\mathrm{ber}\left(R^2\right).$$

It should be noted that the case $P=R$ of Corollary 2.21 is same as the inequality

$$\mathrm{ber}^4(P)\leq\frac{3}{8}\left\||P|^4+|P^*|^4\right\|_{\mathrm{ber}}+\frac{1}{8}\left\||P|^2+|P^*|^2\right\|_{\mathrm{ber}}\mathrm{ber}\left(P^2\right)$$

obtained in [28, Theorem 2.5].
We give the following example which show that $\mathrm{ber}(T)=\max_{1\leq j\leq n}\left|t_{jj}\right|$ for any complex $n\times n$ matrix $T=\left(t_{jk}\right)_{j,k=1}^{n}$ (see, [17, Example 2.17]). Let's think about a situation with finite dimensions. $T=\left(t_{jk}\right)_{j,k=1}^{n}$ be a $n\times n$ matrix. Let $\omega=(\omega_1,\ldots,\omega_n)\in\mathbb{C}^n$ and $Y=\{1,\ldots,n\}$. We can consider $\mathbb{C}^n$ as the set of all functions mapping $Y\to\mathbb{C}$ by $\omega(j)=\omega_j$. Letting z_j be the jth standard basis vector for $\mathbb{C}^n$ under the standard inner product, we can view $\mathbb{C}^n$ as a FHS with kernel

$$k(i,j)=\left\langle z_j,z_i\right\rangle.$$

Note that $k_j=\widehat{k}_j$ for each $j=1,\ldots,n$. We get $t_{jj}=\left\langle Tz_j,z_j\right\rangle$. So, the Berezin set of T is simply

$$\mathrm{Ber}(T)=\left\{t_{jj}:j=1,\ldots,n\right\},$$

which is just the collection of diagonal elements of T. Hence $\mathrm{ber}(T)=\max_{1\leq j\leq n}\left|t_{jj}\right|$.

Acknowledgements

The authors would like to express their sincere thanks to the editor and the anonymous reviewers for their helpful comments and suggestions.

Article Information

Acknowledgements: The authors thank the referees for valuable comments and suggestions which improved the presentation of this paper.

Author's Contributions: The authors contributed equally to the writing of this paper.

Conflict of Interest Disclosure: No potential conflict of interest was declared by the author.

Supporting/Supporting Organizations: No grants were received from any public, private or non-profit organizations for this research.

Ethical Approval and Participant Consent: It is declared that during the preparation process of this study, scientific and ethical principles were followed and all the studies benefited from are stated in the bibliography.

Plagiarism Statement: This article was scanned by the plagiarism program. No plagiarism detected.

Availability of Data and Materials: Not applicable.

References

[1] N. Aronzajn, *Theory of reproducing kernels*, Trans. Amer. Math. Soc., **68** (1950), 337-404.
[2] F. A. Berezin, *Covariant and contravariant symbols for operators*, Math. USSR-Izv., **6** (1972), 1117-1151.
[3] H. Başaran, M. Gürdal, A. N. Güncan, *Some operator inequalities associated with Kantorovich and Hölder-McCarthy inequalities and their applications*, Turkish J. Math., **43**(1) (2019), 523-532.
[4] H. Başaran, M. Gürdal, *Berezin number inequalities via inequality*, Honam Math. J., **43**(3) (2021), 523-537.
[5] H. Başaran, V. Gürdal, *Berezin radius and Cauchy-Schwarz inequality*, Montes Taurus J. Pure Appl. Math., **5**(3) (2023), 16-22.
[6] H. Başaran, V. Gürdal, *On Berezin radius inequalities via Cauchy-Schwarz type inequalities*, Malaya J. Mat., **11**(2) (2023), 127-141.
[7] M. T. Garayev, M. W. Alomari, *Inequalities for the Berezin number of operators and related questions*, Complex Anal. Oper. Theory, **15**(30) (2021), 1-30.
[8] M. Gürdal, H. Başaran, *A-Berezin number of operators*, Proc. Inst. Math. Mech. Natl. Acad. Sci. Azerb., **48**(1) (2022), 77-87.
[9] M. B. Huban, H. Başaran, M. Gürdal, *New upper bounds related to the Berezin number inequalities*, J. Inequal. Spec. Funct., **12**(3) (2021), 1-12.
[10] M. T. Karaev, *Reproducing kernels and Berezin symbols techniques in various questions of operator theory*, Complex Anal. Oper. Theory, **7** (2013), 983-1018.
[11] W. Bani-Domi, F. Kittaneh, *Norm and numerical radius inequalities for Hilbert space operators*, Linear Multilinear Algebra, **69**(5) (2021), 934-945.
[12] S. S. Dragomir, *Power inequalities for the numerical radius of a product of two operators in Hilbert spaces*, Sarajevo J. Math., **5** (2009), 269–278.
[13] F. Kittaneh, *Norm inequalities for sums of positive operators*, J. Operator Theory, **48** (2002), 95–103.
[14] F. Kittaneh, H. R. Moradi, *Cauchy-Schwarz type inequalities and applications to numerical radius inequalities*, Math. Inequal. Appl., **23**(3) (2020), 1117-1125.
[15] M. T. Karaev, *Berezin symbol and invertibility of operators on the functional Hilbert spaces*, J. Funct. Anal., **238** (2006), 181-192.
[16] M. B. Huban, H. Başaran, M. Gürdal, *Some new inequalities via Berezin numbers*, Turk. J. Math. Comput. Sci., **14**(1) (2022), 129-137.
[17] M. B. Huban, H. Başaran, M. Gürdal, *Berezin number inequalities via convex functions*, Filomat, **36**(7) (2022), 2333-2344.
[18] H. Başaran, M. B. Huban, M. Gürdal, *Inequalities related to Berezin norm and Berezin number of operators*, Bull. Math. Anal. Appl., **14**(2) (2022), 1-11.
[19] M. Bakherad, *Some Berezin number inequalities for operator matrices*, Czechoslovak Math. J., **68**(4) (2018), 997-1009.
[20] M. Bakherad, M. T. Garayev, *Berezin number inequalities for operators*, Concr. Oper., **6**(1) (2019), 33-43.
[21] M. Bakherad, M. Hajmohamadi, R. Lashkaripour, S. Sahoo, *Some extensions of Berezin number inequalities on operators*, Rocky Mountain J. Math., **51**(6) (2021), 1941-1951.
[22] A. Abu-Omar, F. Kittaneh, *Numerical radius inequalities for $n \times n$ operator matrices*, Linear Algebra Appl., **468** (2015), 18-26.
[23] M. Bakherad, K. Shebrawi, *Upper bounds for numerical radius inequalities involving off-diagonal operator matrices*, Ann. Funct. Anal., **9**(3) (2018), 297-309.
[24] F. Kittaneh, *Notes on some inequalities for Hilbert space operators*, Publ. Res. Inst. Math. Sci., **24**(2) (1988), 283-293.
[25] J. Aujla, F. Silva, *Weak majorization inequalities and convex functions*, Linear Algebra Appl., **369** (2003), 217-233.
[26] S. S. Sahoo, N. Das, D. Mishra, *Berezin number and numerical radius inequalities for operators on Hilbert spaces*, Adv. Oper. Theory, **5** (2020), 714-727.
[27] M. L. Buzano, *Generalizzatione della disuguaglianza di Cauchy-Schwarz*, Rend. Sem. Mat. Univ. e Politec. Torino, **31**(1971/73) (1974) 405-409.
[28] V. Gürdal, H. Başaran, M. B. Huban, *Further Berezin radius inequalities*, Palest. J. Math., **12**(1) (2023), 757–767.

Fundamental Journal of Mathematics and Applications, 6 (2) (2023) 117-127
Research Article

FUJMA

Fundamental Journal of Mathematics and Applications

Journal Homepage: www.dergipark.org.tr/en/pub/fujma
ISSN: 2645-8845
doi: https://dx.doi.org/10.33401/fujma.1277288

Ricci Soliton Lightlike Submanifolds with Co-Dimension 2

Erol Kılıç[1], Mehmet Gülbahar[2], Ecem Kavuk[1] and Esra Erkan[2*]

[1]*Department of Mathematics, Faculty of Science and Arts, İnönü University, Malatya, Türkiye*
[2]*Department of Mathematics, Faculty of Science and Arts, Harran University, Şanlıurfa, Türkiye*
[*]*Corresponding author*

Article Info

Keywords: *Concircular vector field, Concurrent vector field, Ricci soliton*
2010 AMS: *53C25, 53C40, 53C42*
Received: *4 April 2023*
Accepted: *1 June 2023*
Available online: *11 June 2023*

Abstract

The necessary requirements for half-lightlike and coisotropic lightlike submanifolds to be a Ricci soliton are obtained. Some examples of Ricci soliton half-lightlike and Ricci soliton coisotropic lightlike submanifolds are given. The Ricci soliton equation is investigated on totally geodesic, totally umbilical, and irrotational lightlike submanifolds.

1. Introduction

The concept of Ricci solitons has become a fascinating issue in the differential geometry and this concept has been studied on various submanifolds of Riemannian manifolds. For some applications on Ricci solitons, we touch on [1–8], etc. A (semi-) Riemannian manifold (M,g) is said to be a Ricci soliton if

$$L_\zeta g(X_1,X_2)+2\mathrm{Ric}(X_1,X_2)=2\kappa g(X_1,X_2) \tag{1.1}$$

is satisfied for each tangent vector fields X_1 and X_2. In (1.1), L_ζ indicates the Lie derivative, Ric denotes the Ricci tensor, κ is a scalar and ζ is called the potential vector field. If κ is a function then (M,g) is said to be an almost Ricci soliton. Considering the description of Ricci solitons, every Einstein manifold is a Ricci soliton. This issue is known as shrinking when $\kappa>0$, steady when $\kappa=0$ and expanding when $\kappa<0$.

In addition to this, concircular vector fields are one of the most utilized vector field to characterize a smooth manifold. Concircular vector fields were initially observed in the definition of torse-forming vector field which was introduced by K. Yano [9]. There exist remarkable applications of concircular vector fields in the literature (cf. [10–15]). A vector field ζ is said to be concircular if there is a differentiable function φ such that

$$\nabla_X\zeta=\varphi X$$

is satisfied for each tangent vector field X. If $\varphi=1$, ζ becomes concurrent.

In the degenerate geometry, Ricci soliton lightlike hypersurfaces were studied in [16]. As a continuation of this study, we examine Ricci soliton half-lightlike submanifolds and Ricci soliton coisotropic lightlike submanifolds admitting concircular and concurrent potential vector fields in this paper.

***Email addresses and ORCID numbers*: erol.kilic@inonu.edu.tr, 0000-0001-7536-0404 (E. Kılıç), mehmetgulbahar@harran.edu.tr, 0000-0001-6950-7633 (M. Gülbahar), 23616140002@ogr.inonu.edu.tr, 0000-0002-8922-2691 (E. Kavuk) esraerkan@harran.edu.tr, 0000-0003-0456-6418 (E. Erkan)**
Cite as: E. Kılıç, E. Kavuk, M. Gülbahar, E. Erkan *Ricci Soliton Lightlike Submanifolds with Co-Dimension* 2, Fundam. J. Math. Appl., 6(2) (2023), 117-127.

2. Half-Lightlike Submanifolds

Let $(\widetilde{M},\widetilde{g})$ be a semi-Riemannian manifold equipped with a semi-Riemannian metric $\widetilde{g}$. Presume that (M,g) to be a lightlike submanifold $(\widetilde{M},\widetilde{g})$ with the co-dimension 2. Then the radical distribution $\mathrm{Rad}(T_pM)$ at $p\in M$ is determined by

$$\mathrm{Rad}(T_pM)=\left\{\xi\in T_pM:\widetilde{g}(\xi,X)=0,\forall X\in T_pM\right\}.$$

Denote a complementary non-degenerate vector bundle of $\mathrm{Rad}(TM)$ by $\mathrm{S}(TM)$. We note that a lightlike submanifold is usually indicated by the triple $(M,g,\mathrm{S}(TM))$ [17]. Here, the distribution $\mathrm{S}(TM)$ is said to be a screen distribution and we put

$$TM=\mathrm{Rad}(TM)\oplus\mathrm{S}(TM)$$

where $\oplus_{orth}$ indicates the orthogonal direct sum. If the dimension of $\mathrm{Rad}(TM)$ is equal to 1, then $(M,g,\mathrm{S}(TM))$ is said to be a half-lightlike submanifold [18].

For each half-lightlike submanifold, there are a $1-$dimensional non-degenerate subbundle $\mathbb{D}$ and a $1-$dimensional degenerate subbundle $\mathrm{ltr}(TM)$ such that $\mathbb{D}=Span\{U\}$, $ltr(TM)=Span\{N\}$ and

$$\begin{aligned}\widetilde{g}(\xi,U) &= \widetilde{g}(N,U)=0,\quad \widetilde{g}(U,U)\neq 0,\\ \widetilde{g}(\xi,N) &= 1,\quad \widetilde{g}(N,U)=0\end{aligned}$$

are satisfied.

Let $\widetilde{\nabla}$ denotes the Levi-Civita connection on $(\widetilde{M},\widetilde{g})$ and P denotes the projection from $\Gamma(TM)$ to $\Gamma(\mathrm{S}(TM))$. The Gauss and Weingarten type formulas are formulated by

$$\widetilde{\nabla}_{X_1}X_2 = \nabla_{X_1}X_2+B(X_1,X_2)N+D(X_1,X_2)U, \tag{2.1}$$
$$\widetilde{\nabla}_{X_1}N = -A_NX_1+\rho_1(X_1)N+\rho_2(X_1)U, \tag{2.2}$$
$$\widetilde{\nabla}_{X_1}U = -A_UX_1+\mu_1(X_1)N+\mu_2(X_1)U, \tag{2.3}$$

and

$$\nabla_{X_1}PX_2 = \nabla^*_{X_1}PX_2+C(X_1,X_2)\xi, \tag{2.4}$$
$$\nabla_{X_1}\xi = -A^*_\xi X_1-\rho_1(X_1)\xi, \tag{2.5}$$

where $\nabla_{X_1}X_2,A_NX_1,A_UX_1\in\Gamma(TM)$, $\nabla^*_{X_1}PX_2,A^*_\xi X_1\in\Gamma(\mathrm{S}(TM))$, A_N and A_U are the shape operators on $\Gamma(TM)$, A^*_ξ is the shape operator on $\Gamma(\mathrm{S}(TM))$, $B(X_1,X_2)$ and $D(X_1,X_2)$ are ingredients of the second fundamental form, ρ_1,ρ_2, μ_1,μ_2 are $1-$forms. From (2.1)-(2.5), it is known that the relations

$$\begin{aligned}B(X_1,X_2) &= g(A^*_\xi X_1,X_2),\\ C(X_1,X_2) &= g(A_NX_1,X_2),\\ D(X_1,X_2) &= g(A_UX_1,X_2)-\mu_1(X_1)\eta(X_2),\end{aligned}$$

are satisfied. Here $\eta(X_2)=\widetilde{g}(X_2,N)$ [19].

We note that B and D are symmetric but C is not symmetric. Since the relation

$$(\nabla_{X_3}g)(X_1,X_2)=B(X_3,X_2)\eta(X_1)+B(X_3,X_1)\eta(X_2) \tag{2.6}$$

is satisfied, ∇ is not a metric connection. The Lie derivative of g is formulated by

$$\begin{aligned}(L_{X_3}g)(X_1,X_2) &= X_3g(X_1,X_2)-\widetilde{g}([X_3,X_1],X_2)-\widetilde{g}([X_3,X_2],X_1)\\ &= X_3g(X_1,X_2)-g(\nabla_{X_3}X_1,X_2)-g(\nabla_{X_3}X_2,X_1)+g(\nabla_{X_1}X_3,X_2)+g(\nabla_{X_2}X_3,X_1).\end{aligned} \tag{2.7}$$

From (2.6) and (2.7), we also have

$$(L_{X_3}g)(X_1,X_2) = B(X_3,X_2)\eta(X_1)+B(X_3,X_1)\eta(X_2)+g(\nabla_{X_1}X_3,X_2)+g(\nabla_{X_2}X_3,X_1) \tag{2.8}$$

or we put

$$(L_{X_3}g)(X_1,X_2) = (\nabla_{X_3}g)(X_1,X_2)+g(\nabla_{X_1}X_3,X_2)+g(\nabla_{X_2}X_3,X_1).$$

Indicate the Riemannian curvatures of $(M,g,\mathrm{S}(TM))$ and its ambient manifold by R and $\widetilde{R}$ respectively. Then the following equality holds:

$$\begin{aligned}\widetilde{g}(\widetilde{R}(X_1,X_2)PX_3,PX_4) &= g(R(X_1,X_2)PX_3,PX_4)+B(X_1,PX_3)C(X_2,PX_4)-B(X_2,PX_3)C(X_1,PX_4)\\ &\quad +D(X_1,PX_3)D(X_2,PX_4)-D(X_2,PX_3)D(X_1,PX_4).\end{aligned} \tag{2.9}$$

Let $\{Y_1,Y_2,\ldots,Y_n\}$ be a orthonormal frame field on $\Gamma(\mathrm{S}(TM))$. Then the Ricci type tensor $R^{(0,2)}$ is determined by

$$R^{(0,2)}(X_1,X_2)=\sum_{j=1}^{n} g(R(Y_j,X_1)X_2,Y_j)+\widetilde{g}(R(\xi,X_1)X_2,N). \tag{2.10}$$

We note that $R^{(0,2)}$ is not symmetric. If $\mathrm{S}(TM)$ is integrable, then $R^{(0,2)}$ is symmetric [17].

A half-lightlike submanifold is called totally geodesic if $B=D=0$ and it is said to be irrotational if $B(X,\xi)=0$ for any $X\in\Gamma(TM)$ [20]. A half-lightlike submanifold is said to be totally umbilical if there exists a differentiable transversal vector field H satisfying

$$B(X_1,X_2)N+D(X_1,X_2)U=g(X_1,X_2)H \tag{2.11}$$

for any $X_1,X_2\in\Gamma(TM)$ [21]. In view of (2.11), it is clear that there exist two differentiable functions H_1 and H_2 satisfying

$$B(X_1,X_2)=H_1g(X_1,X_2) \quad \text{and} \quad D(X_1,X_2)=H_2g(X_1,X_2).$$

3. Ricci Soliton Half-Lightlike Submanifolds

Let $(M,g,\mathrm{S}(TM))$ be a half-lighlike submanifold of $(\widetilde{M},\widetilde{g})$ Assume that $\zeta\in\Gamma(T\widetilde{M})$. Hence one can put

$$\zeta=\zeta^{\top}+f_1N+f_2U$$

where $\zeta^{\top}\in\Gamma(TM)$, f_1 and f_2 are differentiable functions on $\Gamma(T\widetilde{M})$. Thus, we get

$$f_1=\widetilde{g}(\zeta,\xi) \quad \text{and} \quad f_2=\varepsilon\widetilde{g}(\zeta,U)$$

where $\varepsilon=\widetilde{g}(U,U)=\mp1$.

Proposition 3.1. *If ζ is concircular, then the following equalities are satisfied for any $X\in\Gamma(TM)$:*

$$\nabla_X\zeta^{\top} = \varphi X+f_1A_NX+f_2A_UX, \tag{3.1}$$
$$B(X,\zeta^{\top}) = -X[f_1]-f_1\rho_1(X)-f_2\mu_1(X), \tag{3.2}$$
$$D(X,\zeta^{\top}) = -X[f_2]-f_1\rho_2(X)-f_2\mu_2(X). \tag{3.3}$$

Proof. If ζ is concircular, then we put

$$\widetilde{\nabla}_X\zeta=\varphi X=\widetilde{\nabla}_X\zeta^{\top}+\widetilde{\nabla}_X(f_1N)+\widetilde{\nabla}_X(f_2U).$$

Using (2.1), (2.2) and (2.3) in the last formula, we get

$$\begin{aligned}\varphi X &= \nabla_X\zeta+B(X,\zeta^{\top})N+D(X,\zeta)U+X[f_1]N-f_1A_NX+f_1\rho_1(X)N+f_1\rho_2(X)U+X[f_2]U\\ &\quad -f_2A_UX+f_2\mu_1(X)N+f_2\mu_2(X)U.\end{aligned}$$

Considering the tangential parts $\mathrm{ltr}(TM)$ and $\mathbb{D}$, the proofs of (3.1), (3.2) and (3.3) are straightforward. □

Putting $\varphi=1$ in Proposition 3.1, we find

Proposition 3.2. *For any half-lightlike submanifold admitting a concurrent vector field ζ, we have*

$$\nabla_X\zeta^{\top}=X+f_1A_NX+f_2A_UX.$$

As a special case for $\zeta=\zeta^{\top}$, we find:

Proposition 3.3. *For any half-lightlike submanifold admitting a concircular vector field $\zeta=\zeta^{\top}$,*

$$B(X,\zeta^{\top})=D(X,\zeta^{\top})=0 \tag{3.4}$$

is satisfied.

As a result of Proposition 3.3, we find the following theorem:

Theorem 3.4. *Let $(M,g,S(TM))$ be a half-lightlike submanifold. If there exists at least one concircular or concurrent vector field $\zeta=\zeta^{\top}$ on $\Gamma(TM)$, then $\nabla_{\zeta^{\top}}g=0$.*

Definition 3.5. *A lightlike submanifold $(M,g,S(TM))$ with a integrable screen distribution is called a Ricci soliton if the relation*

$$(L_{\zeta}g)(X_1,X_2)+2R^{(0,2)}(X_1,X_2)=2\kappa g(X_1,X_2) \tag{3.5}$$

holds for any $X_1,X_2\in\Gamma(TM)$. Here, κ is a constant and ζ is called the potential vector field of $(M,g,S(TM))$.

Remark 3.6. *It is known that the Ricci tensor for any lightlike submanifold is not symmetric in general. Hence (3.5) loses its geometrical meaning since the induced degenerate metric g is symmetric. Thus we investigate Ricci soliton lightlike submanifolds whose screen distribution is integrable throughout the study.*

We shall compute the Lie derivative for half-lightlike submanifolds.

From (2.8) and (3.1), we obtain

$$(L_{\zeta^{\top}}g)(X_1,X_2)=B(X_1,\zeta^{\top})\eta(X_2)+B(X_2,\zeta^{\top})\eta(X_1)+2\varphi g(X_1,X_2)+2f_1g(A_NX_1,X_2)+2f_2g(A_UX_1,X_2). \tag{3.6}$$

If ζ is concurrent, then we easily obtain

$$(L_{\zeta^{\top}}g)(X_1,X_2)=B(X_1,\zeta^{\top})\eta(X_2)+B(X_2,\zeta^{\top})\eta(X_1)+2g(X_1,X_2)+2f_1g(A_NX_1,X_2)+2f_2g(A_UX_1,X_2). \tag{3.7}$$

As a special case for $\zeta=\zeta^{\top}$, we obtain from (3.4) and (3.6) that

$$(L_{\zeta^{\top}}g)(X_1,X_2)=2\varphi g(X_1,X_2).$$

If ζ is concurrent and $\zeta=\zeta^{\top}$, we obtain

$$(L_{\zeta^{\top}}g)(X_1,X_2)=2g(X_1,X_2).$$

By (3.5) and (3.6), we have:

Theorem 3.7. *Let $(M,g,S(TM))$ be a half-lightlike submanifold admitting a concircular vector field ζ. Then, $(M,g,S(TM))$ is a Ricci soliton such that $\zeta^{\top}$ is the potential vector field if and only if the equation*

$$R^{(0,2)}(X_1,X_2)=-\frac{1}{2}B(X_1,\zeta^{\top})\eta(X_2)-\frac{1}{2}B(\zeta^{\top},X_2)\eta(X_1)-f_1g(A_NX_1,X_2)-f_2g(A_UX_1,X_2)+(\kappa-\varphi)g(X_1,X_2)$$

holds for any $X_1,X_2\in\Gamma(TM)$.

In view of (3.5) and (3.7), we have:

Theorem 3.8. *Let $(M,g,S(TM))$ be a half-lightlike submanifold admitting a concurrent vector field ζ. Then, $(M,g,S(TM))$ is a Ricci soliton such that $\zeta^{\top}$ is the potential vector field if and only if the equation*

$$R^{(0,2)}(X_1,X_2)=-\frac{1}{2}B(X_1,\zeta^{\top})\eta(X_2)-\frac{1}{2}B(\zeta^{\top},X_2)\eta(X_1)-f_1g(A_NX_1,X_2)-f_2g(A_UX_1,X_2)+(\kappa-1)g(X_1,X_2)$$

holds for any $X_1,X_2\in\Gamma(TM)$.

Theorem 3.9. *Let $(M,g,S(TM))$ be a half-lightlike submanifold admitting a concircular vector field $\zeta=\zeta^{\top}$. Then, the submanifold is a Ricci soliton such that $\zeta^{\top}$ is the potential vector field if and only if the equation*

$$R^{(0,2)}(X_1,X_2)=(\kappa-\varphi)g(X_1,X_2) \tag{3.8}$$

holds for any $X_1,X_2\in\Gamma(TM)$. It means that the submanifold is an Einstein manifold.

Theorem 3.10. *Let $(M,g,S(TM))$ be a half-lightlike submanifold admitting a concurrent vector field $\zeta=\zeta^{\top}$. The submanifold is a Ricci soliton if and only if the equation*

$$R^{(0,2)}(X_1,X_2)=(\kappa-1)g(X_1,X_2)$$

holds for any $X_1,X_2\in\Gamma(TM)$. In other words, the submanifold is an Einstein manifold. Furthermore if the soliton is steady, then the Ricci curvature of $(M,g,S(TM))$ is negative defined.

In view of Theorem 3.7 we find:

Corollary 3.11. *Let $(M,g,S(TM))$ be a totally geodesic half-lightlike submanifold admitting a concircular vector field ζ. If the submanifold is a Ricci soliton, then we find*

$$R^{(0,2)}(X_1,X_2) = -f_1 g(A_N X_1,X_2) - f_2 g(A_U X_1,X_2) + (\kappa-\varphi)g(X_1,X_2)$$

for any $X_1,X_2 \in \Gamma(S(TM))$.

In view of Theorem 3.8 we find:

Corollary 3.12. *Let $(M,g,S(TM))$ be a totally geodesic half-lightlike submanifold admitting a concurrent vector field ζ. If the submanifold is a Ricci soliton, then we find*

$$R^{(0,2)}(X_1,X_2) = -f_1 g(A_N X_1,X_2) - f_2 g(A_U X_1,X_2) + (\kappa-1)g(X_1,X_2)$$

for any $X_1,X_2 \in \Gamma(S(TM))$.

Corollary 3.13. *Let $(M,g,S(TM))$ be an irrotational half-lightlike submanifold admitting a concircular vector field $\zeta = \xi$. If the submanifold is a Ricci soliton, then we find*

$$R^{(0,2)}(X_1,X_2) = (\kappa-\varphi)g(X_1,X_2)$$

for any $X_1,X_2 \in \Gamma(S(TM))$.

Corollary 3.14. *Let $(M,g,S(TM))$ be an irrotational half-lightlike submanifold admitting a concurrent vector field $\zeta = \xi$. If the submanifold is a Ricci soliton, then we have*

$$R^{(0,2)}(X_1,X_2) = (\kappa-1)g(X_1,X_2)$$

for any $X_1,X_2 \in \Gamma(S(TM))$.

Example 3.15 ([22]). *Consider a submanifold in $\mathbb{R}^5_2$ with the signature $(-,-,+,+,+)$ and local coordinate system $\{z_1,z_2,z_3,z_4,z_5\}$ given by*

$$z_4 = (z_1^2+z_2^2)^{\frac{1}{2}}, \quad z_3 = (1-z_5^2)^{\frac{1}{2}}, \quad z_5,z_1,z_2 > 0.$$

Thus we find

$$\begin{aligned} Rad(TM) &= Span\{\xi = z_1\partial_1 + z_2\partial_2 + z_4\partial_4\}, \\ S(TM) &= Span\{X_1 = z_4\partial_1 + z_1\partial_4, X_2 = -z_5\partial_3 + z_3\partial_5\}, \\ ltr(TM) &= Span\left\{N = \frac{1}{2z_3^2}(z_1\partial_1 - z_2\partial_2 + z_4\partial_4)\right\}, \end{aligned}$$

and

$$\mathbb{D} = Span\{U = z_3\partial_3 + z_5\partial_5\}.$$

Here $\{\partial_1,\partial_2,\partial_3,\partial_4,\partial_5\}$ is the natural frame field on $\mathbb{R}^5_2$. By a straightforward computation, we obtain that $(M,g,S(TM))$ is a half-lightlike submanifold and

$$\widetilde{\nabla}_{X_1}\xi = X_1, \quad \widetilde{\nabla}_{X_2}\xi = 0, \quad \widetilde{\nabla}_{\xi}\xi = \xi$$

which show that

$$\begin{aligned} B(X_1,\xi) &= B(X_2,\xi) = B(X_1,X_2) = B(X_2,X_2) = 0, \quad B(X_1,X_1) = z_2^2, \\ C(X_1,\xi) &= C(X_2,\xi) = C(X_1,X_2) = C(X_2,X_2) = 0, \quad C(X_1,X_1) = -\frac{1}{2}, \\ D(X_1,\xi) &= D(X_2,\xi) = D(X_1,X_2) = D(X_1,X_1) = 0, \quad D(X_2,X_2) = 1. \end{aligned}$$

From (2.9), we find

$$R^{(0,2)}(X_1,X_1) = R^{(0,2)}(X_2,X_2) = R^{(0,2)}(X_1,X_2) = 0.$$

If we consider $\zeta = \varphi(\xi+U)$, where φ is a differentiable function on M and $\zeta^T = \varphi\xi$, then we obtain ζ is concircular and $(M,g,S(TM))$ is a shrinking Ricci soliton such that $\zeta^\top$ is the potential vector field and $\kappa = 1$.

Theorem 3.16 (cf. Theorem 3.2 of [23]). *Let $\widetilde{M}(c)$ be an indefinite space form with constant curvature c and $(M,g,S(TM))$ be a totally umbilical half-lightlike submanifold with the co-dimension 2. Then the following equality holds:*

$$\begin{aligned} R(X_1,X_2)X_3 &= c\{g(X_2,X_3)X_1-g(X_1,X_3)X_2\}+H_1\{g(X_2,X_3)A_NX_1-g(X_1,X_3)A_NX_2\} \\ &\quad +H_2\{g(X_2,X_3)A_UX_1-g(X_1,X_3)A_UX_2\}. \end{aligned} \tag{3.9}$$

Theorem 3.17. *Let $(M,g,S(TM))$ be a totally umbilical half-lightlike submanifold of $\widetilde{M}(c)$ admitting a concircular vector field $\zeta=\zeta^{\top}$. The submanifold is a Ricci soliton such that $\zeta^{\top}$ is the potential vector field if and only if the equation*

$$\kappa = c+\varphi+H_1 traceA_N+H_2 traceA_U \tag{3.10}$$

is satisfied.

Proof. Let $\{Y_1,\ldots,Y_n\}$ be an orthonormal frame field of $\Gamma(\mathrm{S}(TM))$. In view of (2.10) and (3.9), it can be obtained

$$R^{(0,2)}(Y_i,Y_i) = c+H_1\mathrm{trace}A_N+H_2\mathrm{trace}A_U \tag{3.11}$$

for any $i\in\{1,\ldots,n\}$. In view of (3.8) and (3.11) we obtain (3.10). The converse part is straightforward. □

As a result of Theorem 3.17, we obtain

Theorem 3.18. *Let $(M,g,S(TM))$ be a totally umbilical half-lightlike submanifold of $\widetilde{M}(c)$ admitting a concurrent vector field $\zeta=\zeta^{\top}$. The submanifold is a Ricci soliton such that $\zeta^{\top}$ is the potential vector field if and only if the equation*

$$\kappa = c+1+H_1 traceA_N+H_2 traceA_U$$

is satisfied.

4. Coisotropic Lightlike Submanifolds

Let $(M,g,\mathrm{S}(TM))$ be a lightlike submanifold of $(\widetilde{M},\widetilde{g})$ with co-dimension 2. If the dimension of $\mathrm{Rad}(TM)$ is 2, then the submanifold is called a coisotropic lightlike submanifold [24]. For any coisotropic lightlike submanifold, there exists the following quasi-orthonormal basis on $\Gamma(T\widetilde{M})$:

$$\{Y_1,Y_2,\ldots,Y_n,\xi_1,\xi_2,N_1,N_2\}$$

where $\mathrm{S}(TM)=Span\{Y_1,Y_2,\ldots,Y_n\}$, $\mathrm{Rad}(TM)=Span\{\xi_1,\xi_2\}$ and $ltr(TM)=Span\{N_1,N_2\}$. It is known that the relations

$$\widetilde{g}(N_i,\xi_j)=\delta_{ij},\quad \widetilde{g}(N_i,N_j)=0$$

are satisfied for $i,j\in\{1,2\}$. The Gauss and Weingarten formulas are formulated by

$$\widetilde{\nabla}_{X_1}X_2 = \nabla_{X_1}X_2+\sum_{k=1}^{2}D_k(X_1,X_2)N_k, \tag{4.1}$$

$$\widetilde{\nabla}_{X_1}N_k = -A_{N_k}X_1+\sum_{l=1}^{2}\rho_{kl}(X_1)N_l, \tag{4.2}$$

$$\nabla_{X_1}X_2 = \nabla^*_{X_1}PX_2+\sum_{k=1}^{2}C_k(X_1,X_2)\xi_k, \tag{4.3}$$

$$\nabla_{X_1}\xi_k = -A^*_{\xi_k}X_1-\sum_{l=1}^{2}\rho_{kl},(X_1)\xi_l, \tag{4.4}$$

where $\nabla_{X_1}X_2, A_{N_k}X_1\in\Gamma(TM)$, $\nabla^*_{X_1}PX_2, A^*_{\xi_k}X_1\in\Gamma(\mathrm{S}(TM))$, A_{N_k} are the shape operators on $\Gamma(TM)$, $A^*_{\xi_k}$ are the shape operators on $\Gamma(\mathrm{S}(TM))$, $D_k(X_1,X_2)$, $C_k(X_1,X_2)$ are ingredients of the second fundamental forms, ρ_{kl} are $1-$forms for $k,l\in\{1,2\}$. In view of (4.1)-(4.4), we have

$$D_k(X_1,X_2)=g(A^*_{\xi}X_1,X_2),\quad C_k(X_1,X_2)=g(A_{N_k}X_1,X_2)$$

for any $k\in\{1,2\}$. We note that D_k are symmetric but C_k are not symmetric. Using the fact that $\widetilde{\nabla}$ is a metric connection and from (4.1), we find

$$(\nabla_{X_3}g)(X_1,X_2)=D_1(X_3,X_2)\eta_1(X_1)+D_1(X_3,X_1)\eta_1(X_2)+D_2(X_3,X_2)\eta_2(X_1)+D_2(X_3,X_1)\eta_2(X_2)$$

which shows that ∇ is not a metric connection [24]. Here, $\eta_1(X_1)=g(X_1,\xi_1)$ and $\eta_2(X_1)=g(X_1,\xi_2)$.

The Lie derivative is formulated by

$$\begin{aligned}(L_{X_3}g)(X_1,X_2) &= D_1(X_3,X_2)\eta(X_1)+D_1(X_3,X_1)\eta(X_2)+D_2(X_3,X_2)\eta(X_1)+D_2(X_3,X_1)\eta(X_2)\\ &\quad +g(\nabla_{X_1}X_3,X_2)+g(\nabla_{X_2}X_3,X_1)\end{aligned} \tag{4.5}$$

or, equivalently, we have

$$(L_{X_3}g)(X_1,X_2)=(\nabla_{X_3}g)(X_1,X_2)+g(\nabla_{X_1}X_3,X_2)+g(\nabla_{X_2}X_3,X_1).$$

Furthermore, the following equality

$$\widetilde{g}(\widetilde{R}(X_1,X_2)PX_3,PX_4)=g(R(X_1,X_2)PX_3,PX_4)+\sum_{k=1}^{2}D_k(X_1,PX_3)C_k(X_2,PX_4)-\sum_{k=1}^{2}D_k(X_2,PX_3)C_k(X_1,PX_4)$$

holds for any $X_1,X_2,X_3,X_4\in\Gamma(TM)$. The induced Ricci type tensor $R^{(0,2)}$ of M is formulated by

$$R^{(0,2)}(X_1,X_2)=\sum_{j=1}^{n}g(R(Y_j,X_1)X_2,Y_j)+\sum_{k=1}^{2}\widetilde{g}(R(X_1,\xi_k)X_2,N_k). \tag{4.6}$$

We note that $R^{(0,2)}$ is not symmetric. If $\mathrm{S}(TM)$ is integrable, then $R^{(0,2)}$ is symmetric.

A coisotropic lightlike submanifold with co-dimension 2 is said to be totally geodesic if $D_1=D_2=0$ and it is said to be irrotational [20] if $D_k=0$ on $\mathrm{Rad}(TM)$ for any $k\in\{1,2\}$. A coisotropic lightlike submanifold is known as totally umbilical if there is a differentiable transversal vector field H such that

$$D_1(X_1,X_2)N_1+D_2(X_1,X_2)N_2=g(X_1,X_2)H$$

holds for any $X_1,X_2\in\Gamma(TM)$ [22]. In this case, there exist two differentiable functions H_1 and H_2 satisfying

$$D_i(X_1,X_2)=H_ig(X_1,X_2)$$

for any $i\in\{1,2\}$.

5. Ricci Soliton Coisotropic Lightlike Submanifolds

Assume that ζ is a vector field lying on $\Gamma(T\widetilde{M})$. Hence one can put

$$\zeta=\zeta^{\top}+f_1N_1+f_2N_2$$

where $\zeta^{\top}\in\Gamma(TM)$ and f_1,f_2 are differentiable functions on $\Gamma(T\widetilde{M})$. Thus we find

$$f_1=g(\zeta,\xi_1)\quad\text{and}\quad f_2=g(\zeta,\xi_2).$$

Proposition 5.1. *Let $(M,g,S(TM))$ be a coisotropic lightlike submanifold of $(\widetilde{M},\widetilde{g})$. If ζ is concircular, then the following equalities are satisfied for any $X\in\Gamma(TM)$:*

$$\begin{aligned}\nabla_X\zeta^{\top} &= \varphi X+f_1A_{N_1}X+f_2A_{N_2}X,\\ D_1(X,\zeta^{\top}) &= -X[f_1]-f_1\rho_{11}(X)-f_2\rho_{21}(X),\\ D_2(X,\zeta^{\top}) &= -X[f_2]-f_1\rho_{12}(X)-f_2\rho_{22}(X).\end{aligned} \tag{5.1}$$

Proof. If ζ is concircular, we find

$$\widetilde{\nabla}_X\zeta \;=\varphi X=\widetilde{\nabla}_X\zeta^{\top}+\widetilde{\nabla}_X(f_1N_1)+\widetilde{\nabla}_X(f_2N_2).$$

In view of (4.1) and (4.2), we get

$$\begin{aligned}\varphi X &= \nabla_X\zeta^{\top}+D_1(X,\zeta^{\top})N_1+D_2(X,\zeta^{\top})N_2+X[f_1]N_1-f_1A_{N_1}X+f_1\rho_{11}(X)N_1+f_1\rho_{12}(X)N_2+X[f_2]N_2\\ &\quad -f_2A_{N_2}X+f_2\rho_{21}(X)N_1+f_2\rho_{22}(X)N_2.\end{aligned}$$

In view of the last equation, we obtain (3.1), (3.2) and (3.3) immediately. □

Putting $\varphi=1$ in Proposition 5.1, we have:

Proposition 5.2. *For any coisotropic lightlike submanifold admitting a concurrent vector field, we have*

$$\nabla_X \zeta^\top = X + f_1 A_{N_1} X + f_2 A_{N_2} X.$$

As a special case for $\zeta = \zeta^\top$, we have:

Proposition 5.3. *For any coisotropic lightlike submanifold admitting a concircular (or concurrent) vector field $\zeta = \zeta^\top$, we have*

$$D_1(X, \zeta^\top) = D_2(X, \zeta^\top) = 0.$$

Theorem 5.4. *Let $(M, g, S(TM))$ be a coisotropic lightlike submanifold. If there exists at least one concircular or concurrent vector field $\zeta = \zeta^\top$ on $\Gamma(TM)$, then $\nabla_{\zeta^\top} g = 0$.*

Using (4.5) and (5.1), we arrive at

$$\begin{aligned}(L_{\zeta^\top} g)(X_1, X_2) &= D_1(\zeta^\top, X_2)\eta_1(X_1) + D_1(\zeta^\top, X_1)\eta_1(X_2) + D_2(\zeta^\top, X_2)\eta_2(X_1) + D_2(\zeta^\top, X_1)\eta_2(X_2) \\ &\quad + 2g(\varphi X_1, X_2) + 2f_1 g(A_{N_1} X_1, X_2) + 2f_2 g(A_{N_2} X_1, X_2) \end{aligned} \tag{5.2}$$

for any $X_1, X_2 \in \Gamma(TM)$. If ζ is concurrent, then we obtain

$$\begin{aligned}(L_{\zeta^\top} g)(X_1, X_2) &= D_1(\zeta^\top, X_2)\eta_1(X_1) + D_1(\zeta^\top, X_1)\eta_1(X_2) + D_2(\zeta^\top, X_2)\eta_2(X_1) + D_2(\zeta^\top, X_1)\eta_2(X_2) \\ &\quad + 2g(X_1, X_2) + 2f_1 g(A_{N_1} X_1, X_2) + 2f_2 g(A_{N_2} X_1, X_2). \end{aligned} \tag{5.3}$$

As a special case for $\zeta = \zeta^\top$, we obtain

$$(L_{\zeta^\top} g)(X_1, X_2) = 2\varphi g(X_1, X_2).$$

If ζ is concurrent and $\zeta = \zeta^\top$, we find

$$(L_{\zeta^\top} g)(X_1, X_2) = 2g(X_1, X_2).$$

From (3.5) and (5.2), we have

Theorem 5.5. *Let $(M, g, S(TM))$ be a coisotropic lightlike submanifold admitting a concircular vector field ζ. Then, $(M, g, S(TM))$ is a Ricci soliton such that $\zeta^\top$ is the potential vector field if and only if the equation*

$$\begin{aligned}R^{(0,2)}(X_1, X_2) &= \frac{1}{2}\Big[-D_1(\zeta^\top, X_2)\eta_1(X_1) - D_1(\zeta^\top, X_1)\eta_1(X_2) - D_2(\zeta^\top, X_2)\eta_2(X_1) \\ &\quad - D_2(\zeta^\top, X_1)\eta_2(X_2) - 2f_1 g(A_{N_1} X_1, X_2) - 2f_2 g(A_{N_2} X_1, X_2)\Big] + (\kappa - \varphi) g(X_1, X_2)\end{aligned}$$

holds for any $X_1, X_2 \in \Gamma(TM)$.

From (3.5) and (5.3), we have:

Theorem 5.6. *Let $(M, g, S(TM))$ be a coisotropic lightlike submanifold admitting a concurrent vector field ζ. Then, $(M, g, S(TM))$ is a Ricci soliton such that $\zeta^\top$ is the potential vector field if and only if the equation*

$$R^{(0,2)}(X_1, X_2) = \frac{1}{2}\begin{bmatrix} -D_1(\zeta^\top, X_2)\eta_1(X_1) - D_1(\zeta^\top, X_1)\eta_1(X_2) - D_2(\zeta^\top, X_2)\eta_2(X_1) \\ -D_2(\zeta^\top, X_1)\eta_2(X_2) - 2f_1 g(A_{N_1} X_1, X_2) - 2f_2 g(A_{N_2} X_1, X_2) \end{bmatrix} + (\kappa - 1) g(X_1, X_2)$$

is satisfied for any $X_1, X_2 \in \Gamma(TM)$.

Theorem 5.7. *Let $(M, g, S(TM))$ be a coisotropic lightlike submanifold admitting a concircular vector field $\zeta = \zeta^\top$. Then, the submanifold is a Ricci soliton such that $\zeta^\top$ is the potential vector field if and only if the equation*

$$R^{(0,2)}(X_1, X_2) = (\kappa - \varphi) g(X_1, X_2) \tag{5.4}$$

holds for any $X_1, X_2 \in \Gamma(TM)$. It means that $(M, g, S(TM))$ is an Einstein manifold.

Theorem 5.8. *Let $(M, g, S(TM))$ be a coisotropic lightlike submanifold admitting a concurrent vector field $\zeta = \zeta^\top$. Then, the submanifold is a Ricci soliton with the potential vector field $\zeta^\top$ if and only if the equation*

$$R^{(0,2)}(X_1, X_2) = (\kappa - 1) g(X_1, X_2)$$

is satisfied for any $X_1, X_2 \in \Gamma(TM)$. It means that the submanifold is an Einstein manifold. Furthermore if the soliton is steady, then the Ricci curvature of $(M, g, S(TM))$ is negative defined.

In view of Theorem 5.5 we find:

Corollary 5.9. *Let $(M,g,S(TM))$ be a totally geodesic coisotropic lightlike submanifold admitting a concircular vector field ζ. If the submanifold is a Ricci soliton, then the equation*

$$R^{(0,2)}(X_1,X_2) = (\kappa-\varphi)g(X_1,X_2) - f_1 g(A_{N_1}X_1,X_2) - f_2 g(A_{N_2}X_1,X_2)$$

is satisfied.

As a result of Theorem 5.6 we find:

Corollary 5.10. *Let $(M,g,S(TM))$ be a totally geodesic coisotropic lightlike submanifold admitting a concurrent vector field ζ. If the submanifold is a Ricci soliton, then the equation*

$$R^{(0,2)}(X_1,X_2) = (\kappa-1)g(X_1,X_2) - f_1 g(A_{N_1}X_1,X_2) - f_2 g(A_{N_2}X_1,X_2)$$

is satisfied.

Example 5.11. *Consider a submanifold in $\mathbb{R}^6_3$ given by*

$$z_4 = (z_1^2+z_2^2)^{\frac{1}{2}}, \quad z_3 = (z_5^2+z_6^2)^{\frac{1}{2}}, \quad z_1,z_2,z_3,z_4 > 0.$$

Then we find

$$\begin{aligned}
Rad(TM) &= Span\{\xi_1 = z_1\partial_1 + z_2\partial_2 + z_4\partial_4, \quad \xi_2 = z_3\partial_3 + z_5\partial_5 + z_6\partial_6\},\\
S(TM) &= Span\{X_1 = z_4\partial_1 + z_1\partial_4, X_2 = z_3\partial_5 + z_5\partial_3\},\\
ltr(TM) &= Span\left\{N_1 = \frac{1}{2z_2^2}(z_1\partial_1 - z_2\partial_2 + z_3\partial_3), \quad N_2 = \frac{1}{2z_5^2}(z_3\partial_3 - z_5\partial_5 + z_6\partial_6)\right\},
\end{aligned}$$

where $\{\partial_1,\partial_2,\partial_3,\partial_4,\partial_5,\partial_6\}$ is the natural frame field on $\mathbb{R}^6_3$. Therefore $(M,g,S(TM))$ is a coisotropic lightlike submanifold. By a straightforward computation, we obtain

$$\begin{aligned}
&\widetilde{\nabla}_{X_1}\xi_1 = X_1, && \widetilde{\nabla}_{X_1}\xi_2 = 0, && \widetilde{\nabla}_{X_2}\xi_1 = 0, && \widetilde{\nabla}_{X_2}\xi_2 = X_2,\\
&\widetilde{\nabla}_{\xi_1}\xi_1 = \xi_1, && \widetilde{\nabla}_{\xi_1}\xi_2 = \widetilde{\nabla}_{\xi_2}\xi_1 = 0, && \widetilde{\nabla}_{\xi_2}\xi_2 = \xi_2, && \widetilde{\nabla}_{\xi_2}N_2 = N_2.\\
&\widetilde{\nabla}_{\xi_1}N_1 = N_1, && \widetilde{\nabla}_{\xi_1}N_2 = 0, && \widetilde{\nabla}_{\xi_2}N_1 = 0,
\end{aligned}$$

In view of (4.1)-(4.4), we obtain

$$D_1(\xi_1,\xi_1) = D_2(\xi_2,\xi_2) = D_1(\xi_1,\xi_2) = 0.$$

Therefore, we have $R^{(0,2)}(X_1,X_2) = 0$. If we consider $\zeta = \varphi(\xi_1+\xi_2)$, where φ is a differentiable function and $\zeta = \zeta^T$, then we find $(M,g,S(TM))$ is a Ricci soliton such that $\zeta^\top$ is the potential vector field and $\kappa = 1$. Thus, the submanifold is a shrinking Ricci soliton.

Example 5.12. *Consider a submanifold in $\mathbb{R}^5_2$ with the signature $(-,-,+,+,+)$ given by*

$$M = \left\{(u^2, u^2w, u^2\cos v, u^2\sin v, u^2w) : \ v\in[0,2\pi), u,w\in\mathbb{R}\right\}.$$

Then we have

$$\begin{aligned}
Rad(TM) &= Span\{\xi_1 = 2u(\partial_1 + w\partial_2 + \cos v\partial_3 + \sin v\partial_4 + w\partial_5), \quad \xi_2 = u^2(\partial_2+\partial_5)\},\\
S(TM) &= Span\{X_1 = u^2(-\sin v\partial_3 + \cos v\partial_4)\},\\
ltr(TM) &= Span\left\{N_1 = \frac{1}{2u}(-\partial_1 + w\partial_2 + \cos v\partial_3 + \sin v\partial_4 + w\partial_5), \quad N_2 = \frac{1}{2u^2}(-\partial_2+\partial_5)\right\},
\end{aligned}$$

where $\{\partial_1,\partial_2,\partial_3,\partial_4,\partial_5\}$ is the natural frame field on $\mathbb{R}^5_2$. Therefore, $(M,g,S(TM))$ is a coisotropic lightlike hypersurface of $\mathbb{R}^5_2$. By a straightforward computation, we find

$$\widetilde{\nabla}_{X_1}\xi_1 = \frac{2}{u}X_1, \quad \widetilde{\nabla}_{\xi_2}\xi_1 = \frac{2}{u}\xi_2, \quad \widetilde{\nabla}_{\xi_1}\xi_1 = \frac{2}{u}\xi_1,$$

which show that ξ_1 is a concircular vector field on $(M,g,S(TM))$ and $(L_{\xi_1}g)(X_1,X_1) = 2u^2$. By a direct computation, we get

$$R(X_1,\xi_1)X_1 = X_1, \quad R(X_1,\xi_2)X_1 = 0$$

which shows that $R^{(0,2)}(X_1,X_1) = 0$. This fact shows that $(M,g,S(TM))$ is almost Ricci soliton such that $\kappa = \frac{2}{u^2}$.

Theorem 5.13 (Theorem 3.1 in [24]). *Let $(M,g,S(TM))$ be a totally umbilical lightlike submanifold of $\widetilde{M}(c)$. Then the following equality holds*

$$R(X_1,X_2)X_3 = c\{g(X_2,X_3)X_1 - g(X_1,X_3)X_2\} + \sum_{i=1}^{2}[H_i\{g(X_2,X_3)A_{N_i}X_1 - g(X_1,X_3)A_{N_i}X_2\}], \tag{5.5}$$

where the mean curvature vector field $H = H_1N + H_2U$.

Theorem 5.14. *Let $(M,g,S(TM))$ be a totally umbilical lightlike submanifold of $\widetilde{M}(c)$ admitting a concircular vector field $\zeta = \zeta^{\top}$. The submanifold is a Ricci soliton such that $\zeta^{\top}$ is the potential vector field if and only if the equation*

$$\kappa = c + \varphi + \sum_{i=1}^{2} H_i traceA_{N_i}$$

is satisfied.

Proof. Let $\{Y_1,\ldots,Y_n\}$ be an orthonormal frame field on the screen distribution. From (4.6) and (5.5), we find

$$R^{(0,2)}(Y_j,Y_j) = c + \sum_{i=1}^{2} H_1 \text{trace}A_{N_i} \tag{5.6}$$

for any $j \in \{1,\ldots,n\}$. From (5.4) and (5.6), the proof is straightforward. □

As a result of Theorem 5.14, we obtain:

Theorem 5.15. *Let $(M,g,S(TM))$ be a totally umbilical lightlike submanifold of $\widetilde{M}(c)$ admitting a concurrent vector field $\zeta = \zeta^{\top}$. The submanifold is a Ricci soliton with the potential vector field $\zeta^{\top}$ if and only if the equation*

$$\kappa = c + 1 + \sum_{i=1}^{2} H_i traceA_{N_i}$$

is satisfied.

Article Information

Acknowledgements: The authors would like to express their sincere thanks to the editor and the anonymous reviewers for their helpful comments and suggestions.

Author's contributions: All authors contributed equally to the writing of this paper. All authors read and approved the final manuscript.

Conflict of Interest Disclosure: No potential conflict of interest was declared by the author.

Supporting/Supporting Organizations: No grants were received from any public, private or non-profit organizations for this research.

Ethical Approval and Participant Consent: It is declared that during the preparation process of this study, scientific and ethical principles were followed and all the studies benefited from are stated in the bibliography.

Plagiarism Statement: This article was scanned by the plagiarism program. No plagiarism detected.

Availability of data and materials: Not applicable.

References

[1] M. T. K. Abbassi, N. Amri, C. L. Bejan, *Conformal vector fields and Ricci soliton structures on natural Riemann extensions*, Mediterr. J. Math., **18**(2) (2021), 1–16.
[2] C. L. Bejan, M. Crasmareanu, *Second order parallel tensors and Ricci solitons in 3-dimensional normal paracontact geometry*, Ann. Global Anal. Geom., **46**(2) (2014), 117–127.
[3] A. M. Blaga, C. Özgür, *Almost η-Ricci and almost η-Yamabe solitons with torse-forming potential vector field*, Quaest. Math., **45**(1) (2022), 143–163.
[4] B. Y. Chen, S. Deshmukh, *Geometry of compact shrinking Ricci solitons*, Balkan J. Geom. Appl., **19**(1) (2014), 13–21.
[5] S. Deshmukh, H. Alodan, H. Al-Sodais, *A note on Ricci solitons*, Balkan J. Geom. Appl., **16**(1) (2011), 48–55.
[6] S. Y. Perktaş, S. Keleş, *Ricci solitons in 3-dimensional normal almost paracontact metric manifolds*, Int. Electron. J. Geom., **8**(2) (2015), 34–45.
[7] A. Sardar, U. C. De, *η-Ricci solitons on para-Kenmotsu manifolds*, Differ. Geom. Dyn. Syst., **22** (2020), 218–228.
[8] H. İ. Yoldaş, Ş. Eken Meriç, E. Yaşar, *Some special vector fields on a cosymplectic manifold admitting a Ricci soliton*, Miskolc Math. Notes, **22**(2) (2021), 1039–1050.
[9] K. Yano, *On the torse-forming direction in Riemannian spaces*, Proceedings of the Imperial Academy, **20**(6) (1944), 340-345.
[10] B. Y. Chen, *Some results on concircular vector fields and their applications to Ricci solitons*, Bull. Korean Math. Soc., **52**(5) (2015), 1535–1547.

[11] B. Y. Chen, *Concircular vector fields and pseudo-Kaehler manifolds*, Kragujevac J. Math., **40**(1) (2016), 7–14.
[12] B. Y. Chen, S. Deshmukh, *Some results about concircular vector fields on Riemannian manifolds*, Filomat, **34**(3) (2020), 835–842.
[13] S. Deshmukh, K. İlarslan, H. Alsodais, U. C. De, *Spheres and Euclidean spaces via concircular vector fields*, Mediterr. J. Math., **18**(5) (2021), 1–14.
[14] D. A. Kaya, L. Onat, *Almost Ricci solitons and concircular vector fields*, An. Ştiinţ. Univ. Al. I. Cuza Iaşi. Mat. (N.S.), **64** (2018), 199-204.
[15] S. Khan, A. Mahmood, A. T. Ali, *Concircular vector fields for Kantowski-Sachs and Bianchi type-III spacetimes*, Int. J. Geom. Methods Mod. Phys., **15**(08) (2018), 1850126.
[16] E. Kılıç, M. Gülbahar, E. Kavuk, *Concurrent vector fields on lightlike hypersurfaces*, Mathematics, **9**(1) (2020), 59.
[17] K. L. Duggal, A. Bejancu, *Lightlike Submanifolds of Semi-Riemannian Manifolds and Applications*, Springer Dordrecht: Kluwer Academic Publishers, London, UK, 1996.
[18] K. L. Duggal, A. Bejancu, *Lightlike submanifolds of codimension two*, Toyama Math. J., **15** (1992), 59–82.
[19] K. L. Duggal, B. Şahin, *Screen conformal half-lightlike submanifolds*, Int. J. Math. Math. Sci., **2004**(68) (2004), 3737–3753.
[20] D. N. Kupeli, *Singular Semi-Riemannian Geometry*, Kluwer Academic, 1996.
[21] K. L. Duggal, D. H. Jin, *Totally umbilical lightlike submanifolds*, Kodai Math. J., **26** (2003), 49-–68.
[22] K. L. Duggal, B. Şahin, *Differential Geometry of Lightlike Submanifolds*, Springer Science, Business Media: Berlin, Germany, 2011.
[23] K. L. Duggal, D. H. Jin, *Half-lightlike submanifolds of codimension 2*, Toyama Math. J., **22** (1999), 121–161.
[24] D.H. Jin, *Geometry of coisotropic submanifolds*, J. Korean Soc. Math. Educ. Ser. B Pure Appl. Math., **8**(1) (2001), 33—46.

Fundamental Journal of Mathematics and Applications, 6 (2) (2023) 128-136
Research Article

FUJMA

Fundamental Journal of Mathematics and Applications

Journal Homepage: www.dergipark.org.tr/en/pub/fujma
ISSN: 2645-8845
doi: https://dx.doi.org/10.33401/fujma.1239100

Qualitative Behavior of the Difference Equation $x_{n+1} = \frac{\alpha x_{n-m}+\eta x_{n-k}+\sigma x_{n-l}+\delta x_n}{\beta+\gamma x_{n-k}x_{n-l}(x_{n-k}+x_{n-l})}$

Mohamed Abd El-Moneam

Mathematics Department, Faculty of Science, Jazan University, Kingdom of Saudi Arabia

Article Info

Keywords: *Difference equations, Rational difference equations, qualitative properties of solutions of difference equations, Equilibrium, Oscillates, Prime period two solution, Globally asymptotically stable*
2010 AMS: *39A10, 39A11, 39A99, 34C99*
Received: *19 January 2023*
Accepted: *5 May 2023*
Available online: *25 June 2023*

Abstract

In this paper, we discuss some qualitative properties of the positive solutions to the following rational nonlinear difference equation $x_{n+1} = \frac{\alpha x_{n-m}+\eta x_{n-k}+\sigma x_{n-l}+\delta x_n}{\beta+\gamma x_{n-k}x_{n-l}(x_{n-k}+x_{n-l})}$, $n = 0,1,2,\ldots$ where the parameters $\alpha,\beta,\gamma,\delta,\eta,\sigma \in (0,\infty)$, while m,k,l are positive integers, such that $m < k < l$. The initial conditions $x_{-m},\ldots,x_{-k},\ldots,x_{-l},\ldots,x_{-1},\ldots,x_0$ are arbitrary positive real numbers. We will give some numerical examples to illustrate our results.

1. Introduction

The study of solution of nonlinear rational recursive sequence of high order is quite challenging and rewarding. Every dynamical system $a_{n+1} = f(a_n)$ determines a difference equation and vice versa. An interesting class of nonlinear difference equations is the class of solvable difference equations, and one of the interesting problems is to find equations that belong to this class and to solve them in closed form or in explicit form [1–25]. Note that most of these equation often show increasingly complex behavior such as the existence of a bounded. The qualitative study of difference equations is a fertile research area and increasingly attracts many mathematicians. This topic draws its importance from the fact that many real life phenomena are modeled using difference equations. The applications of these difference equations can be found on the economy, biology and so on. It is known that nonlinear difference equations are capable of producing a complicated behavior regardless its order. The objective of this article is to investigate some qualitative behavior of the solutions of the nonlinear difference equation

$$x_{n+1} = \frac{\alpha x_{n-m}+\eta x_{n-k}+\sigma x_{n-l}+\delta x_n}{\beta+\gamma x_{n-k}x_{n-l}(x_{n-k}+x_{n-l})}, \qquad n = 0,1,2,\ldots \tag{1.1}$$

where the parameters $\alpha,\beta,\gamma,\delta,\eta,\sigma \in (0,\infty)$, while m,k,l are positive integers, such that $m < k < l$. The initial conditions $x_{-m},\ldots,x_{-k},\ldots,x_{-l},\ldots,x_{-1},\ldots,x_0$ are arbitrary positive real numbers equation (1.1) has been discussed in [26] when $m = 1, k = 2$ and $l = 4$, and in [27] when $\delta = 0$, where some global behavior of the more general nonlinear rational difference equation (1.1), we need the following well-known definitions and results [28–34].

Definition 1.1. *A difference equation of order $(k+1)$ is of the form*

$$x_{n+1} = F(x_n, x_{n-1},\ldots,x_{-k}), \quad n = 0,1,2,\ldots \tag{1.2}$$

Email address and ORCID number: maliahmedibrahim@jazanu.edu.sa, 0000-0002-1676-2662
Cite as: El-Moneam, M. A., *Qualitative Behavior of the difference equation* $x_{n+1} = \frac{\alpha x_{n-m}+\eta x_{n-k}+\sigma x_{n-l}+\delta x_n}{\beta+\gamma x_{n-k}x_{n-l}(x_{n-k}+x_{n-l})}$, Fundam. J. Math. Appl., 6(2) (2023), 128-136.

where F is a continuous function which maps some set J^{k+1} into J and J is a set of real numbers. An equilibrium point $\widetilde{x}$ of this equation is a point that satisfies the condition $\widetilde{x} = F(\widetilde{x},\widetilde{x},\ldots,\widetilde{x})$. That is, the constant sequence $\{x_n\}_{n=-k}^{\infty}$ with $x_n = \widetilde{x}$ for all $n \geq -k$ is a solution of that equation.

Definition 1.2. *Let $\widetilde{x} \in (0,\infty)$ be an equilibrium point of the difference equation (1.2). Then*

(i) An equilibrium point $\widetilde{x}$ of the difference equation (1.2) is called locally stable if for every $\varepsilon > 0$ there exists $\delta > 0$ such that, if $x_{-k},\ldots,x_{-1},x_0 \in (0,\infty)$ with $|x_{-k}-\widetilde{x}|+\ldots+|x_{-1}-\widetilde{x}|+|x_0-\widetilde{x}| < \delta$, then $|x_n-\widetilde{x}| < \varepsilon$ for all $n \geq -k$.

(ii) An equilibrium point $\widetilde{x}$ of the difference equation (1.2) is called locally asymptotically stable if it is locally stable and there exists $\gamma > 0$ such that, if $x_{-k},\ldots,x_{-1},x_0 \in (0,\infty)$ with $|x_{-k}-\widetilde{x}|+\ldots+|x_{-1}-\widetilde{x}|+|x_0-\widetilde{x}| < \gamma$, then

$$\lim_{n\to\infty} x_n = \widetilde{x}.$$

(iii) An equilibrium point $\widetilde{x}$ of the difference equation (1.2) is called a global attractor if for every $x_{-k},\ldots,x_{-1},x_0 \in (0,\infty)$ we have

$$\lim_{n\to\infty} x_n = \widetilde{x}.$$

(iv) An equilibrium point $\widetilde{x}$ of the equation (1.2) is called globally asymptotically stable if it is locally stable and a global attractor.

(v) An equilibrium point $\widetilde{x}$ of the difference equation (1.2) is called unstable if it is not locally stable.

Definition 1.3. *A sequence $\{x_n\}_{n=-k}^{\infty}$ is said to be periodic with period p if $x_{n+p} = x_n$ for all $n \geq -k$. A sequence $\{x_n\}_{n=-k}^{\infty}$ is said to be periodic with prime period p if p is the smallest positive integer having this property.*

Definition 1.4. *We say that a sequence $\{x_n\}_{n=-l}^{\infty}$ is bounded and persisting if there exists positive constants m and M such that*

$$m \leq x_n \leq M \quad \text{for all} \quad n \geq -k.$$

Definition 1.5. *A positive semicycle of $\{x_n\}_{n=-k}^{\infty}$ consists of "a string" of terms $x_l,x_{l+1},\ldots,x_m$ all greater than or equal to $\tilde{x}$, with $l \geq -k$ and $m \leq \infty$ such that*

$$\text{either} \quad l = -k \quad \text{or} \quad l > -k \quad \text{and} \quad x_{l-1} < \tilde{x},$$

and

$$\text{either} \quad m = \infty \quad \text{or} \quad m < \infty \quad \text{and} \quad x_{m+1} < \tilde{x}.$$

A negative semicycle of $\{x_n\}_{n=-k}^{\infty}$ consists of "a string" of terms $x_l,x_{l+1},\ldots,x_m$ all less than $\tilde{x}$, with $l \geq -k$ and $m \leq \infty$ such that

$$\text{either} \quad l = -k \quad \text{or} \quad l > -k \quad \text{and} \quad x_{l-1} \geq \tilde{x},$$

and

$$\text{either} \quad m = \infty \quad \text{or} \quad m < \infty \quad \text{and} \quad x_{m+1} \geq \tilde{x}.$$

Definition 1.6. *The linearized equation of equation (1.2) about the equilibrium point $\widetilde{x}$ is the linear difference equation*

$$y_{n+1} = \sum_{i=0}^{k} \frac{\partial F(\widetilde{x},\widetilde{x},\ldots,\widetilde{x})}{\partial x_{n-i}} y_{n-i}. \tag{1.3}$$

Now assume that the characteristic equation associated with equation (1.3) is

$$p(\lambda) = p_0\lambda^k + p_1\lambda^{k-1} + \ldots + p_{k-1}\lambda + p_k = 0 \tag{1.4}$$

where

$$p_i = \partial F(\widetilde{x},\widetilde{x},\ldots,\widetilde{x})/\partial x_{n-i}.$$

Theorem 1.7. *Assume that $p_i \in R$, $i = 1,2,\ldots,$ and $k \in \{0,1,2,\ldots\}$. Then*

$$\sum_{i=1}^{k} |p_i| < 1$$

is a sufficient condition for the asymptotic stability of the difference equation

$$x_{n+k} + p_1x_{n+k-1} + \ldots + p_kx_n = 0, \quad n = 0,1,2,\ldots$$

Theorem 1.8 (The Linearized Stability Theorem)**.** *Suppose F is a continuously differentiable function defined on an open neighbourhood of the equilibrium $\widetilde{x}$. Then the following statements are true.*

(i) If all roots of the characteristic equation (1.4) of the linearized equation (1.3) have an absolute value less than one, then the equilibrium point $\widetilde{x}$ is locally asymptotically stable.

(ii) If at least one root of equation (1.4) has an absolute value greater than one, then the equilibrium point $\widetilde{x}$ is unstable.

2. Change of Variables

By using the change of variables $x_n = \left(\frac{\beta}{\gamma}\right)^{\frac{1}{3}} y_n$, the equation (1.1) reduces to the following difference equation

$$y_{n+1} = \frac{ry_{n-m}+ty_{n-k}+uy_{n-l}+sy_n}{1+y_{n-k}y_{n-l}\left(y_{n-k}+y_{n-l}\right)}, \qquad n = 0,1,2,\ldots \tag{2.1}$$

where $r = \frac{\alpha}{\beta} > 0$, $s = \frac{\delta}{\beta} > 0$, $u = \frac{\sigma}{\beta} > 0$, $t = \frac{\eta}{\beta} > 0$ and the initial conditions $y_{-l},\ldots,y_{-k},\ldots,y_{-m},\ldots,y_{-l},y_0 \in (0,\infty)$. In the next section, we shall study the global behavior of equation (2.1).

3. The Dynamics of Equation (2.1)

The equilibrium points $\tilde{y}$ of the equation (2.1) are the positive solutions of the equation

$$\tilde{y} = \frac{[r+s+t+u]\tilde{y}}{1+2\tilde{y}^3}. \tag{3.1}$$

Thus $\tilde{y}_1 = 0$ is always an equilibrium point of the equation (2.1). If $(r+s+t+u) > 1$, then the only positive equilibrium point $\tilde{y}_2$ of equation (2.1) is given by

$$\tilde{y}_2 = \left(\frac{[r+s+t+u]-1}{2}\right)^{\frac{1}{3}}. \tag{3.2}$$

Let us introduce a continuous function $F : (0,\infty)^4 \to (0,\infty)$ which is defined by

$$F(v_0,v_1,v_2,v_3) = \frac{rv_0+sv_1+tv_2+uv_3}{1+v_2^2v_3+v_2v_3^2}. \tag{3.3}$$

Consequently, we get

$$\frac{\partial F(v_0,v_1,v_2,v_3)}{\partial v_0} = \frac{r}{1+v_2^2v_3+v_2v_3^2},$$

$$\frac{\partial F(v_0,v_1,v_2,v_3)}{\partial v_1} = \frac{s}{1+v_2^2v_3+v_2v_3^2},$$

$$\frac{\partial F(v_0,v_1,v_2,v_3)}{\partial v_2} = \frac{t(1+v_2^2v_3+v_2v_3^2)-(rv_0+sv_1+tv_2)(2v_2v_3+v_3^2)}{(1+v_2^2v_3+v_2v_3^2)^2},$$

$$\frac{\partial F(v_0,v_1,v_2,v_3)}{\partial v_3} = \frac{u(1+v_2^2v_3+v_2v_3^2)-(rv_0+sv_1+tv_2+uv_3)(v_2^2+2v_2v_3)}{(1+v_2^2v_3+v_2v_3^2)^2}.$$

At $\tilde{y}_1 = 0$, we have $\frac{\partial F(0,0,0,0)}{\partial v_0} = r$, $\frac{\partial F(0,0,0,0)}{\partial v_1} = s$, $\frac{\partial F(0,0,0,0)}{\partial v_2} = t$, $\frac{\partial F(0,0,0,0)}{\partial v_3} = u$, and the linearized equation of equation (2.1) about $\tilde{y}_1 = 0$, is the equation

$$z_{n+1} - \rho_0 z_n - \rho_1 z_{n-m} - \rho_2 z_{n-k} - \rho_3 z_{n-l} = 0 \tag{3.4}$$

where $\rho_0 = s$, $\rho_1 = r$, $\rho_2 = t$, $\rho_3 = u$. At $\tilde{y}_2 = \left(\frac{[r+s+t+u]-1}{2}\right)^{\frac{1}{3}}$, we have

$$\frac{\partial F(\tilde{y}_2,\tilde{y}_2,\tilde{y}_2,\tilde{y}_2)}{\partial v_0} = \frac{r}{1+2\tilde{y}_2^3} = \frac{r}{1+([r+s+t+u]-1)} = \frac{r}{[r+s+t+u]},$$

$$\frac{\partial F(\tilde{y}_2,\tilde{y}_2,\tilde{y}_2,\tilde{y}_2)}{\partial v_1} = \frac{s}{1+2\tilde{y}_2^3} = \frac{s}{1+([r+s+t+u]-1)} = \frac{s}{[r+s+t+u]},$$

$$\frac{\partial F(\tilde{y}_2,\tilde{y}_2,\tilde{y}_2,\tilde{y}_2)}{\partial v_2} = \frac{2t-3([r+s+t+u]-1)}{2[r+s+t+u]},$$

$$\frac{\partial F(\tilde{y}_2,\tilde{y}_2,\tilde{y}_2,\tilde{y}_2)}{\partial v_3} = \frac{2u-3([r+s+t+u]-1)}{2[r+s+t+u]}.$$

And the linearized equation of equation (2.1) about $\tilde{y}_2 = \left(\frac{[r+s+t+u]-1}{2}\right)^{\frac{1}{3}}$ is the equation

$$z_{n+1} - \rho_0 z_n - \rho_1 z_{n-m} - \rho_2 z_{n-k} - \rho_3 z_{n-l} = 0, \tag{3.5}$$

where $\rho_0 = \frac{s}{[r+s+t+u]}$, $\rho_1 = \frac{r}{[r+s+t+u]}$, $\rho_2 = \frac{2t-3([r+s+t+u]-1)}{2[r+s+t+u]}$, $\rho_3 = \frac{2u-3([r+s+t+u]-1)}{2[r+s+t+u]}$.

Theorem 3.1. *(i) If $[r+s+t+u] < 1$, then the equilibrium point $\tilde{y}_1 = 0$ is locally asymptotically stable.*

(ii) If $[r+s+t+u] > 1$, then the equilibrium point $\tilde{y}_1 = 0$ is unstable.

(iii) If $[r+s+t+u] > 1$, $2t > 3([r+s+t+u]-1)$, then the equilibrium point $\tilde{y}_2 = \left(\frac{[r+s+t+u]-1}{2}\right)^{\frac{1}{3}}$ is unstable.

Proof. With reference to Theorem 1.7, we deduce from equation (3.5) that $|\rho_0|+|\rho_1|+|\rho_2|+|\rho_3| = [r+s+t+u] < 1$, and then the proof of parts (i), (ii) follow. Also, from equation (3.5) we deduce for $[r+s+t+u] > 1$ that $|\rho_0|+|\rho_1|+|\rho_2|+|\rho_3| = 1 + \frac{3([r+s+t+u]-1)}{[r+s+t+u]} > 1$, and hence the proof of part (iii) follows. □

Theorem 3.2. *Assume that $[r+s+t+u] > 1$, and let $\{y_n\}_{n=-l}^{\infty}$ be a solution of equation (2.1) such that*

$$\begin{aligned} &y_{-l}, y_{-l+2}, \ldots, y_{-l+2n}, \ldots, y_{-k}, y_{-k+2}, \ldots, y_{-k+2n}, \ldots, \\ &y_{-m+1}, y_{-m+3}, \ldots, y_{-m+2n+1}, \ldots, y_0 \geq \tilde{y}_2 \\ &\textit{and} \\ &y_{-l+1}, y_{-l+3}, \ldots, y_{-l+2n+1}, \ldots, y_{-k+1}, y_{-k+3}, \ldots, \\ &y_{-k+2n+1}, \ldots, y_{-m}, y_{-m+2}, \ldots, y_{-m+2n}, \ldots, y_{-1} < \tilde{y}_2. \end{aligned} \tag{3.6}$$

Then $\{y_n\}_{n=-l}^{\infty}$ oscillates about $\tilde{y}_2 = \left(\frac{[r+s+t+u]-1}{2}\right)^{\frac{1}{3}}$ with a semicycle of length one.

Proof. Assume that (3.6) holds. Then

$$y_1 = \frac{ry_{-m}+sy_0+ty_{-k}+uy_{-l}}{1+y_{-k}y_{-l}(y_{-k}+y_{-l})} < \frac{ry_{-m}+sy_0+ty_{-k}+uy_{-l}}{1+2\tilde{y}_2^3} < \frac{[r+s+t+u]\tilde{y}_2}{1+([r+s+t+u]-1)} = \tilde{y}_2$$

and

$$y_2 = \frac{ry_{-m+1}+sy_1+ty_{-k+1}+uy_{-l+1}}{1+y_{-k+1}y_{-l+1}(y_{-k+1}+y_{-l+1})} \geq \frac{ry_{-m+1}+sy_1+ty_{-k+1}+uy_{-l+1}}{1+2\tilde{y}_2^3} \geq \frac{[r+s+t+u]\tilde{y}_2}{1+([r+s+t+u]-1)} = \tilde{y}_2$$

and hence the proof follows by induction. □

Theorem 3.3. *Assume that $[r+s+t+u] < 1$, then the equilibrium point $\tilde{y}_1 = 0$ of equation (2.1) is globally asymptotically stable.*

Proof. We have shown in Theorem 3.3 that if $[r+s+t+u] < 1$ then the equilibrium point $\tilde{y}_1 = 0$ is locally asymptotically stable. It remains to show that $\tilde{y}_1 = 0$ is a global attractor. To this end, let $\{y_n\}_{n=-l}^{\infty}$ be a solution of equation (2.1). It suffics to show that $\lim_{n\to\infty} y_n = 0$. Since

$$0 \leq y_{n+1} = \frac{ry_{n-m}+sy_n+ty_{n-k}+uy_{n-l}}{1+y_{n-k}y_{n-l}(y_{n-k}+y_{n-l})} \leq ry_{n-m}+sy_n+ty_{n-k}+uy_{n-l} < y_{n-k}.$$

Then we have $\lim_{n\to\infty} y_n = 0$. This completes the proof. □

Theorem 3.4. *Assume that $[r+s+t+u] > 1$, then equation (2.1) possesses an unbounded solution.*

Proof. With the aid of Theorem 3.2, we have

$$\begin{aligned} y_{2n+2} &= \frac{ry_{-m+2n+1}+sy_{2n+1}+ty_{-k+2n+1}+uy_{-l+2n+1}}{1+y_{-k+2n+1}\,y_{-l+2n+1}(y_{-k+2n+1}+y_{-l+2n+1})} > \frac{ry_{-m+2n+1}+sy_{2n+1}+ty_{-k+2n+1}+uy_{-l+2n+1}}{1+2\tilde{y}_2^3} \\ &> \frac{ry_{-m+2n+1}+sy_{2n+1}+ty_{-k+2n+1}+uy_{-l+2n+1}}{1+([r+s+t+u]-1)} = \frac{ry_{-m+2n+1}+sy_{2n+1}+ty_{-k+2n+1}+uy_{-l+2n+1}}{[r+s+t+u]}, \end{aligned}$$

and

$$\begin{aligned} y_{2n+3} &= \frac{ry_{-m+2n+2}+sy_{2n+2}+ty_{-k+2n+2}+uy_{-l+2n+2}}{1+y_{-k+2n+2}\,y_{-l+2n+2}(y_{-k+2n+2}+y_{-l+2n+2})} \leq \frac{ry_{-m+2n+2}+sy_{2n+2}+ty_{-k+2n+2}+uy_{-l+2n+2}}{1+2\tilde{y}_2^3} \\ &\leq \frac{ry_{-m+2n+2}+sy_{2n+2}+ty_{-k+2n+2}+uy_{-l+2n+2}}{1+([r+s+t+u]-1)} = \frac{ry_{-m+2n+2}+sy_{2n+2}+ty_{-k+2n+2}+uy_{-l+2n+2}}{[r+s+t+u]}. \end{aligned}$$

From which it follows that

$$\lim_{n\to\infty} y_{2n} = \infty \quad \textit{and} \quad \lim_{n\to\infty} y_{2n+1} = 0.$$

Hence, the proof of Theorem 3.4 is now completed. □

Theorem 3.5. *(i) If m is odd, and k,l are even, equation (2.1) has prime period two solution if $(r-[s+t+u])<1$ and has not prime period two solution if $(r-[s+t+u])\geq 1$.*
(ii) If m is even and k,l are odd, equation (2.1) has not prime period two solution.
(iii) If all m,k,l are even, equation (2.1) has prime period two solution.
(iv) If all m,k,l are odd, equation (2.1) has prime period two solution if $(r-[s+t+u])>1$, and has not prime period two solution if $(r-[s+t+u])\leq 1$.
(v) If m,k are even and l is odd, equation (2.1) has not prime period two solution if $[r+s+t]+1>u$.
(vi) If m,k are odd and l is even, equation (2.1) has prime period two solution if $([r+t]-[s+u])>1$, and has not prime period two solution if $([r+t]-[s+u])\leq 1$.
(vii) If m,l are odd and k is even, equation (2.1) has prime period two solution if $([r+u]-[s+t])>1$, and has not prime period two solution if $([r+u]-[s+t])\leq 1$.
(viii) If m,l are even and k is odd, equation (2.1) has not prime period two solution.

Proof. Assume that there exists distinct positive solutions

$$\ldots,\phi,\psi,\phi,\psi,\ldots$$

of prime period two of equation (2.1).

(i) If m is odd, and k,l are even, then $y_{n+1}=y_{n-m}$ and $y_n=y_{n-k}=y_{n-l}$. It follows from equation (2.1) that

$$\phi=\frac{r\phi+[s+t+u]\,\psi}{1+2\psi^3}, \quad \psi=\frac{r\psi+[s+t+u]\,\phi}{1+2\phi^3}.$$

Consequently, we have

$$0<2\phi\psi(\phi+\psi)=1-(r-[s+t+u]). \tag{3.7}$$

We deduce that (3.7) is always true if $(r-[s+t+u])<1$ and hence equation (2.1) has prime period two solution. If $(r-[s+t+u])\geq 1$, we have a contradiction, and hence equation (2.1) has not prime period two solution.

(ii) If m is even, and k,l are odd, then $y_n=y_{n-m}$,and $y_{n+1}=y_{n-k}=y_{n-l}$. It follows from equation (2.1) that

$$\phi=\frac{[t+u]\,\phi+[r+s]\,\psi}{1+2\phi^3}, \quad \psi=\frac{[t+u]\,\psi+[r+s]\phi}{1+2\psi^3}.$$

Consequently, we have

$$0<2\,(\phi+\psi)\,(\phi^2+\psi^2)=-\,([r+s+t+u]+1). \tag{3.8}$$

Since $[r+s+t+u]>0$, we have a contradiction. Hence equation (2.1) has not prime period two solution.

(iii) If all m,k,l are even, then $y_n=y_{n-m}=y_{n-k}=y_{n-l}$. It follows from equation (2.1) that

$$\phi=\frac{[r+s+t+u]\,\psi}{1+2\psi^3}, \quad \psi=\frac{[r+s+t+u]\,\phi}{1+2\phi^3}.$$

Consequently, we get

$$0<2\phi\psi(\phi+\psi)=[r+s+t+u]+1. \tag{3.9}$$

Since $[r+s+t+u]>0$, the formula (3.9) is always true. Hence equation (2.1) has prime period two solution.

(iv) If all m,k,l are odd, then $y_{n+1} = y_{n-m} = y_{n-k} = y_{n-l}$. It follows from equation (2.1) that

$$\phi = \frac{r\psi + [s+t+u]\,\phi}{1+2\phi^3}, \quad \psi = \frac{r\phi + [s+t+u]\,\psi}{1+2\psi^3}.$$

Consequently, we get

$$0 < 2(\phi+\psi)(\phi^2+\psi^2) = (r-[s+t+u])-1. \tag{3.10}$$

If $(r-[s+t+u]) > 1$, the formula (3.10) is always true, and hence equation (2.1) has prime period two solution. If $(r-[s+t+u]) \leq 1$, we have a contradiction and hence equation (2.1) has not prime period two solution.

(v) If m,k are even, and l is odd, then $y_n = y_{n-k} = y_{n-m}$, and $y_{n+1} = y_{n-l}$. It follows from equation (2.1) that

$$\phi = \frac{[r+s+t]\,\psi + u\phi}{1+\psi^2\phi+\psi\phi^2}, \quad \psi = \frac{[r+s+t]\,\phi + u\psi}{1+\phi^2\psi+\phi\psi^2}.$$

Consequently, we have

$$0 < \phi\psi(\phi+\psi) = u - ([r+s+t]+1). \tag{3.11}$$

Since $[r+s+t]+1 > u$, we have a contradiction. Hence equation (2.1) has not a prime period two solution.

(vi) If m,k are odd, and l is even, then $y_{n+1} = y_{n-m} = y_{n-k}$, and $y_n = y_{n-l}$. It follows from equation (2.1) that

$$\phi = \frac{[r+t]\,\phi + [s+u]\,\psi}{1+\phi\psi(\phi+\psi)}, \quad \psi = \frac{[r+t]\,\psi + [s+u]\,\phi}{1+\phi\psi(\phi+\psi)}.$$

Consequently, we have

$$0 < \phi\psi(\phi+\psi) = ([r+t]-[s+u])-1. \tag{3.12}$$

If $([r+t]-[s+u]) > 1$,the formula (3.12) is always true, and hence equation (2.1) has prime period two solution. If $([r+t]-[s+u]) \leq 1$, we have a contradiction. Hence equation (2.1) has not a prime period two solution.

(vii) If m,l are odd, and k is even, then $y_{n+1} = y_{n-m} = y_{n-l}$, and $y_n = y_{n-k}$. It follows from equation (2.1) that

$$\phi = \frac{[r+u]\,\phi + [s+t]\,\psi}{1+\phi\psi(\phi+\psi)}, \quad \psi = \frac{[r+u]\,\psi + [s+t]\,\phi}{1+\phi\psi(\phi+\psi)}.$$

Consequently, we have

$$0 < \phi\psi(\phi+\psi) = ([r+u]-[s+t])-1. \tag{3.13}$$

If $([r+u]-[s+t]) > 1$, the formula (3.13) is always true, and hence equation (2.1) has prime period two solution. If $([r+u]-[s+t]) \leq 1$, we have a contradiction. Hence equation (2.1) has not a prime period two solution.

(viii) If m,l are even, and k is odd, then $y_n = y_{n-m} = y_{n-l}$, and $y_{n+1} = y_{n-k}$. It follows from equation (2.1) that

$$\phi = \frac{[r+s+u]\,\psi + t\phi}{1+\psi^2\phi+\psi\phi^2}, \quad \psi = \frac{[r+s+u]\,\phi + t\psi}{1+\phi^2\psi+\phi\psi^2},$$

Consequently, we have

$$0 < \phi\psi(\phi+\psi) = t - ([r+s+u]+1). \tag{3.14}$$

Since $[r+s+u]+1 > t$, we have a contradiction. Hence equation (2.1) has not a prime period two solution. Hence the proof of Theorem (3.5) is now completed.

□

4. Numerical Examples

In order to illustrate the results of the previous section and to support our theoretical discussions, we consider some numerical examples in this section. These examples represent different types of qualitative behavior of solutions of equation (2.1).

Example 4.1. *Figure 4.1 shows that the solution of equation (2.1) is bounded if* $x_{-3}=1,\ x_{-2}=2,\ x_{-1}=3,\ x_0=4,\ m=1,\ k=2,\ l=3,\ r=0.1,\ s=0.2,\ t=0.3,\ u=0.25,$ *i.e.* $[r+s+t+u]<1.$

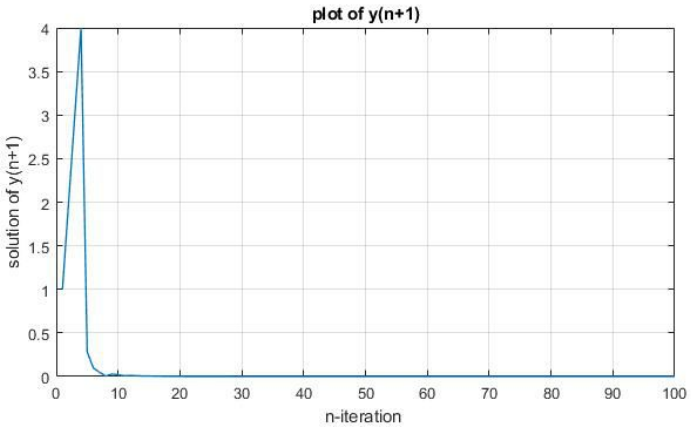

Figure 4.1: The solution of equation (2.1) is bounded.

.

Example 4.2. *Figure 4.2 shows that the solution of equation (2.1) is unbounded if* $x_{-3}=1,\ x_{-2}=2,\ x_{-1}=3,\ x_0=4,\ m=1,\ k=2,\ l=3,\ r=1,\ s=2,\ t=3,\ u=4,$ *i.e.* $[r+s+t+u]>1.$

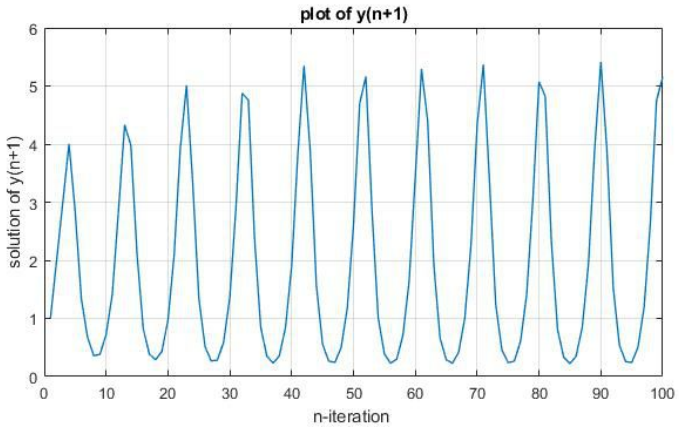

Figure 4.2: The solution of equation (2.1) is unbounded.

Example 4.3. *Figure 4.3 shows that equation (2.1) is globally asymptotically stable if* $x_{-4}=1,\ x_{-3}=2,\ x_{-2}=3,\ x_{-1}=4,\ x_0=5,\ m=2,\ k=3,\ l=4,\ r=0.1,\ s=0.5,\ t=0.2,\ u=0.25,$ *i.e.* $[r+s+t+u]<1.$

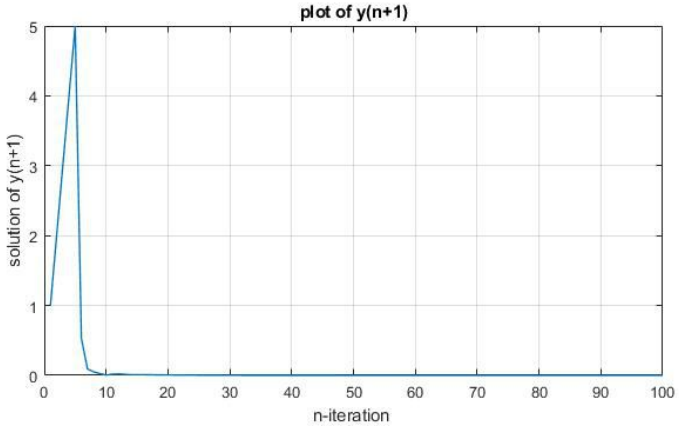

Figure 4.3: The solution of equation (2.1) is globally asymptotically stable.

Example 4. *Figure 4.4 shows that equation (2.1) has no positive prime period two solutions if* $x_{-3}=1,\ x_{-2}=2,\ x_{-1}=3,\ x_0=4,\ m=2,\ k=1,\ l=3,\ r=100,\ s=300,\ t=400,\ u=500.$

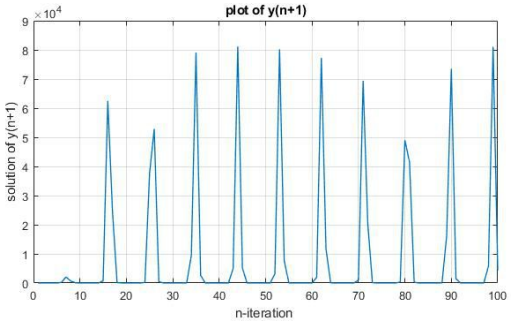

Figure 4.4: The solution of equation (2.1) has no positive prime period two solutions.

5. Conclusions

In this article, we have shown that equation (2.1) has two equilibrium points $\tilde{y}_1=0$ and $\tilde{y}_2=\left(\frac{[r+s+t+u]-1}{2}\right)^{\frac{1}{3}}$. If $[r+s+t+u]<1$, we have proved that $\tilde{y}_1=0$ is globally asymptotically stable, while if $[r+s+t+u]>1$, the solution of equation (2.1) oscillates about the point $\tilde{y}_2=\left(\frac{[r+s+t+u]-1}{2}\right)^{\frac{1}{3}}$ with a semicycle of length one. When $[r+s+t+u]>1$, we have proved that the solution of equation (2.1) is unbounded. The periodicity of the solution of equation (2.1) has been discussed in details in Theorem 3.5.

Article Information

Acknowledgements: The author thank the referees for valuable comments and suggestions which improved the presentation of this paper.

Author's Contributions: The article has a single author. The author has seen the final version of the article and approved its publication.

Conflict of Interest Disclosure: No potential conflict of interest was declared by the author.

Supporting/Supporting Organizations: No grants were received from any public, private or non-profit organizations for this research.

Ethical Approval and Participant Consent: It is declared that during the preparation process of this study, scientific and ethical principles were followed and all the studies benefited from are stated in the bibliography.

Plagiarism Statement: This article was scanned by the plagiarism program. No plagiarism detected.

Availability of Data and Materials: Not applicable.

References

[1] R. P. Agarwal, E. M. Elsayed, *On the solution of fourth-order rational recursive sequence*, Adv. Stud. Contemp. Math., **20**(4) (2010), 525–545.

[2] A. M. Alotaibi, M. A. El-Moneam, *On the dynamics of the nonlinear rational difference equation* $x_{n+1}=\frac{\alpha x_{n-m}+\delta x_n}{\beta+\gamma x_{n-k}\ x_{n-l}(x_{n-k}+x_{n-l})}$, AIMS Mathematics, **7**(5) (2022), 7374–7384.

[3] R. Devault, W. Kosmala, G. Ladas, S. W. Schaultz, *Global behavior of* $y_{n+1}=\frac{p+y_{n-k}}{qy_n+y_{n-k}}$, Nonlinear Anal. Theory Methods Appl., **47** (2004), 83–89.

[4] Q. Din, *Dynamics of a discrete Lotka-Volterra model*, Adv. Differ. Equ., **95** (2013).

[5] Q. Din, *On a system of rational difference equation*, Demonstratio Mathematica, (in press).

[6] E. M. Elabbasy, H. El-Metwally, E. M. Elsayed, *On the difference equation* $x_{n+1}=ax_n-\frac{bx_n}{cx_n-dx_{n-1}}$, Adv. Differ. Equ., (2006), Article ID 82579, 1–10.

[7] H. El-Metwally, E. A. Grove, G. Ladas, and H.D.Voulov, On the global attractivity and the periodic character of some difference equations, J. Differ. Equations Appl., **7** (2001), 837–850.

[8] M. A. El-Moneam, *On the dynamics of the higher order nonlinear rational difference equation*, Math. Sci. Lett. **3**(2) (2014), 121–129.

[9] M. A. El-Moneam, *On the dynamics of the solutions of the rational recursive sequences*, Br. J. Math. Comput. Sci., **5**(5) (2015), 654–665.

[10] M. A. El-Moneam, S. O. Alamoudy, *On study of the asymptotic behavior of some rational difference equations*, DCDIS Series A: Mathematical Analysis, **21**(2014), 89–109.

[11] M. A. El-Moneam, E. M. E. Zayed, *Dynamics of the rational difference equation*, Inf. Sci. Lett., **3**(2) (2014), 1–9.

[12] M. A. El-Moneam, E. M. E. Zayed, *On the dynamics of the nonlinear rational difference equation* $x_{n+1} = Ax_n + Bx_{n-k} + Cx_{n-l} + \frac{bx_{n-k}}{dx_{n-k} - ex_{n-l}}$, J. Egypt. Math. Soc., **23** (2015), 494–499.

[13] E. M. Elsayed, *Solution and attractivity for a rational recursive sequence*, Discrete Dyn. Nat. Soc., **2011**, Article ID 982309, (2011).

[14] E. M. Elsayed, T. F. İbrahim, *Solutions and periodicity of a rational recursive sequences of order five*, (Accepted and to appear 2012-2013, Bull. Malaysian Math. Sci. Soc.).

[15] E. A. Grove, G. Ladas, Periodicities in Nonlinear Difference Equations, Chapman & Hall / CRC, Vol. 4, 2005.

[16] T. F. İbrahim, *Boundedness and stability of a rational difference equation with delay*, Rev. Roum. Math. Pures Appl. *57* (2012), 215–224.

[17] T. F. İbrahim, *Periodicity and global attractivity of difference equation of higher order*, J. Comput. Anal. Appl., **16**, (2014).

[18] T. F. İbrahim, *Three-dimensional max-type cyclic system of difference equations*, Int. J. Phys. Sci., **8**(15) 2013, 629–634.

[19] T. F. İbrahim, N. Touafek, *On a third-order rational difference equation with variable coefficients*, DCDIS Series B: Applications & Algorithms (Dyn. Contin. Discret. I.) **20**(2) (2013), 251–264.

[20] V. L. Kocic, G. Ladas, *Global Behavior of Nonlinear Difference Equations of Higher Order with Applications*, Kluwer Academic Publishers, Dordrecht, 1993.

[21] D. Şimsek, C. Çınar, İ. Yalçınkaya, *On the recursive sequence* $x_{n+1} = \frac{x_{n-3}}{1+x_{n-1}}$, Int. J. Contemp. Math. Sci., **1**(10) (2006), 475–480.

[22] S. Stević ´, *Global stability and asymptotics of some classes of rational difference equations*, J. Math. Anal. Appl., **316** (2006) 60–68.

[23] N. Touafek, E. M. Elsayed, *On the solutions of systems of rational difference equations*, Math. Comput. Modelling, **55** (2012), 1987–1997.

[24] N. Touafek, E. M. Elsayed, On the periodicity of some systems of nonlinear difference equations, Bull. Math. Soc. Sci. Math. Roum., Nouv. Sr 2012., **55**(103), 217–224.

[25] İ. Yalçınkaya, *On the max-type equation* $x_(n+1) = max(1/x(n), A(n)x(n-1))$, Discrete Dyn. Nat. Soc., 2012, Article ID 327437, (2012), 9 pages.

[26] M. E. Erdoğan, C. Çınar, İ. Yalçınkaya, *On the dynamics of the recursive sequence* $x_{n+1} = \frac{x_{n-1}}{\beta + \gamma x_{n-2}^2 x_{n-4} + \gamma x_{n-2} x_{n-4}^2}$, Comput. Math. Appl., **61** (2011), 533–537.

[27] E. M. E. Zayed, *On the dynamics of the nonlinear rational difference equation*, DCDIS Series A: Mathematical Analysis, (to appear).

[28] E. M. E. Zayed, M. A. El-Moneam, *On the rational recursive two sequences* $x_{n+1} = ax_{n-k} + bx_{n-k} / (cx_n + \delta dx_{n-k})$, Acta Math. Vietnamica, **35**(2010), 355–369.

[29] E. M. E. Zayed, M. A. El-Moneam, *On the global attractivity of two nonlinear difference equations*, J. Math. Sci., **177** (2011), 487–499.

[30] E. M. E. Zayed, M. A. El-Moneam, *On the rational recursive sequence* $x_{n+1} = (A + \alpha_0 x_n + \alpha_1 x_{n-\sigma}) / (B + \beta_0 x_n + \beta_1 x_{n-\tau})$, Acta Math. Vietnamica, **36** (2011), 73–87.

[31] E. M. E. Zayed, M. A. El-Moneam, *On the global asymptotic stability for a rational recursive sequence*, Iran J. Sci. Technol. Trans. A Sci., **A4** (2011), 333–339.

[32] E. M. E. Zayed, M. A. El-Moneam, *On the rational recursive sequence* $x_{n+1} = \frac{\alpha_0 x_n + \alpha_1 x_{n-l} + \alpha_2 x_{n-m} + \alpha_3 x_{n-k}}{\beta_0 x_n + \beta_1 x_{n-l} + \beta_2 x_{n-m} + \beta_3 x_{n-k}}$, WSEAS Trans. Math., **11**(5) (2012), 373–382.

[33] E. M. E. Zayed, M. A. El-Moneam, *On the qualitative study of the nonlinear difference equation* $x_{n+1} = \frac{\alpha x_{n-\sigma}}{\beta + \gamma x_{n-\tau}^p}$, Fasc. Math., **50** (2013), 137–147.

[34] E. M. E. Zayed, M. A. El-Moneam, *Dynamics of the rational difference equation* $x_{n+1} = \gamma x_n + \frac{\alpha x_{n-l} + \beta x_{n-k}}{A x_{n-l} + B x_{n-k}}$, Comm. Appl. Nonl. Anal., **21** (2014), 43–53.